Stony Brook University

Slow Onset Inhibition of KasA by Thiolactomycin: Mechanistic Insights and Lead Optimization for Anti-Bacterial Drug Discovery

A Dissertation Presented

by

Carl A. Machutta

to

The Graduate School

in Partial Fulfillment of the Requirements

for the Degree of

Doctor of Philosophy

in

Chemistry

(Chemical Biology)

Stony Brook University

August 2008

Carl A. Machutta

We, the dissertation committee for the above candidate for the

Doctor of Philosophy degree, hereby recommend

acceptance of this dissertation.

Peter J. Tonge Ph.D. Advisor
Professor, Department of Chemistry

Daniel P. Raleigh Ph.D. Chairman of Defense
Professor, Department of Chemistry

Iwao Ojima Ph.D.
Distinguished Professor, Department of Chemistry

Lizbeth Hedstrom Ph.D.
Professor, Department of Biochemistry
Brandeis University

This dissertation is accepted by the Graduate School

Lawrence Martin
Dean of the Graduate School

Abstract of the Dissertation

Slow Onset Inhibition of KasA by Thiolactomycin: Mechanistic Insights and Lead Optimization for Anti-Bacterial Drug Discovery

by

Carl A. Machutta

Doctor of Philosophy

in

Chemistry

(Chemical Biology)

Stony Brook University

2008

Mycobacterium tuberculosis (MTB) is a global health threat and novel chemotherapeutics are urgently needed for the treatment of multi-drug resistant and extensively drug resistant strains. The type II fatty acid biosynthesis pathway (FASII) is the target for current frontline drugs such as isoniazid (INH), as well as for the development of novel inhibitors. KasA, the FASII β keto-acyl ACP synthase, initiates each cycle of fatty acid elongation by catalyzing the Claisen condensation of malonyl-ACP with the growing acyl chain and is essential to mycobacterial viability. The FASII cycle is a historically efficacious antimicrobial drug target and the KasA inhibitor

thiolactomycin (TLM) is a lead compound for drug development. Attempts to obtain KasA from heterologous expression in *E. coli* were unsuccessful and the protein has been expressed in *M. smegmatis*. Acyl-CoA substrates, typically used to study other FAS enzymes, are inactive with KasA. Consequently, acyl carrier protein (ACP) substrates based on the mycobacterial ACP have been used for kinetic and inhibition studies. Fluorescence quenching, and kinetic assays have been used to characterize the binding of TLM to KasA. Interestingly, while TLM binds only weakly to the free enzyme (K_d = 226 μM), the inhibitor binds more tightly to the KasA acyl-enzyme intermediate (K_d = 20 μM). Our rigorous characterization of KasA inhibition by TLM has also shown that binding to the acyl-KasA intermediate is characterized by an additional slow step rationalizing why pre-incubation of enzyme and inhibitor reduces the apparent IC_{50}. The slow association of TLM with acyl-KasA and C171Q KasA, a mutant thought to mimic the acyl-enzyme intermediate, was quantified using a fluorescence decay assay to obtain k_{obs} values using a two step binding model. The observed K_i* value correlates with the lower IC_{50} value obtained upon pre-incubation. Our development of an efficient source of recombinant protein has afforded us the opportunity to corroborate our biochemical data with the first KasA X-ray structural models to be reported. Finally, interligand-NOE NMR technology along with insights gained from the above biochemical and structural characterization have been used to guide the synthesis of novel TLM analogues as potential anti-TB therapeutics.

Table of Contents

List of Figures

List of Tables

Acknowledgement

Despite the relief I feel in completing this dissertation, I now find myself faced with the far more daunting task of repaying an entire life worth of favors and in expressing my gratitude and appreciation to a network of family, friends and mentors. Firstly, I thank the teachers of the Levittown Public School District. There enthusiasm and commitment to excellence provided me with the foundation needed for academic success. Particularly, I'd like the thank Mr. Castle, both my physical science and high school chemistry teacher, and Mr. Sobanski, my high school math teacher for three years. There passion for learning and teaching has had a profound impact on my academic career and my personal life.

I thank my dissertation advisor Prof. Peter J. Tonge, who has always provided support and advise while giving me the latitude to suffer the abrasions and contusions needed to truly learn. He has enabled me to travel across the US and around the world, he is a role model, a dear friend and I will miss him when I leave.

I thank my family and friends who have provided both logistical and moral support through the years. They have opened there homes and hearts to me and without them I could not have completed this degree.

And to my parents, you'll never know how much I appreciate you; I thank you and I love you very much.

List of Publications

1. "Inhibition of KasA, the Mycobacterial β-Ketoacyl Synthase I, by Thiolactomycin: Structural and Functional Insights for Lead Optimization" **Carl Machutta**, Sylvia R. Luckner, Kanishk Kapilashrami, Bela Ruzsicska, Caroline Kisker, Peter J. Tonge. *(In Preparation)*

2. "Enzymology of Fatty Acid Biosynthesis and Oxidation" Huaning Zhang, **Carl Machutta**, Peter J. Tonge. Comprehensive Natural Products Chemistry II. *(Review In Preparation)*

3. "Rational Design of Thiolactomycin Pantetheine Adducts with Increased Affinity for β-ketoacyl Synthases using ILOE-NMR" **Carl Machutta**, Francis Picart, B Gopal Reddy, Pilho Kim, Cynthia Dowd, Clifton Barry and Peter J. Tonge. *(In Preparation)*

4. "Slow Onset Inhibition of KasA by Thiolactomycin: Mechanistic Insights for Lead Optimization" **Carl Machutta** and Peter J. Tonge (2008) *FASEB J.* 2008 22:792.6

5. "Characterization of The β-Keto-Acyl-ACP Synthase, KasA from *Mycobacterium tuberculosis*" **Carl Machutta** and Peter J. Tonge. (2006), *FASEB J.* 2006 *20*, A462-e-463.

6. "Substrate Recognition by the Human Fatty-acid Synthase" Loretha Carlisle-Moore, Chris R. Gordon, **Carl Machutta**, W. Todd Miller, and Peter J. Tonge. J. Biol. Chem., Vol. 280, Issue 52, 42612-42618, December 30, 2005

7. "Crystal structure of *Mycobacterium tuberculosis* MenB, a key enzyme in vitamin K2 biosynthesis" James J. Truglio, Karsten Theis, Yuguo Feng, Ramona Gajda, **Carl Machutta**, Peter J. Tonge, and Caroline Kisker, J. Biol. Chem., Vol. 278, Issue 43, 42352-42360, October 24, 2003

Chapter 1

Mycobacterium Tuberculosis and Anti-Bacterial Drug Discovery

The Tuberculosis Global Health Threat

Infection Treatment

Emergence of Drug Resistance

Cell Wall Biosynthesis

Inhibitors of Bacterial Fatty Acid Biosynthesis

Natural Products as Lead Molecules for Drug Discovery

References

The Tuberculosis Global Health Threat

Mycobacterium tuberculosis (MTB), the causative agent in tuberculosis (TB), is a global health threat. The WHO estimates that nearly one third of the world's population is infected with MTB, and that 10% of these individuals will develop active infections(*1, 2*). The pandemic affects nearly every country on earth with the burden in some areas in sub-Saharan Africa as high a 70% of the population. According to the WHO each year 1.6 million people die and there were an estimated 9.2 million new infections of TB in 2006. Thus, TB remains one of the greatest contributors to adult mortality among infectious diseases. TB is a deadly coinfection in HIV/AIDS patients and is a common phenomenon throughout the world but serves to compound the disease burden in sub-Saharan Africa. One in three patients with HIV/AIDS will die of TB making it the leading cause of death in these individuals (*1*). This common coinfection in immunocompromised individuals can act to exacerbate TB's progression through the population.

MTB, a gram positive bacillus, was first discovered as the intracellular pathogen responsible for TB in 1882 by a German physician Dr. Robert Koch. He later won the Nobel Prize for this work in 1905. The history of tuberculosis however extends far beyond this discovery with evidence of TB infection found in Peruvian and Egyptian mummies dating TB infection in humans to at least 4000 years ago(*3*). Thus, the bacteria are believed to have coevolved

with humankind contributing to the organisms interesting and effective pathogenesis and to its very complex host pathogen interactions(*4*).

MTB pathogenesis is characterized by different types of infection with the vast majority of these patients developing respiratory TB. The remaining TB cases are classified as extra-pulmonary or disseminated TB. The disseminated disease is characterized by granuloma or granular tumor formation (below) in tissues other than the lung including the kidney, brain, bone and lymph nodes.

The infection can persist in two distinct states, latent and active. The vast majority of the 1.9 billion people infected with MTB are latent infections with only 8 million patients developing the active form annually(*5*). The major cell type involved in the host pathogen interaction is the alveolar macrophage(*6*). Typically, aerosolized droplets containing MTB enter the lung and condense on the alveolar surface. The bacilli are met, as are any bacteria, by alveolar machrophages in the lumen of the lung and the interaction involves the non specific phagocytosis of MTB into a phagocytic vacuole(*6, 7*). This vacuole in the case of other bacterial infections would develop into a caustic and degradative environment, the lysosome, but in the case of MTB an active process prevents the development of the lysosome. The active prevention of the development of the lysosome by the bacillus involves many complex host pathogen interactions with both well understood and unclear mechanisms.

Recently Ser/Thr kinases have been shown to be secreted by MTB to modulate cell signaling within the macrophage and prevent phago-lysosomal fusion(*8, 9*). Calcium signaling within the macrophage has also been shown to be essential for the maturation of the phagosome into a bacteriacidal phagolysosome(*10*). MTB is thought to block calcium signaling through the specific inhibition of sphingosine kinase thus preventing phagosome maturation(*11, 12*). These complex host pathogen interactions, that are intensely studied but not well understood, combined with the waxy protective cell wall found in MTB (more below) allow for the infection to persist in the latent state within the macrophage for, in some cases, decades(*7*). The transition between these latent and active states, though also unclear, often involves weakening of the host immune system.

In the case of active infection in elderly patients and those infected by HIV/AIDS, MTB proliferates at the site of infection and the host response leads to a granulomatous inflammatory condition. The formation of granuloma, a collection of immune and inflammatory cells responding to the bacterial infection, precedes cell death or necrosis at the center of the granular formation(*13*). The area of necrosis, in the case of respiratory TB, eventually causes a perforation of the lung tissue. Subsequently, the lung collapses resulting in a loss of respiratory function and death.

Infection Treatment

The unique host pathogen interactions in MTB infection and persistence in the human macrophage coupled with MTB's extraordinarily slow growth rate (doubling time 24 hours) make the TB treatment regimen difficult and lengthy(*14*). The frontline drug used to treat TB is isoniazid (INH) and is part of a six to nine month drug regimen including at least three other antibiotics, Rifampicin, Pyrazinamide and Ethambutol (Figure 1).

The minimum inhibitory concentration (MIC), molecular target and mutations correlated with resistance are summarized in Table 2. MIC is defined as the minimum inhibitor concentration required to observe a 99% reduction in bacterial viability in culture.

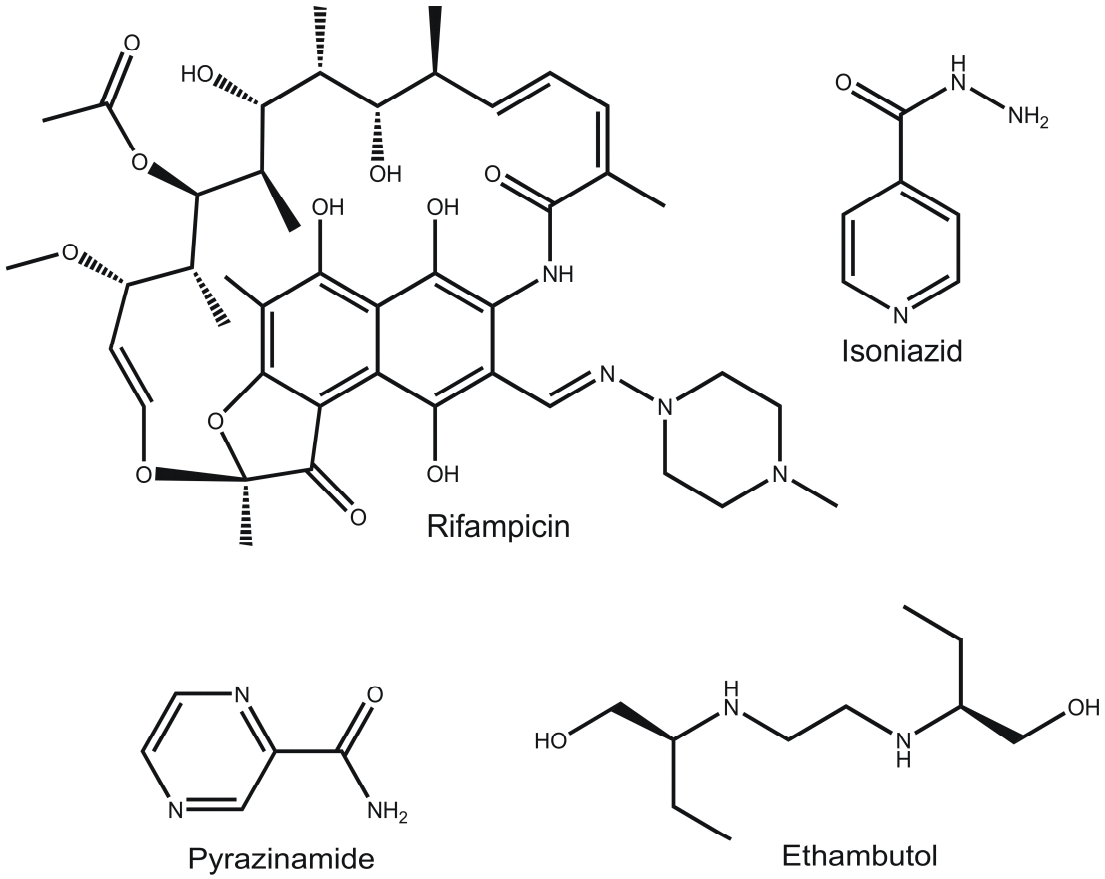

Figure 1: *Frontline drugs used for tuberculosis treatment*

Chemotherapeutic intervention in TB infection first utilized streptomycin in 1944 which is now known to inhibit protein synthesis. This drug is not widely used today due to its toxicity and lack of oral bioavailability meaning it is administered by injection only(*15*). INH is an inhibitor of fatty acid biosynthesis (FASII) through its interaction with one or more components of the cycle, the enoyl acyl carrier protein reductase InhA and the ketoacyl synthase KasA (below). The drug was introduced in 1952 but resistance

emerged shortly thereafter requiring the incorporation of other drugs into the treatment regimen(*16*).

Pyrazinamide, introduced in 1954, was proposed to inhibit fatty acid synthesis (FASI) based on binding experiments with 5-Cl-pyrazinamide(*17*) but was later shown to bind the 5-chloro-analogue but not pyrazinamide(*18*). Based on the drugs synergistic effect with molecules known to interfere with membrane potential, pyrazinamide is thought to effect membrane energetics; however an exact molecular explanation for the drugs efficacy has remained elusive(*19*).

Ethambutol was introduced in 1962 and is widely established as an inhibitor of arabinogalactan biosynthesis(*20, 21*). This compound was followed by Rifampacin in 1963. Rifampacin, a transcriptional inhibitor that binds to the RNA polymerase β-subunit *rpoB*, is the most recent addition to the frontline drugs used to treat TB. This antiquated drug regimen highlights the need to introduce modern chemotherapeutics for the treatment of MTB infection.

Drug	First Year in Clinical Use	MIC (μg/ml)	Molecular Target	Mutations correlated with drug resistance	Ref.
Isoniazid	1952	0.016	InhA, KasA others	katG, InhA, KasA others	(*22, 23*)
Pyrazinamide	1954	12-25 dependent on assay	Unknown possibly FASI	pncA (prodrug activation)	(*15, 24*)
Ethambutol	1962	1.0	arabinogalactan synthesis	embB	(*15, 25*)
Rifampacin	1963	32	transcription	rpoB	(*15, 25*)
Streptomycin	1944	4.0	30S ribosomal subunit	rpsL and rrs	(*15, 25*)

Table 1: *Summary of Minimum Inhibitory Concentration (MIC) and other Data for Frontline Tuberculosis Drugs*

These drugs, summarized in Table 1, possess potent anti-TB activity but are far from ideal therapeutic agents. The side effects of these drugs can be brutally painful and even deadly. Ethambutol has been associated with optic neuropathy causing irreversible blindness. All of the drugs have been linked to liver failure, rifampicin has limited efficacy in HIV/AIDS patients due to an interaction with anti-retroviral drugs while still relatively minor effects; weakness, fatigue, vomiting, weight loss and rash hamper patient compliance leading to the emergence of drug resistant strains.

Emergence of Drug Resistance

Despite the complexities involved in the treatment of TB infection, physicians with adequate access to resources can provide drug therapy with

a high cure rate. The success of TB therapy is dependent on the physician's strict adherence to the four drug regimen, and patient compliance with the prescribed regimen.

As described above, brutal side effects lead to patient non-compliance or in the case of toxicity an abandonment of therapy, this in turn leads to the emergence of drug resistance through natural selection. That is, individual bacteria within the infecting population possess random mutations that confer resistance and therefore a selective advantage over susceptible bacteria. When the drug is removed prematurely this population flourishes giving rise to a new drug resistant population.

Additionally, the improper treatment of patients by health professionals leads to drug resistance. For example, when prescribed alone INH leads to a high frequency of resistance. Failure to use a four drug therapy is thought to be a contributing factor in the outbreak of multi-drug resistant TB (MDR-TB) in NYC in the 1990s(*26, 27*). MDR-TB is defined as simultaneous resistance to both rifampicin and INH and the emergence of 450,000 new cases annually lengthens the treatment to up 24 months with a 20 fold increase in cost. NYC spent $1 billion on just 4000 cases of MDR-TB, where a full six month supply of drugs for susceptible strains would cost just $16-25. A massive surge in resources devoted to TB control following the NYC outbreak resulted in a 59% decrease in TB cases with a 91% decrease in MDR-TB(*27*), showing

that adequate TB control programs can prevent the emergence of MDR-TB and are a sound investment. According to the Global Alliance for TB Drug Development the global economic TB burden amounts to $12 billion per year. Due to TB's close association with impoverished developing countries, the urgency for the development of novel chemotherapeutics therefore goes far beyond saving lives in the clinic.

Recently, drug resistance has worsened with the emergence of extensively drug resistant strains (XDR-TB). XDR-TB is resistant to all of the first line drugs as well as the second line fluoroquinolones (Ciprofloxacin) and at least one of the three injectable second line drugs. The emergence of this dangerous, virtually untreatable strain compounds the global TB burden and is an imminent threat to both the developed and undeveloped world. One example from each of the six classes of second line drugs is shown in Figure 2 and summarized in Table 2.

Table2: *Summary of Secondline Drugs for TB Treatment*

Drugs	Class	Molecular Target	IV or OA‡	Ref:
Amikacin	aminoglycocides	Protein Synthesis, 30S ribosomal subunit	IV	
Capromycin	polypeptides	Various	IV	
Ethionamide	thioamides	InhA	OA	(*28*)
Ciprofloxacin	fluoroquinolones	DNA gyrase	OA	
Cycloserine	N/A*	peptidoglygan synthesis *Alr*	OA	
para-amino-salicylic acid	N/A*	Unknown; Folate synthesis Iron transport	OA	

* Only drug in this class
‡ (IV) Intravenous, (OA) Orally Available

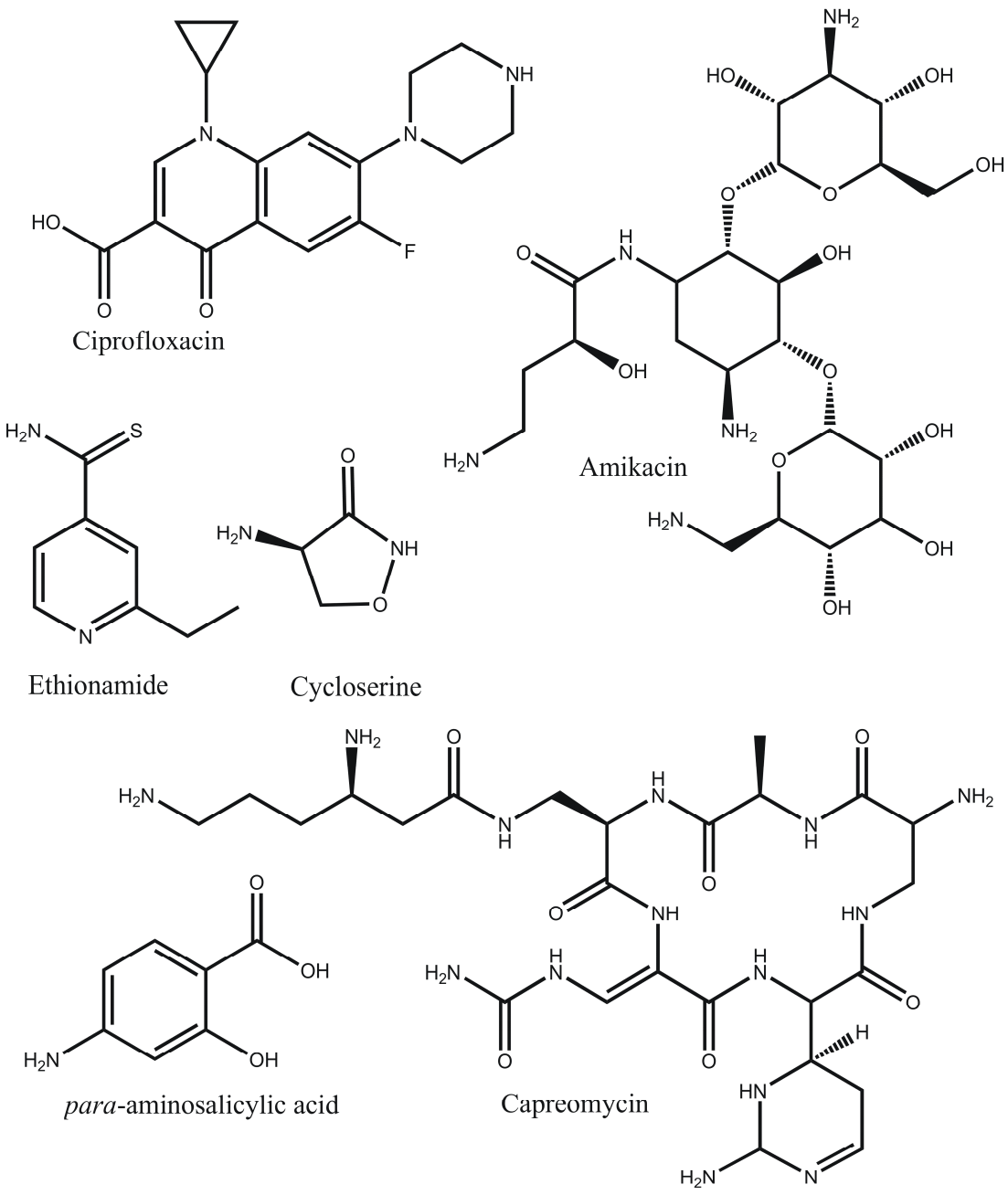

Figure 2: *Second Line TB Drugs*

As highlighted by the success of TB control program reinvestment in NYC, the WHO created the DOTS or Directly Observed Therapy Short-course in

1995(*27, 29*). The DOTS program was created to ensure patients were following their treatment regimen with consistent, proper dosing. Patients following a DOTS short course regimen will be given the four frontline drugs for an initial intensive phase lasting two months. This is followed by a continuation phase with rifampicin and isoniazid for an additional four months(*29*). The WHO reports 84% of patients registered and treated with DOTS as successfully treated. Despite these improvements in TB treatment the global incidence of TB continues to rise today. The increasing incidence is fueled by the HIV/AIDS pandemic and the emergence of drug resistance highlighting the urgent need for the addition of novel chemotherapeutics to the current armamentarium.

Cell Wall Biosynthesis

Cell wall biosynthesis is a historically efficacious drug target and is a widely used target for chemotherapeutic intervention in a variety of bacterial infections(*30*). In mycobacteria the cell wall is comprised of mycolic acids, very long chain lipids that provide protection and allow the bacteria to persist in the human macrophage(*31, 32*). The complex cell wall structure (Figure 3) is thought to contribute to the pathogenesis of MTB and is the subject of intense research.

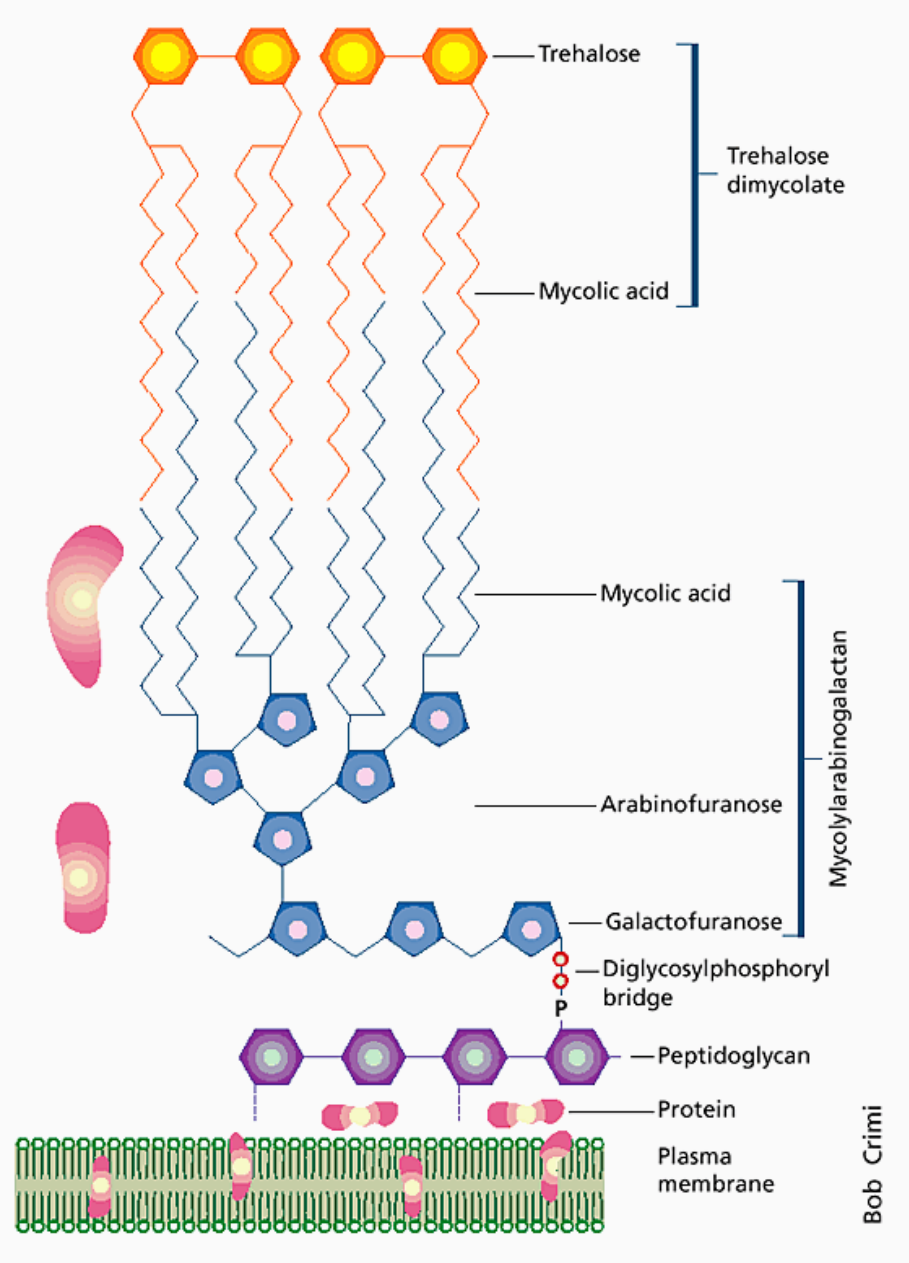

Figure 3: *Mycobacterial Cell Wall*

Mycolic acids are synthesized from long chain (C50+) fatty acids that are in turn synthesized by the dissociated fatty acid synthesis (FAS-II) pathway (below). Isoniazid inhibits the synthesis of mycolic acids through an effect on one or more cellular targets including the FAS-II enoyl reductase InhA.

Although the mycobacterial FAS-II pathway catalyzes the extension of fatty acids using the standard cycle of condensation, keto-reduction, dehydration and reduction reactions (Figure 4), the MTB FAS-II enzymes are atypical due to their very long chain length specificity. Mycobacteria are also unusual because they possess both a FAS-I cycle, typically found in eukaryotes, and a bacterial FAS-II cycle, making it the first prokaryote shown to have both pathways(*33*).

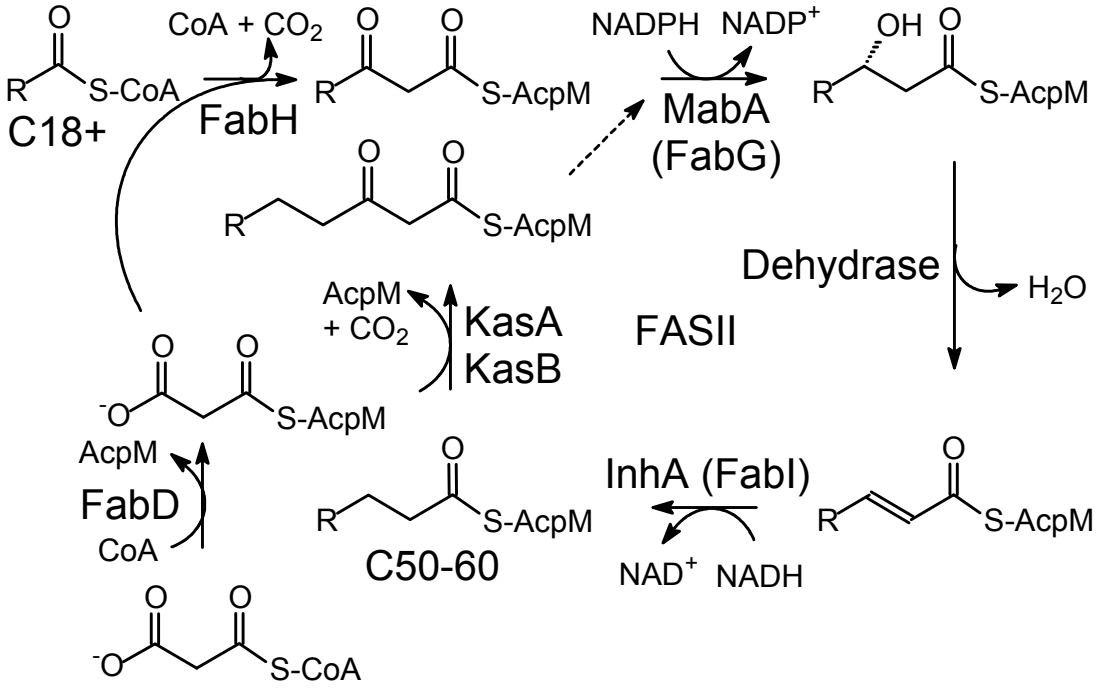

Figure 4: *MTB Fatty Acid Biosynthesis FASII Cycle*

The *de novo* production of fatty acids in MTB from malonyl-CoA and acetyl-CoA is achieved through the FAS-I or associated fatty acid synthesis

cycle. This is homologous to the mammalian FAS-I multienzyme complex. In FAS-I all of the catalytic steps are contained on a single multi-functional 550kDa polypeptide that includes an acyl carrier protein (Acp) domain. The products of FAS-I, primarily palmitic acid (C16) are released by a separate enzyme, thioesterase. The expression of FAS-I in humans is tightly regulated by diet and is thought to be evolutionarily important during cycles of feast and famine. Up-regulation of FAS-I has been shown in breast cancer cells to supply fatty acids for the rapidly dividing tumor and is a drug target for anti-tumor drug discovery(*34*).

Fatty acid biosynthesis plays a central role in the metabolism of all living systems and with the advent of *E. coli* based molecular biology, the enzymes involved in bacterial fatty acid biosynthesis (FASII) have been extensively studied in this organism. In the FAS-II pathway, the growing fatty acids are shuttled through the cycle attached to the phosphopantetheine prosthetic group of a small (13kDa) acidic protein, acyl carrier protein (Acp). The acyl chain is linked to the phosphopantetheine through a thioester. The mycobacterial specific AcpM is shown in Figure 5 and is distinct from other Acps in that it has an extended C-terminal tail thought to accommodate and solublize the longer acyl chain lengths in MTB.

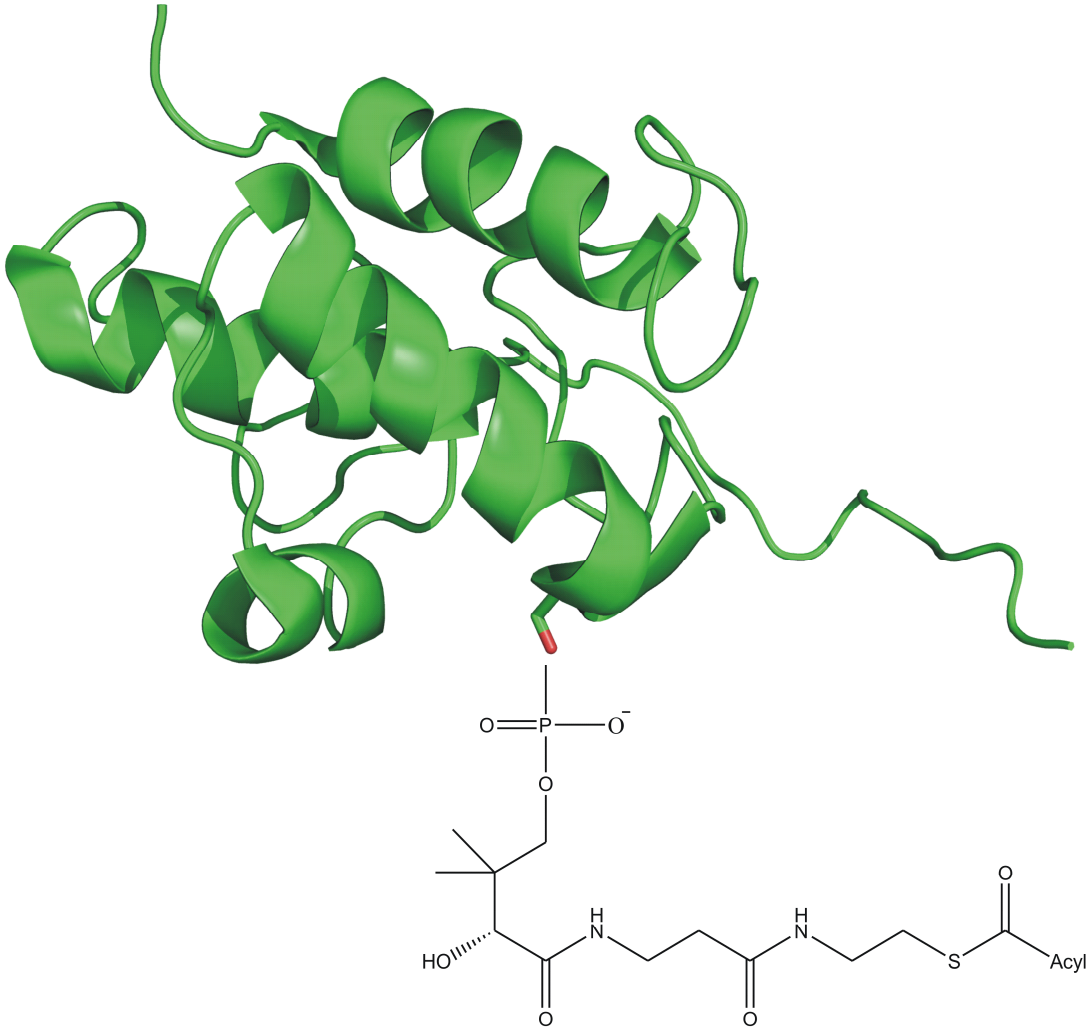

Figure 5: *Mycobacterial Acyl Carrier Protein (AcpM) with phosphopantetheine prosthetic group attached to Serine 41 through a phosphodiester linakge and thioester linkage to the growing fatty acyl chain*

Initially the C18-CoA product of the FAS-I pathway is condensed with malonyl-AcpM to generate a β-ketoacyl-AcpM by the β-ketoacyl synthase FabH, and this product is then reduced, dehydrated and reduced by the consecutive action of a β-ketoacyl dehydrogenase (MabA), a dehydrase and the enoyl reductase InhA (Figure 4). Subsequent rounds of elongation use the same enzymes except that the condensation reaction utilizes the AcpM-specific β-ketoacyl synthases KasA or KasB, which are homologues of the FabB and FabF synthases found in *E. coli* (*35, 36*). KasA, KasB and FabH all catalyze a Claisen condensation between malonyl-AcpM and acyl-CoA or acyl-AcpM, and whereas the initiation and elongation β-ketoacyl synthases share conserved three dimensional structures, they differ in there active site triad which is Cys-His-Asn in FabH and Cys-His-His in KasA/KasB (FabB/FabF)(*37*). The active site triad and conserved thiolase fold of FabB are shown in Figure 6.

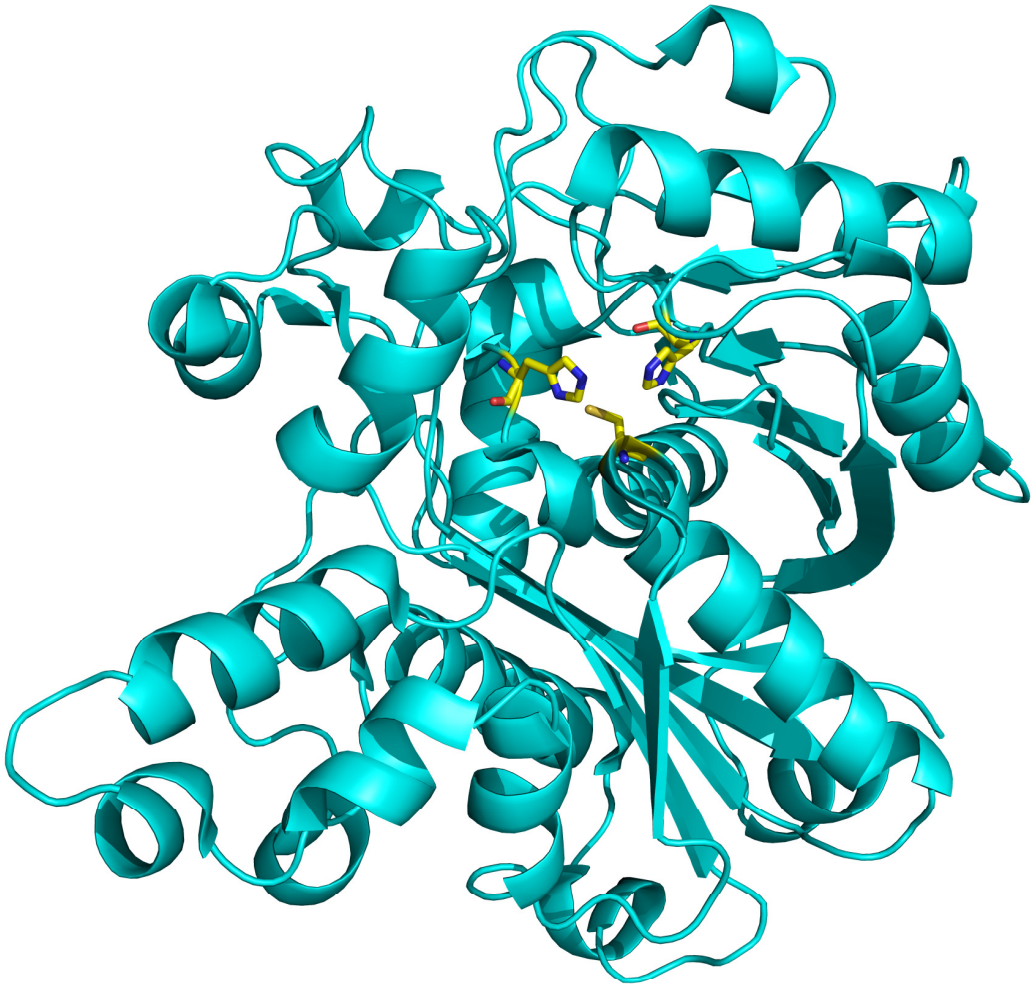

Figure 6: *E.coli β-ketoacyl-ACP synthase FabB (KAS-I)*

Cys-His-His Catalytic Triad Shown in Yellow

The fundamental importance of FAS to cellular structure, function and metabolism has made the enzymes involved in this pathway subject to thorough research. The high degree of conservation between components in the FAS-II pathway in bacteria and the distinction of mammalian FAS from

bacterial FAS make this cycle an attractive target for chemotherapy development. Many component enzymes in FASII have been explicitly shown to be essential in a variety of bacterial pathogens through knockdown and knockout experiments as well as through the use of target specific inhibitors. Bergler *et al*. showed FabI, the enoyl reductase in *E. coli*, to be essential using a temperature sensitive *fabI* mutant(*38*). Lai and Cronan showed that FabH is essential for growth in both gram positive and gram negative bacteria using genetic deletion experiments(*39*). However, the FabH gene has been shown to not be essential for growth in MTB(*40*). The essentiality of KasA was confirmed using conditional depletion experiments and specific inhibitors known to inhibit KAS enzymes(*41*). Experiments confirming the essentiality of MabA (*42, 43*) and the recently discovered dehydrase, HadA-C, followed suit completing the validation of each component in the pathway. Additionally, currently marketed anti-bacterial agents further validate this pathway as a target for drug discovery with two major target classes being the enoyl-ACP reductase and the β-ketoacyl-ACP synthase.

Inhibitors of Bacterial Fatty Acid Biosynthesis

The two major areas of FAS inhibition studies are targeted toward the enoyl reductase (ER) and ketoacyl synthase(KAS). Triclosan, a widely used broad spectrum antibiotic, is found in a number of anti-bacterial products such

as toothpaste, hand sanitizer and soap. Though initially considered a non-specific biocide, triclosan is now known to be a potent ER inhibitor. A 2% triclosan bath is recommended to decolonize patients known to be exposed to methicillin resistant *staphylococcus aureus* (MRSA). Structure activity relationship (SAR) studies have been conducted with the triclosan pharmacaphore leading to potent ER inhibitors with activity against MTB, MDR-TB, *staphylococcus aureus*, and *francisella tularensis* (Figure 7B) (*44, 45*). Isoniazid is a potent slow-onset inhibitor of MTB's enoyl reductase InhA, but it is first activated by a catalase peroxidase enzyme KatG to form an adduct with the InhA nicotinamide cofactor (Figure 7A) (*22*).

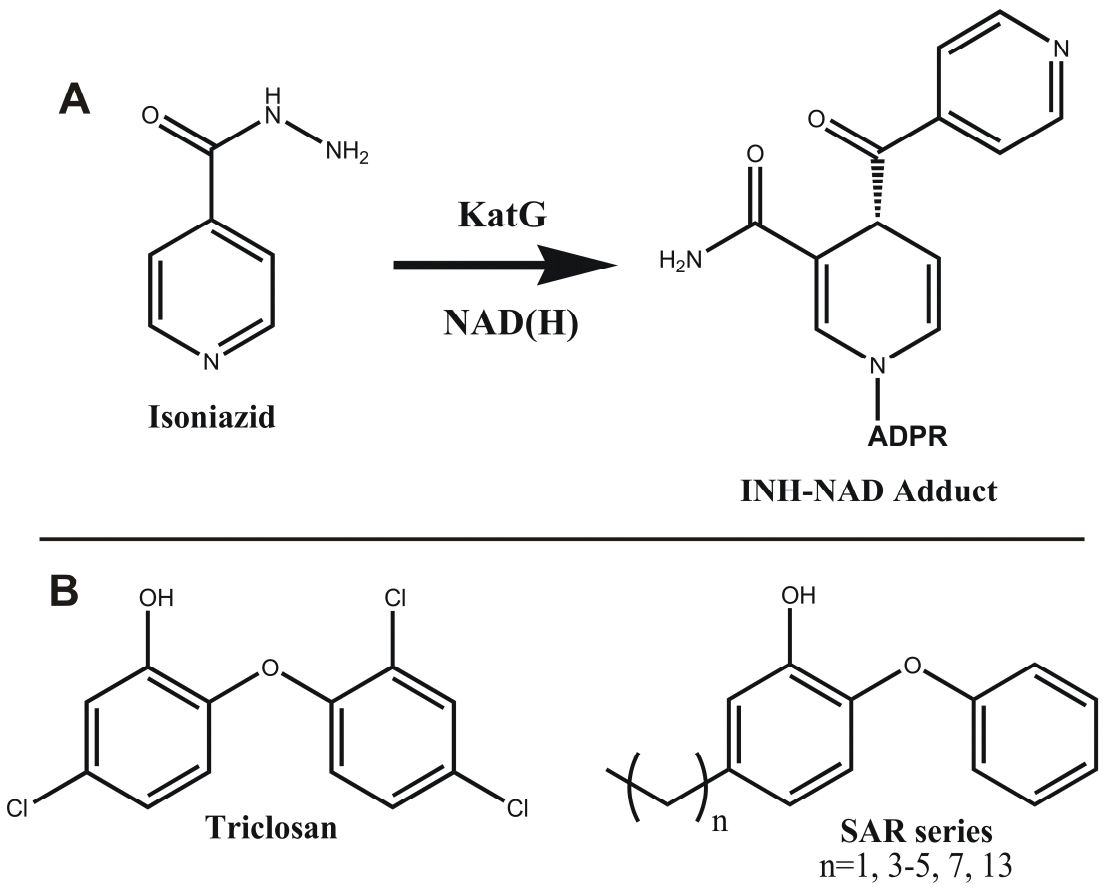

Figure 7: *Inhibitors of ER-InhA; A. Isoniazid activation by KatG*

B. Triclosan and Analog SAR series (44)

Ketoacyl synthase inhibitors, though not used clinically, are important for their potential development into drugs. Cerulenin is an irreversible KAS inhibitor that reacts with the active site cysteine in KAS enzymes, though its development as a lead molecule has largely been abandoned due to its cross reactivity with the mammalian FAS-I. Recently, three KAS inhibitors were discovered using a high-throughput antisense RNA technology. The expression of FabF (KAS-II) and/or FabH (KAS-III) antisense RNA would

cause the bacterial strain to exhibit hypersensitivity in the presence of KAS specific inhibitors and a screen to identify such molecules was conducted. The screen led to the identification of Phomallenic acids, platencin and platencimycin (Figure 8). Thiolactomycin, also a KAS inhibitor, is selective for FAS-II and is summarized and discussed in depth in Chapters 2 and 4. These KAS inhibitors, shown in Figure 8, are all natural products highlighting the utility of nature in generating potent and selective lead molecules. Arguably, nature's selection of these enzymes for inhibition further validates the essentiality of the FAS pathway.

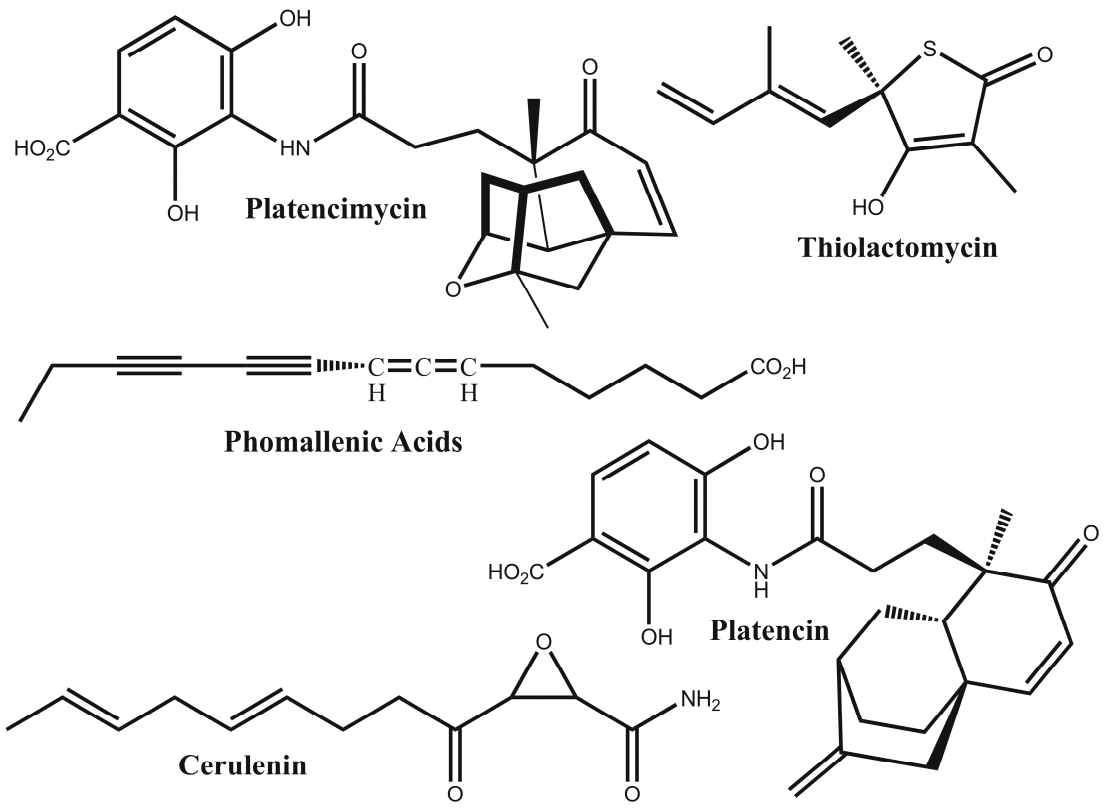

Figure 8: *KAS inhibitors*

Natural Product as Lead Molecules for Drug Discovery

Natural product inhibitors are historically efficacious in the treatment of bacterial infections. Fifty years of anti-bacterial drug discovery efforts have yielded a variety of diverse chemical entities, mostly natural products, with potent broad spectrum activity(*46*). The history of natural product antibiotics has its roots in the initial observation in 1929 by Alexander Fleming that *Penicillin notatum* inhibited bacterial growth. The isolation of penicillin from this organism in the late 1930's set the stage for the next half century of drug discovery(*47*) and the identification of streptomycin by Waksman *et al.* followed soon after. Physicians and scientist alike widely held the seductive notion that bacterial infections would soon be eradicated; but nearly eighty years later infectious disease is still a leading cause of death. Modern drug discovery still utilizes natural products and with 70 out of 90 of the antibiotics marketed from 1982-2002 being derived from natural products, the utility of generating lead compounds from nature is clear(*48, 49*).

The urgent need for the development of novel chemotherapeutics to treat bacterial infections, particularly MTB infection, coupled with the validation of fatty acid biosynthesis as a drug target and the utility of natural products in generating lead molecules; we set out to develop a drug discovery program based around the FAS-II β-ketoacyl synthase and the natural product thiolactomycin. Experiments and results to this end are described herein.

References:

1. Bloom, B. R., and Murray, C. J. (1992) Tuberculosis: commentary on a reemergent killer, *Science (New York, N.Y 257*, 1055-1064.
2. Kochi, A. (1991) The global tuberculosis situation and the new control strategy of the World Health Organization, *Tubercle 72*, 1-6.
3. Zink, A. R., Sola, C., Reischl, U., Grabner, W., Rastogi, N., Wolf, H., and Nerlich, A. G. (2003) Characterization of Mycobacterium tuberculosis complex DNAs from Egyptian mummies by spoligotyping, *Journal of clinical microbiology 41*, 359-367.
4. Donoghue, H. D., Spigelman, M., Greenblatt, C. L., Lev-Maor, G., Kahila Bar-Gal, G., Matheson, C., Vernon, K., G Nerlich, A., and R Zink, A. (2004) Tuberculosis: from prehistory to Robert Koch, as revealed by ancient DNA, *The Lancet Infectious Diseases 4*, 584-592.
5. Dye, C., Scheele, S., Dolin, P., Pathania, V., and Raviglione, M. C. (1999) Consensus statement. Global burden of tuberculosis: estimated incidence, prevalence, and mortality by country. WHO Global Surveillance and Monitoring Project, *Jama 282*, 677-686.
6. Chackerian, A. A., Alt, J. M., Perera, T. V., Dascher, C. C., and Behar, S. M. (2002) Dissemination of Mycobacterium tuberculosis is influenced by host factors and precedes the initiation of T-cell immunity, *Infection and immunity 70*, 4501-4509.
7. Dannenberg, A. M., Jr. (1982) Pathogenesis of pulmonary tuberculosis, *The American review of respiratory disease 125*, 25-29.
8. Szekely, R., Waczek, F., Szabadkai, I., Nemeth, G., Hegymegi-Barakonyi, B., Eros, D., Szokol, B., Pato, J., Hafenbradl, D., Satchell, J., Saint-Joanis, B., Cole, S. T., Orfi, L., Klebl, B. M., and Keri, G. (2008) A novel drug discovery concept for tuberculosis: Inhibition of bacterial and host cell signalling, *Immunology letters 116*, 225-231.
9. Walburger, A., Koul, A., Ferrari, G., Nguyen, L., Prescianotto-Baschong, C., Huygen, K., Klebl, B., Thompson, C., Bacher, G., and

Pieters, J. (2004) Protein kinase G from pathogenic mycobacteria promotes survival within macrophages, *Science (New York, N.Y 304*, 1800-1804.

10. Kusner, D. J. (2005) Mechanisms of mycobacterial persistence in tuberculosis, *Clinical immunology (Orlando, Fla 114*, 239-247.
11. Malik, Z. A., Denning, G. M., and Kusner, D. J. (2000) Inhibition of Ca(2+) signaling by Mycobacterium tuberculosis is associated with reduced phagosome-lysosome fusion and increased survival within human macrophages, *The Journal of experimental medicine 191*, 287-302.
12. Malik, Z. A., Thompson, C. R., Hashimi, S., Porter, B., Iyer, S. S., and Kusner, D. J. (2003) Cutting edge: Mycobacterium tuberculosis blocks Ca2+ signaling and phagosome maturation in human macrophages via specific inhibition of sphingosine kinase, *J Immunol 170*, 2811-2815.
13. Saunders, B. M., and Britton, W. J. (2007) Life and death in the granuloma: immunopathology of tuberculosis, *Immunology and cell biology 85*, 103-111.
14. Hiriyanna, K. T., and Ramakrishnan, T. (1986) Deoxyribonucleic acid replication time in Mycobacterium tuberculosis H37 Rv, *Archives of microbiology 144*, 105-109.
15. Sacchettini, J. C., Rubin, E. J., and Freundlich, J. S. (2008) Drugs versus bugs: in pursuit of the persistent predator Mycobacterium tuberculosis, *Nature reviews 6*, 41-52.
16. Middlebrook, G. (1952) Sterilization of tubercle bacilli by isonicotinic acid hydrazide and the incidence of variants resistant to the drug in vitro, *American review of tuberculosis 65*, 765-767.
17. Zimhony, O., Cox, J. S., Welch, J. T., Vilcheze, C., and Jacobs, W. R., Jr. (2000) Pyrazinamide inhibits the eukaryotic-like fatty acid synthetase I (FASI) of Mycobacterium tuberculosis, *Nature medicine 6*, 1043-1047.

18. Boshoff, H. I., Mizrahi, V., and Barry, C. E., 3rd. (2002) Effects of pyrazinamide on fatty acid synthesis by whole mycobacterial cells and purified fatty acid synthase I, *Journal of bacteriology 184*, 2167-2172.
19. Zhang, Y., Wade, M. M., Scorpio, A., Zhang, H., and Sun, Z. (2003) Mode of action of pyrazinamide: disruption of Mycobacterium tuberculosis membrane transport and energetics by pyrazinoic acid, *The Journal of antimicrobial chemotherapy 52*, 790-795.
20. Beggs, W. H., and Andrews, F. A. (1974) Chemical characterization of ethambutol binding to Mycobacterium smegmatis, *Antimicrobial agents and chemotherapy 5*, 234-239.
21. Takayama, K., and Kilburn, J. O. (1989) Inhibition of synthesis of arabinogalactan by ethambutol in Mycobacterium smegmatis, *Antimicrobial agents and chemotherapy 33*, 1493-1499.
22. Rawat, R., Whitty, A., and Tonge, P. J. (2003) The isoniazid-NAD adduct is a slow, tight-binding inhibitor of InhA, the Mycobacterium tuberculosis enoyl reductase: adduct affinity and drug resistance, *Proceedings of the National Academy of Sciences of the United States of America 100*, 13881-13886.
23. Gumbo, T., Louie, A., Liu, W., Brown, D., Ambrose, P. G., Bhavnani, S. M., and Drusano, G. L. (2007) Isoniazid bactericidal activity and resistance emergence: integrating pharmacodynamics and pharmacogenomics to predict efficacy in different ethnic populations, *Antimicrobial agents and chemotherapy 51*, 2329-2336.
24. Barco, P., Cardoso, R. F., Hirata, R. D., Leite, C. Q., Pandolfi, J. R., Sato, D. N., Shikama, M. L., de Melo, F. F., Mamizuka, E. M., Campanerut, P. A., and Hirata, M. H. (2006) pncA mutations in pyrazinamide-resistant Mycobacterium tuberculosis clinical isolates from the southeast region of Brazil, *The Journal of antimicrobial chemotherapy 58*, 930-935.
25. Menner, N., Gunther, I., Orawa, H., Roth, A., Rambajan, I., Wagner, J., Hahn, H., Persaud, S., and Ignatius, R. (2005) High frequency of

multidrug-resistant Mycobacterium tuberculosis isolates in Georgetown, Guyana, *Trop Med Int Health 10*, 1215-1218.

26. Frieden, T. R., Sterling, T., Pablos-Mendez, A., Kilburn, J. O., Cauthen, G. M., and Dooley, S. W. (1993) The emergence of drug-resistant tuberculosis in New York City, *The New England journal of medicine 328*, 521-526.
27. Hayward, A. C., and Coker, R. J. (2000) Could a tuberculosis epidemic occur in London as it did in New York?, *Emerging infectious diseases 6*, 12-16.
28. Banerjee, A., Dubnau, E., Quemard, A., Balasubramanian, V., Um, K. S., Wilson, T., Collins, D., de Lisle, G., and Jacobs, W. R., Jr. (1994) inhA, a gene encoding a target for isoniazid and ethionamide in Mycobacterium tuberculosis, *Science (New York, N.Y 263*, 227-230.
29. Cox, H. S., Morrow, M., and Deutschmann, P. W. (2008) Long term efficacy of DOTS regimens for tuberculosis: systematic review, *BMJ (Clinical research ed 336*, 484-487.
30. Heath, R. J., and Rock, C. O. (2004) Fatty acid biosynthesis as a target for novel antibacterials, *Curr Opin Investig Drugs 5*, 146-153.
31. Liu, J., Barry, C. E., 3rd, Besra, G. S., and Nikaido, H. (1996) Mycolic acid structure determines the fluidity of the mycobacterial cell wall, *The Journal of biological chemistry 271*, 29545-29551.
32. Barry, C. E., 3rd, Lee, R. E., Mdluli, K., Sampson, A. E., Schroeder, B. G., Slayden, R. A., and Yuan, Y. (1998) Mycolic acids: structure, biosynthesis and physiological functions, *Progress in lipid research 37*, 143-179.
33. Brindley, D. N., Matsumura, S., and Bloch, K. (1969) Mycobacterium phlei Fatty Acid Synthetase[mdash]A Bacterial Multienzyme Complex, *Nature 224*, 666-669.
34. Carlisle-Moore, L., Gordon, C. R., Machutta, C. A., Miller, W. T., and Tonge, P. J. (2005) Substrate recognition by the human fatty-acid synthase, *The Journal of biological chemistry 280*, 42612-42618.

35. Edwards, P., Nelsen, J. S., Metz, J. G., and Dehesh, K. (1997) Cloning of the fabF gene in an expression vector and in vitro characterization of recombinant fabF and fabB encoded enzymes from Escherichia coli, *FEBS Lett 402*, 62-66.
36. Schaeffer, M. L., Agnihotri, G., Volker, C., Kallender, H., Brennan, P. J., and Lonsdale, J. T. (2001) Purification and biochemical characterization of the Mycobacterium tuberculosis beta-ketoacyl-acyl carrier protein synthases KasA and KasB, *The Journal of biological chemistry 276*, 47029-47037.
37. Olsen, J. G., Kadziola, A., von Wettstein-Knowles, P., Siggaard-Andersen, M., and Larsen, S. (2001) Structures of beta-ketoacyl-acyl carrier protein synthase I complexed with fatty acids elucidate its catalytic machinery, *Structure 9*, 233-243.
38. Bergler, H., Fuchsbichler, S., Hogenauer, G., and Turnowsky, F. (1996) The enoyl-[acyl-carrier-protein] reductase (FabI) of Escherichia coli, which catalyzes a key regulatory step in fatty acid biosynthesis, accepts NADH and NADPH as cofactors and is inhibited by palmitoyl-CoA, *European journal of biochemistry / FEBS 242*, 689-694.
39. Lai, C. Y., and Cronan, J. E. (2003) Beta-ketoacyl-acyl carrier protein synthase III (FabH) is essential for bacterial fatty acid synthesis, *The Journal of biological chemistry 278*, 51494-51503.
40. Sassetti, C. M., Boyd, D. H., and Rubin, E. J. (2003) Genes required for mycobacterial growth defined by high density mutagenesis, *Molecular microbiology 48*, 77-84.
41. Bhatt, A., Kremer, L., Dai, A. Z., Sacchettini, J. C., and Jacobs, W. R., Jr. (2005) Conditional depletion of KasA, a key enzyme of mycolic acid biosynthesis, leads to mycobacterial cell lysis, *Journal of bacteriology 187*, 7596-7606.
42. Parish, T., Roberts, G., Laval, F., Schaeffer, M., Daffe, M., and Duncan, K. (2007) Functional complementation of the essential gene fabG1 of Mycobacterium tuberculosis by Mycobacterium smegmatis

fabG but not Escherichia coli fabG, *Journal of bacteriology 189*, 3721-3728.

43. Silva, R. G., Rosado, L. A., Santos, D. S., and Basso, L. A. (2008) Mycobacterium tuberculosis beta-ketoacyl-ACP reductase: alpha-secondary kinetic isotope effects and kinetic and equilibrium mechanisms of substrate binding, *Archives of biochemistry and biophysics 471*, 1-10.
44. Sullivan, T. J., Truglio, J. J., Boyne, M. E., Novichenok, P., Zhang, X., Stratton, C. F., Li, H. J., Kaur, T., Amin, A., Johnson, F., Slayden, R. A., Kisker, C., and Tonge, P. J. (2006) High affinity InhA inhibitors with activity against drug-resistant strains of Mycobacterium tuberculosis, *ACS chemical biology 1*, 43-53.
45. Xu, H., Sullivan, T. J., Sekiguchi, J. I., Kirikae, T., Ojima, I., Stratton, C. F., Mao, W., Rock, F. L., Alley, M. R., Johnson, F., Walker, S. G., and Tonge, P. J. (2008) Mechanism and Inhibition of saFabI, the Enoyl Reductase from Staphylococcus aureus, *Biochemistry*.
46. Silver, L. L. (2003) Novel inhibitors of bacterial cell wall synthesis, *Curr Opin Microbiol 6*, 431-438.
47. Chain, E., Florey, H. W., Gardner, A. D., Heatley, N. G., Jennings, M. A., Orr-Ewing, J., and Sanders, A. G. (1940) PENICILLIN AS A CHEMOTHERAPEUTIC AGENT, *The Lancet 236*, 226-228.
48. Newman, D. J., Cragg, G. M., and Snader, K. M. (2003) Natural products as sources of new drugs over the period 1981-2002, *Journal of natural products 66*, 1022-1037.
49. Pelaez, F. (2006) The historical delivery of antibiotics from microbial natural products--can history repeat?, *Biochem Pharmacol 71*, 981-990.

Chapter 2

Slow Onset Inhibition of KasA by Thiolactomycin

β-Ketoacyl Synthases

KAS validation

Isoniazid target controversy

Thiolactomycin; a lead molecule for antimicrobial drug discovery

KAS inhibition and the Acyl-enzyme Intermediate

KasA Characterization and TLM Inhibition Mechanism

Materials and Methods

Results

Discussion

Mechanistic Insights for Lead Optimization

References

β-ketoacyl synthases

Carbon-carbon bond formation in the biosynthesis of natural products is a fundamentally important chemical reaction in the cellular metabolism of all living systems. In the biosynthesis of fatty acids and polyketides the decarboxylating Claisen condensation that leads to carbon-carbon bond formation is catalyzed by a class of enzymes collectively known as the condensing enzymes(*1, 2*). These condensing enzymes belong to a superfamily, the thiolase superfamily, based on their common three dimensional fold, the thiolase fold, first characterized in a degradative thiolase from *Saccharomyces cerevisiae(3, 4)*. Curiously, the enzymes catalyzing the polyketide and fatty acid claisen condensation, as well as other members of the superfamily, lack sequence similarity yet share the same basic thiolase fold (Figure 1). The thiolase family of enzymes primarily form dimers with each subunit (monomer) sharing a common superfamily topology(*5*). The monomer can be divided into N and C terminal halves each having a βαβαβαββ topology. Figure 1 shows the *E. coli* Kas-I (FabB) involved in the fatty acid biosynthesis cycle with the conserved Cys-His-His catalytic triad and the conserved catalytic Nα3 α-helix shown in yellow. The conserved substrate binding loops at Cβ4-Cβ5 and Cβ3-Cα3 are shown in red.

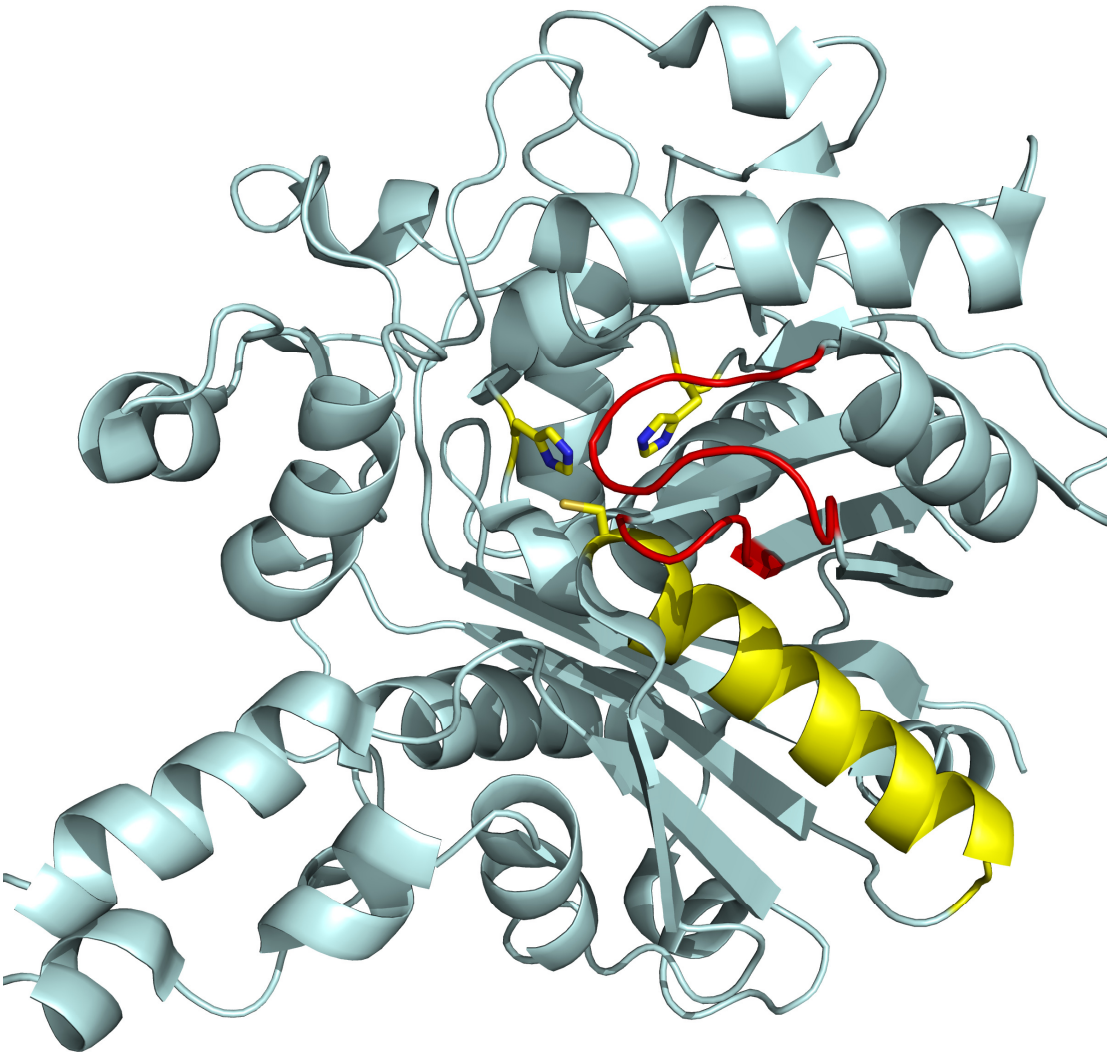

Figure 1*: Apo structure of E. coli KAS-I (FabB)*

Conserved βαβαβαββ topology

Catalytic triad and catalytic helix Nα3 shown in yellow

Conserved thiolase superfamily substrate binding loops

Cβ4-Cβ5 and Cβ3-Cα3 shown in red

The thiolase superfamily can be subdivided into three major categories; the ketoacyl synthases (KAS), the polyketide synthases (PKS), and the biosynthetic and degradative thiolases(*2*). The KAS enzyme subfamily, of particular interest in our anti-bacterial drug discovery project, functions in the synthesis of fatty acids and can be further broken into three subdivisions. The elongating condensing enzymes KAS-I and KAS-II that are structurally similar but differ in substrate specificity. These enzymes catalyze an acyl carrier protein (Acp) dependent reaction using a Cys-His-His catalytic triad. The third class, the initiation condensation enzymes (KAS III), catalyze a coenzyme-A (CoA) dependent reaction utilizing a Cys-His-Asn catalytic triad(*6*).

The β-ketoacyl synthases (KAS) catalyze the condensation between malonyl-Acp and the relevant acyl group using a ping pong mechanism in which the acyl group is first transferred to an active site cysteine residue, which then subsequently reacts with malonyl-Acp after the holo or empty acyl carrier molecule (CoA or Acp) has dissociated (Figure 2).

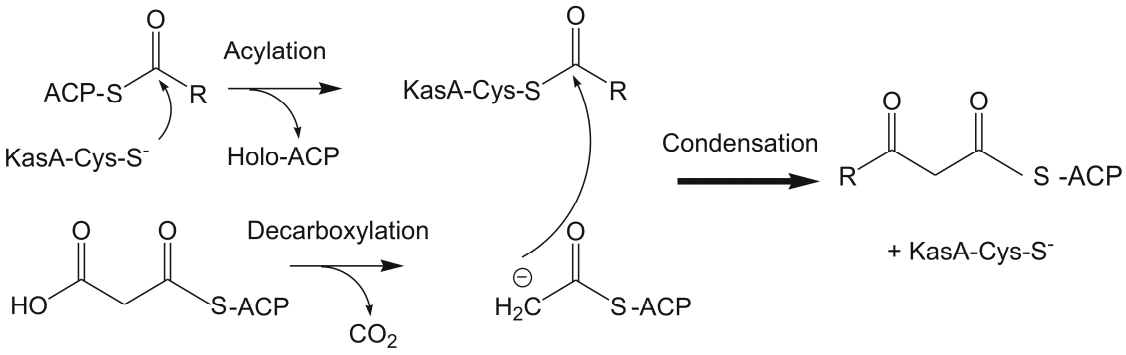

Figure 2: *Ping Pong Catalytic Mechanism for KasA active site acylation occurs by nucleophilic attack of the carbonyl carbon of acyl-Acp by the thiolate of Cys 171(KasA numbering). Dissociation of Holo-Acp and binding of the second substate, malonyl-Acp, is followed by decarboxylation and carbanion formation. Condensation and carbon-carbon bond formation occurs through the nucleophilic attack of the malonyl-AcpM carbanion on acyl-KasA thioester by the carbanion to form the β-keto acyl-AcpM product and free enzyme.*

In the first step the formation of the cysteine thiolate is assisted by an α-helix dipole(*6, 7*). The reactivity of the cysteine is promoted by its position at the N-terminal end of helix Nα3 lowering its pK and thereby increasing its nucleophilicity(*6*). The decarboxylation of malonyl-Acp and subsequent formation of a carbanion is assisted by two active site histidines (*7, 8*). Nucleophilic attack of the acyl-enzyme thioester and carbon-carbon bond

formation is promoted by stabilization of the negative charge in the thio oxide tetrahedral intermediate by an oxyanion hole formed by the backbone amides of C163, F 392 in *E. coli* FabB (C171, F404 in KasA) (*9*).

KAS validation

The KAS enzymes are ubiquitously expressed in bacteria, plants and in human mitochondria (mtKAS). They have been shown to be essential in a variety of pathogenic and non-pathogenic organisms. In many bacteria including *E. coli*, *Streptococcus pneumoniae(10), S. aureus (11, 12),* and *P. falciparum* (*13*) as well as in plants the KAS-I and KAS-II enzymes are referred to as FabB and FabF, respectively. In mycobacteria however KAS-I and KAS-II are known as KasA and KasB, respectively(*14, 15*).

KasA has been shown to be essential in mycobacteria by showing that conditional depletion of KasA induces cell lysis (*16*). In this study Jacobs *et al.* developed CESTET or *c*onditional *e*xpression and *s*pecialized *t*ransduction *e*ssentiality *t*est to confirm the essentiality of KasA(*16*). The genetic tool combines conditional gene expression (where gene expression is dependent on an outside stimulus), with specialized transduction (transfer of a specific segment of DNA), allowing the generation of a conditional null *kasA* mutant.

This technique overcame the inability to generate *kasA* deletion mutants (also suggesting KasA is essential) by utilizing an acetamidase promoter to express KasA during transductant generating experiments. Although KasA inhibitors are not used in the clinic, many KAS inhibitors have shown efficacy against TB (*17*) and other pathogens (*11, 12*) further validating its essentiality and making it an attractive target for drug discovery.

Isoniazid Target Controversy

In addition to the validation of KasA as a target for anti-microbial chemotherapy development, it has also been suggested that KasA is involved in the complex anti-microbial action of frontline drug INH. Barry and colleagues purified an 80kDa covalent complex containing KasA, INH and AcpM (mycobacterial Acp) from INH treated mycobacteria(*15*). Additionally, the formation of this complex correlated with the accumulation of hexacosanoic acid (C26) consistant with KasA inhibition and KasA mutations in patient isolates resistant to INH occurred at a frequency of 5-20 %(*14, 15*). Taken together these data highlight the complexity of INH activity and suggest that KasA is involved in the anti-microbial mechanism of INH either directly or indirectly. Curiously, Tonge and colleagues (*18*) showed that mutations in InhA that correlate with drug resistance have the same affinity for the active drug as *wild-type,* showing that decreased affinity of the drug for

the target cannot explain the resistance mechanism(*18*). It is suggested that these data can only be explained in the context of the interactions within the high molecular weight FAS-II complex first purified by Bloch and colleagues (*19*) and now shown to contain InhA, MabA and KasA(*20*). If the interactions within the complex have a functional effect on the catalytic activity of the individual enzymes, this may be the context that one would explain the apparently conflicting proposals for the *in vivo* activity of INH. *In vitro* reconstitution of the FAS-II pathway to test this hypothesis will require an efficient source of each component enzyme and a deep understanding of the enzyme's *in vitro* activity. KasA being at the center of the INH target controversy combined with its validation as an essential enzyme has made it an alluring target for further studies and for our anti-TB compound development program.

Thiolactomycin; a lead molecule for antimicrobial drug discovery

Thiolactomycin (TLM), (Figure 4) a natural product thiolactone isolated from Nocardia sp., is a selective and reversible FAS-II inhibitor that is known to inhibit KAS enzymes(*7, 21*). TLM has activity against both gram positive and gram negative bacteria(*22, 23*) as well as MTB (MIC 62.5 μM)(*17, 24*), but does not inhibit the mammalian FAS-I enzyme(*25*). The specificity of TLM for the bacterial ketoacyl synthases coupled with its moderate antibacterial

activity and low toxicity in rats, make it an attractive lead compound for anti-microbial drug discovery(*26*). TLM resistant *E. coli* strains contain mutations in the *fabB* gene(*27*) and overproduction of FabB confers TLM resistance *in vivo* (*28*) suggesting that FabB is the major cellular target. Based on kinetic and structural data, TLM is thought to be a competitive inhibitor of malonyl-Acp (*7, 29*). Previous investigators have reported a range of IC_{50} values for the inhibition of KAS enzymes by TLM that appear to depend on the assay conditions that are used(*30, 31*). Curiously, TLM has been shown to be a competitive inhibitor of the pea KASIII at low concentrations but an uncompetitive inhibitor at high concentrations(*32*). This complex kinetic behavior has been suggested to result from the "poor fit of TLM in the active site" with a reported IC_{50} value of 0.7mM(*32*). In a direct binding fluorescence titration experiment, *E. coli* FabF showed a higher K_d than expected based on measured IC_{50} values (*7*). These data indeed show that the TLM inhibition mechanism is "complex" but lack a clearly defined model for TLM binding.

The first synthesis of TLM was reported in 1984, and modern synthetic routes have subsequently been developed for this compound, thus increasing the likelihood that TLM could be optimized as a lead compound for anti-TB drug discovery(*33-35*). A recently published SAR study revealed the essential role of the 5 position isoprene for the inhibition of the MTB KasA enzyme by TLM (*24*). The synthetic routes to TLM are discussed in depth in Chapter 4 as it relates to our rational drug design and SAR efforts.

KAS Inhibition and the Acyl-enzyme Intermediate

A recently discovered natural product, platencimycin (Figure 4), is a potent and selective KAS inhibitor with broad spectrum activity against gram positive bacteria (*11*). Wang *et al* (*11*) demonstrated that platencimycin bound with higher affinity to the covalent acyl-enzyme intermediate of FabF rather than to the free enzyme. They analyzed the interaction of platencimycin with an *E. coli* FabF mutant in which the active site cysteine is replaced by a glutamine, based on the proposal that this replacement mimics the structural changes associated with acylation and due to the increased decarboxylation activity of the mutant enzyme(*36*).

Based on the observation that several modular polyketide KAS domains possess a cysteine to glutamine mutation (abrogating KAS activity) and the observation that active site cysteine modification with iodoacetamide increased the uncoupled malonyl decarboxylase activity of yeast and fungal type-I FASs (a structurally similar modification); Witkowski *et al.* showed that a Cys to Gln mutation indeed mimics the acyl-enzyme intermediate. In this study they showed that C161Q (*E. coli* FabB numbering) had an increase in decarboxylation activity by 2 orders of magnitude. Additionally, they showed that the structural change mimicked the interaction of the carbonyl oxygen of the acyl-enzyme thioester with the backbone amides in the oxyanion hole.

The similarity of the *WT* acyl-enzyme, mutant, and iodoacetamide modified structures are shown in Figure 3. The role of the oxyanion hole in increasing the acyl-enzyme thioester's susceptibility to nucleophilic attack renders this structure particularly unstable to base catalyzed hydrolysis. The mutant and iodoacetamide modification are highly stable acyl-enzyme mimics and allow for studies where long term stabilization of the wild type acyl-enzyme thioester is unrealistic (*i.e.* crystallography, and mass spectrometry)

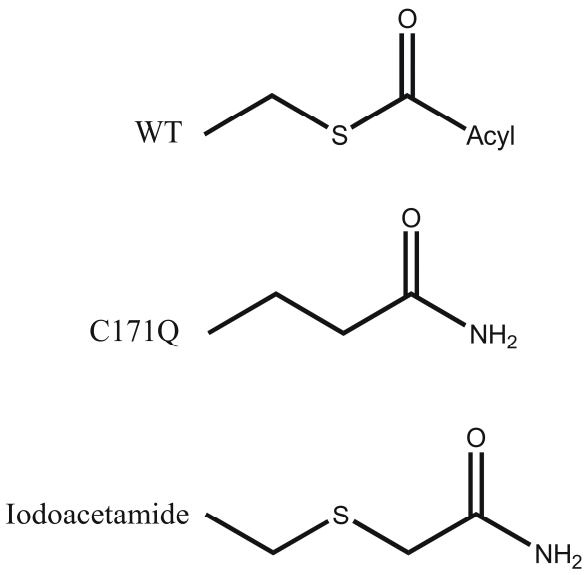

Figure 3: *KAS active site structural modifications (KasA numbering)*

Cerulenin, which is also a natural product, irreversibly modifies uncomplexed KAS enzymes via the formation of a covalent adduct with the active site cysteine. The development of cerulenin as a drug has not been widely pursued due the lack of specificity of the compound which inhibits both

the bacterial FAS-II as well as the eukaryotic FAS-I ketoacyl synthases(*37*). These KAS inhibitors are shown in Figure 4.

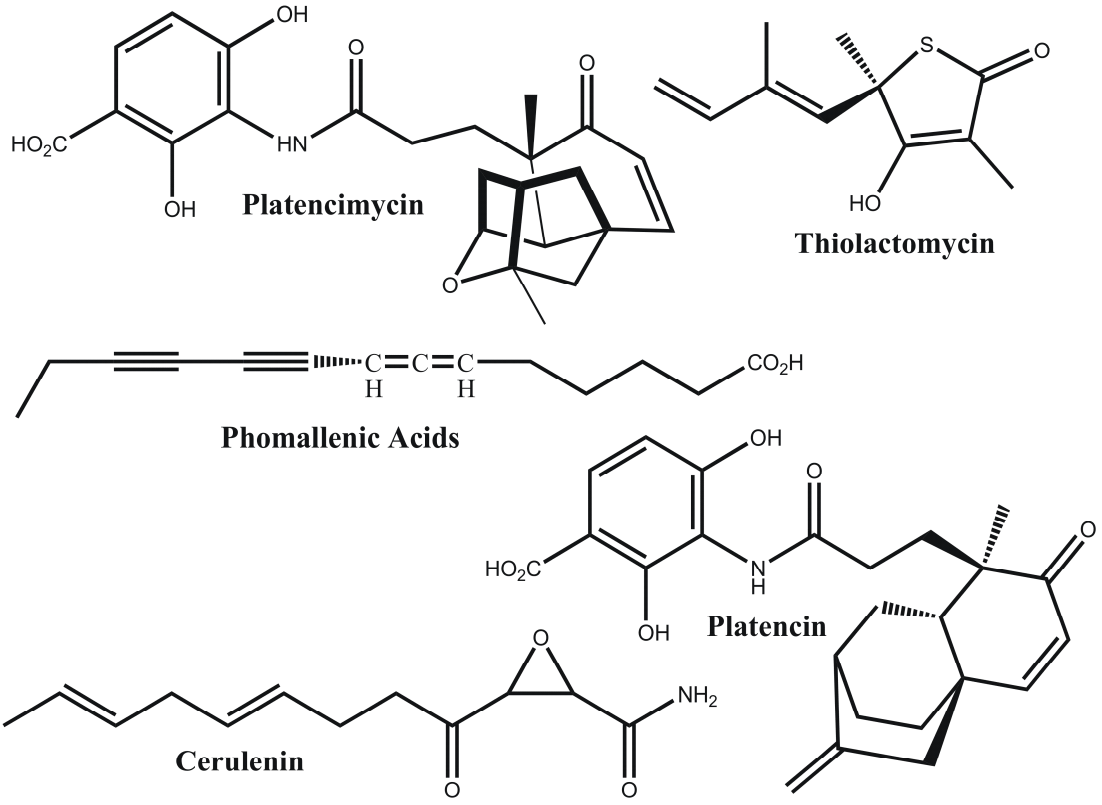

Figure 4: *Structures of KAS inhibitors*

KasA Characterization and TLM Inhibition Mechanism

In order to direct the synthesis of additional TLM analogues, we undertook a detailed analysis of KasA inhibition by TLM. Soluble KasA was obtained using *M. smegmatis* as an expression host in order to overcome solubility issues when the protein is expressed in *E. coli*(*38*). While CoA-based

substrates are commonly used in assays of other FAS-II enzymes, these substrates are inactive with KasA, mitigating the preparation of substrates based on the mycobacterial AcpM carrier. Assays conducted with the AcpM-based substrates together with direct fluorescence binding experiments have provided a detailed understanding of the interaction of TLM with KasA, and have shown that TLM preferentially binds to the acyl-enzyme intermediate of KasA. In addition, we have shown that TLM is a slow-onset inhibitor of the KasA acyl-enzyme but not the apo-enzyme. The C171Q KasA mutant, that is thought to mimic the acyl-enzyme, also shows more potent slow-onset inhibiton relative to wild-type apo enzyme.

These data serve to explain complexities found in the literature and may also explain why structure based inhibitor design based on the lower affinity TLM apo-enzyme structure has been unsuccessful. Our extensive efforts to understand the fundamental structural difference between the high affinity TLM acyl-enzyme complex and the low affinity TLM apo-enzyme complex, as an extension of our TLM-KasA biochemical experiments and to aid in our own structure based inhibitor design, are discussed in depth in Chapter 3.

MATERIALS AND METHODS:

Materials

CoA substrates were purchased from Sigma, and PCR and mutagenesis primers were purchased from Integrated DNA Technologies (IDT). Precast SDS-PAGE gels, columns and resins were purchased from Bio-Rad. pET expression vectors were purchased from Novagen and restriction enzymes and buffers were purchased from New England Biolabs (NEB). TLM purified from Nocardia was generously provided by Cynthia Dowd, and Clifton Barry III (NIAID). Buffers, growth media and other reagents were purchased from Fisher Scientific. We thank Dr. Scott Franzblau at the Institute for Tuberculosis Research, University of Illinois for a gift of the pFCPA plasmid.

KasA Expression and Purification

The KasA gene was initially PCR amplified from genomic DNA and inserted into an *E. coli* expression vector (pET28a(+)) as described previously (*38*). Subsequently, the KasA gene was subcloned into the mycobacterial expression vector pFPCA(*39*) following PCR amplification using the forward and reverse primers shown in table 1 and digestion with the BglII and EcoRI

restriction enzymes so that the gene was in frame with a N-terminal His tag. The BglII digestion site yields an identical overhang to that of BamHI facilitating proper ligation into the target vector.

Table 1: *KasA Cloning Primers*

Forward	5`-GGAAGATCTGGAGGATAACAAAGATGGG-3`
Reverse	5`-CCGGAATTCTCAGTAACGCCCGAAGGCA-3`

Plasmid was isolated from *E. coli* XL1-Blue cells and transformed into *Mycobacterium smegmatis* strain mc^2155 competent cells by electroporation at 2.5kV, 25μF, and 720Ω with a 20ms time constant using 2 μL vector (160μg/mL) and 200 μL of competent cells. Colonies were selected using 7H10 solid media containing 30μg/mL kanamycin, 200μg/mL ampicillin and 15 μg/mL cyclohexamide. Kanamycin resistance is conferred by the aminoglycoside transferase, *aph*, gene encoded by the pFPCA vector while the *M. smegmatis* strain itself is resistant to ampicilin and cyclohexamide(*40*). These antibiotics prevent contamination by other commonly used *E. coli* strains whose short doubling time relative to *M. smegmatis* (20 minutes versus 4 hours(*41*)) make sterile growth conditions a particularly important technical concern.

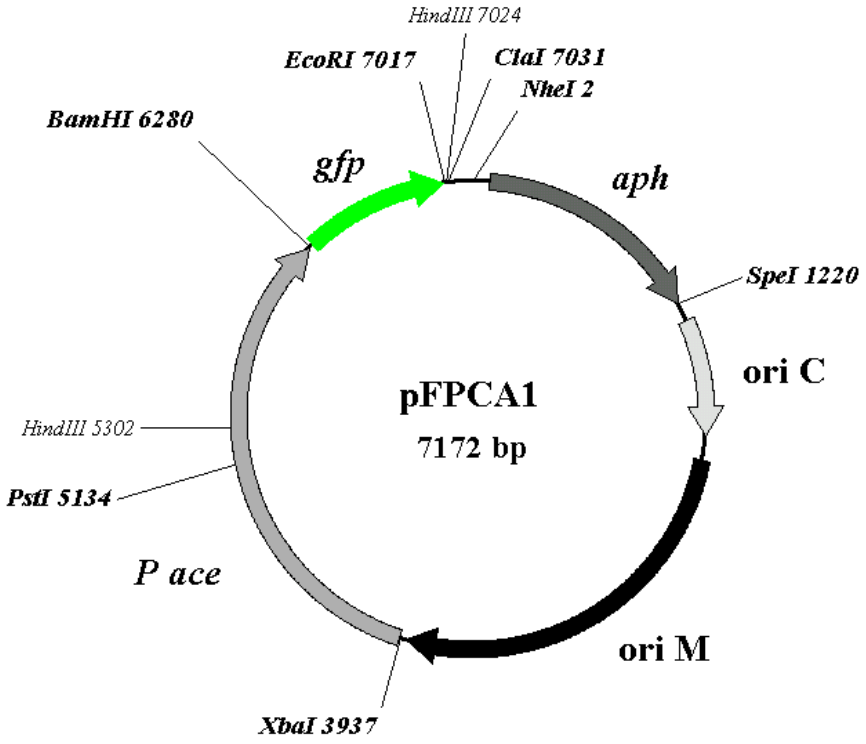

Figure 5: *pFPCA1 vector; origins of replication for both M. smegmatis (ori M) and E.coli (ori C), acetamidase promoter (P ace), kanamycin resistance gene aminoglycoside phosphotransferase (aph) and multiple cloning sites are illustrated. The GFP gene insert was excised by digestion with BamHI and EcoRI and the KasA gene was inserted*

Individual *M. smegmatis* colonies were cultivated using 7H9 liquid media supplemented with glycerol, grown to an optical density (OD_{600}) of 0.6-0.8 and protein expression was induced with 0.2% acetamide. Cells from a 2 L culture were harvested by centrifugation and lysed by sonication. The KasA protein

was subsequently purified using standard Ni affinity chromatography (7 mL column) followed by chromatography on G-25 resin (1x50 cm column) using 50mM NaPO4, pH 8.5, 0.3M NaCl as the eluent.

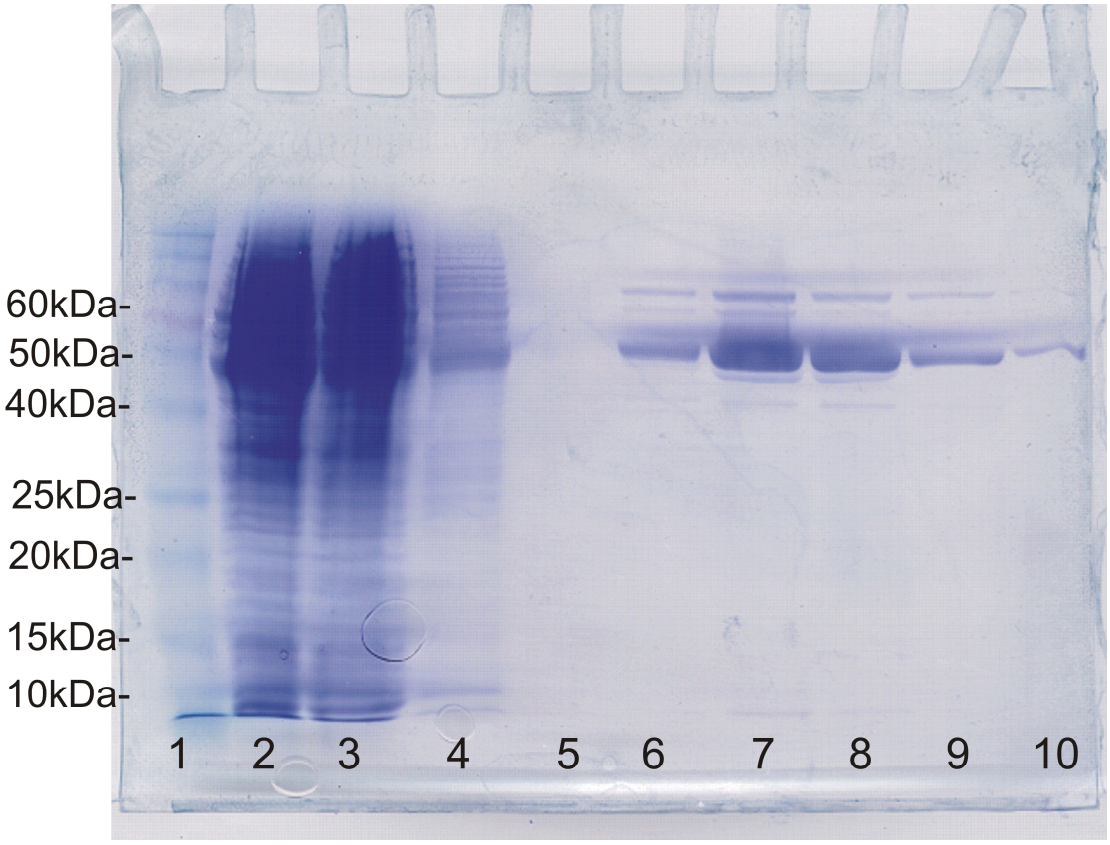

Figure 6: *12% SDS-PAGE gel of KasA His-Tag purification profile.*

Legend for Figure 6	
Lane	Sample Description
1	Invitrogen Benchmark Protein Standard
2	overexpressed KasA in *M. smegmatis* (mc^2155) cell free extract
3	Column Flow-through (5mM imidazole, 0.5M NaCl, 20mM Tris pH 7.9)
4	Column wash (60mM imidazole, 0.5M NaCl, 20mM Tris pH 7.9)
5	Elution Fraction 1 (linear gradient from 5mM to 1M imidazole)
6	Elution Fraction 2 (linear gradient from 5mM to 1M imidazole)
7	Elution Fraction 3 (linear gradient from 5mM to 1M imidazole)
8	Elution Fraction 4 (linear gradient from 5mM to 1M imidazole)
9	Elution Fraction 5 (linear gradient from 5mM to 1M imidazole)
10	Elution Fraction 6 (linear gradient from 5mM to 1M imidazole)

AcpM Expression and Substrate Synthesis

The mycobacterial acyl carrier protein (AcpM) was cloned, expressed and purified as previously described(*38*). Briefly, pETacpM plasmid transformants were selected on kanamycin (30µg/mL) LB media and single colonies were cultivated to an OD_{600} of 0.8-1.0 and induced with 0.7 mM isopropyl thiogalactopyranoside (IPTG). Isopropyl alcohol (IPA) precipitation and anion exchange column chromatography yielded three forms of AcpM, apo, holo and acyl-AcpM. Subsequently, an AKTA FPLC protein purification system was used to obtain pure apo-ACPM from the modified forms of the protein. Fractions containing the three AcpM species were dialyzed into 20mM Tris

pH 8.0 buffer and injected in 2 mL volumes onto a Mono Q 10/100 GL column (GE healthcare) which had been equilibrated with 20mM Tris pH 8.0. Elution of the different AcpM species was achieved using a shallow linear gradient of NaCl. Apo-ACPM eluted at 320 mM NaCl.

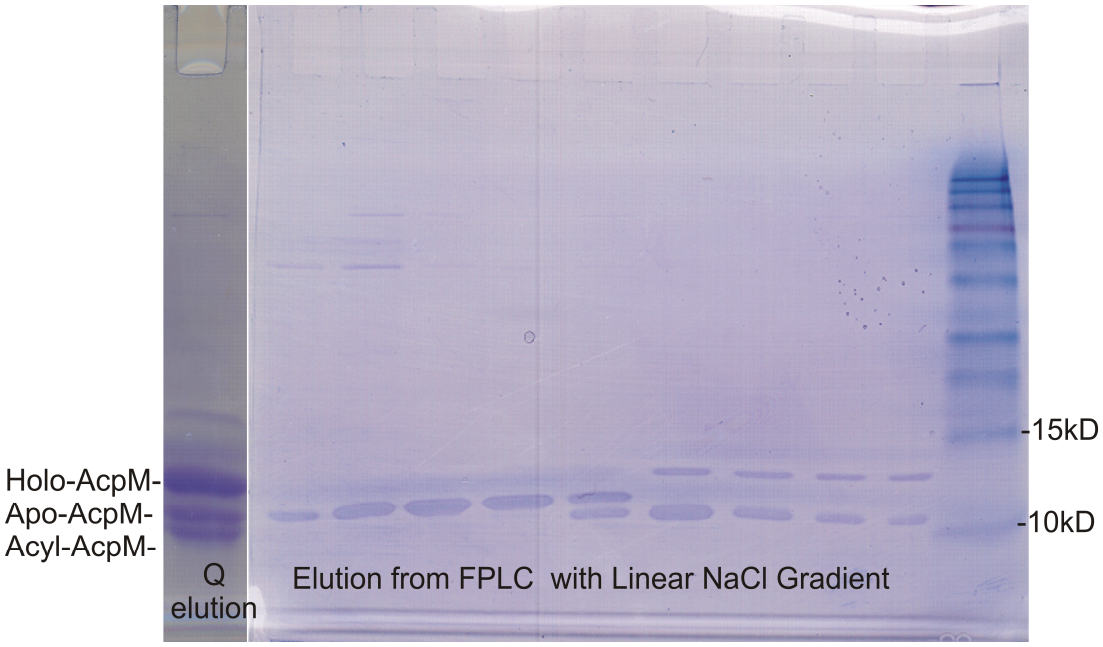

Figure 7: *15% SDS-PAGE gel; Initial Q-column elution showing 3 AcpM isoforms, FPLC elution profile showing separation of fractions containing apo-AcpM and acyl/holo-AcpM mixture*

Homogeneous apo-ACPM was incubated in ACPS reaction buffer (50mM Tris, pH8.5, 25mM $MgCl_2$, 5mM $MnCl_2$, 1 mM DTT) with a 2 molar excess of

either malonyl-CoA or palmitoyl-CoA (Sigma) and 6μM holo-Acp synthase ACPS (purified as described below) for 90 minutes at 30°C. The final reaction mixture was exchanged into 20mM Tris pH 8.0 and purified by AKTA-FPLC ion exchange chromatography as described above. Malonyl-AcpM and palmitoyl-AcpM eluted at slightly higher NaCl concentrations than the apo form.

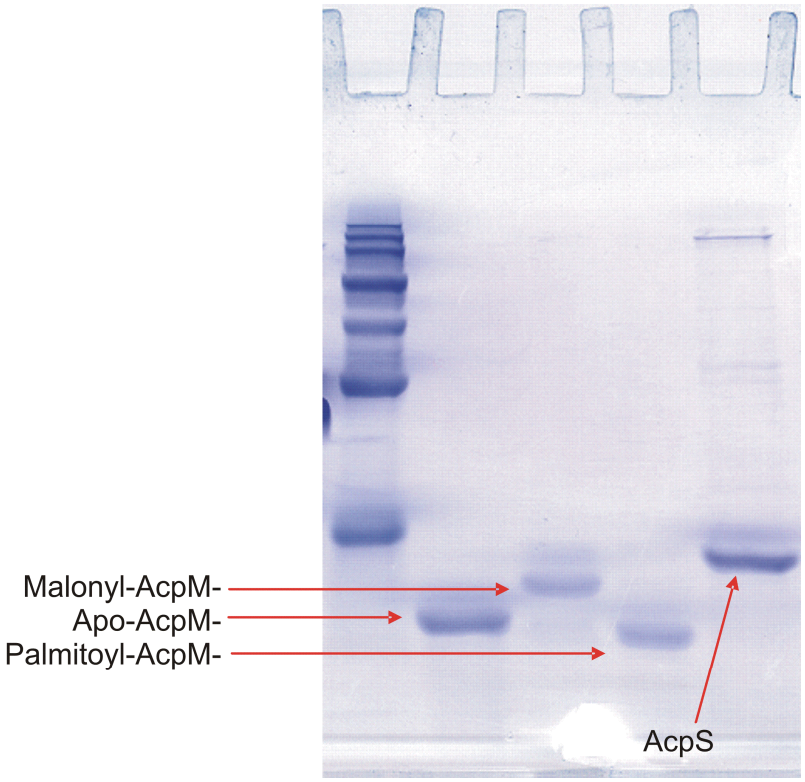

Figure 8: *Gel shift assay for AcpS activity; Confirms the synthesis of Malonyl-AcpM and Palmitoyl-AcpM substrates by a change in position on a 15% SDS-PAGE gel. Notice the position of Palmitoyl-AcpM is lower than would be expected based on molecular weight. This can be explained by the increased hydrophobic interaction of the palmitoyl chain with the SDS increasing the R_f value. (personal communication Dr. John Shanklin, BNL)*

The identity of apo-AcpM starting material and synthesized substrates was confirmed with electro-spray ionization (ESI) mass spectrometry (MS). Samples were exchange into DD-H_2O using a centricon concentrator and injected onto an ESI-MS in positive ion mode in 5-15µl volumes. ESI-MS spectra for apo-AcpM, malonyl-AcpM and palmitoyl-AcpM are shown.

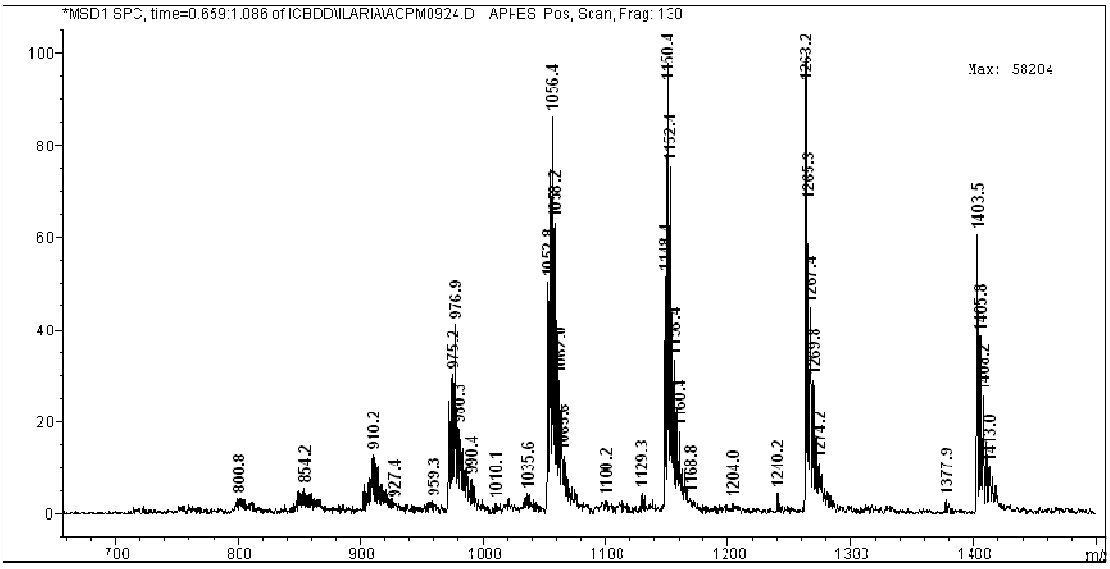

ESI-MS spectrum deconvolutes to 12,622 Da the exact mass of Apo-AcpM

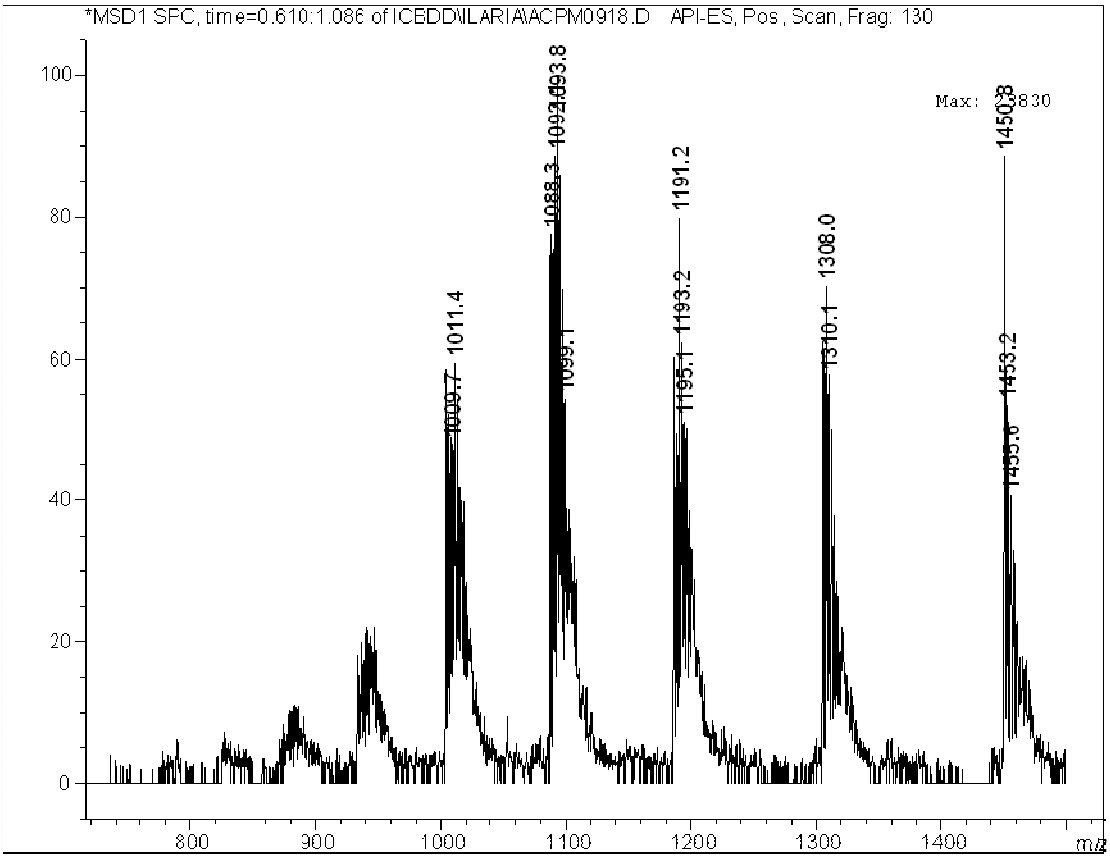

ESI spectrum deconvolutes to 13,048 Da the exact mass of malonyl-AcpM

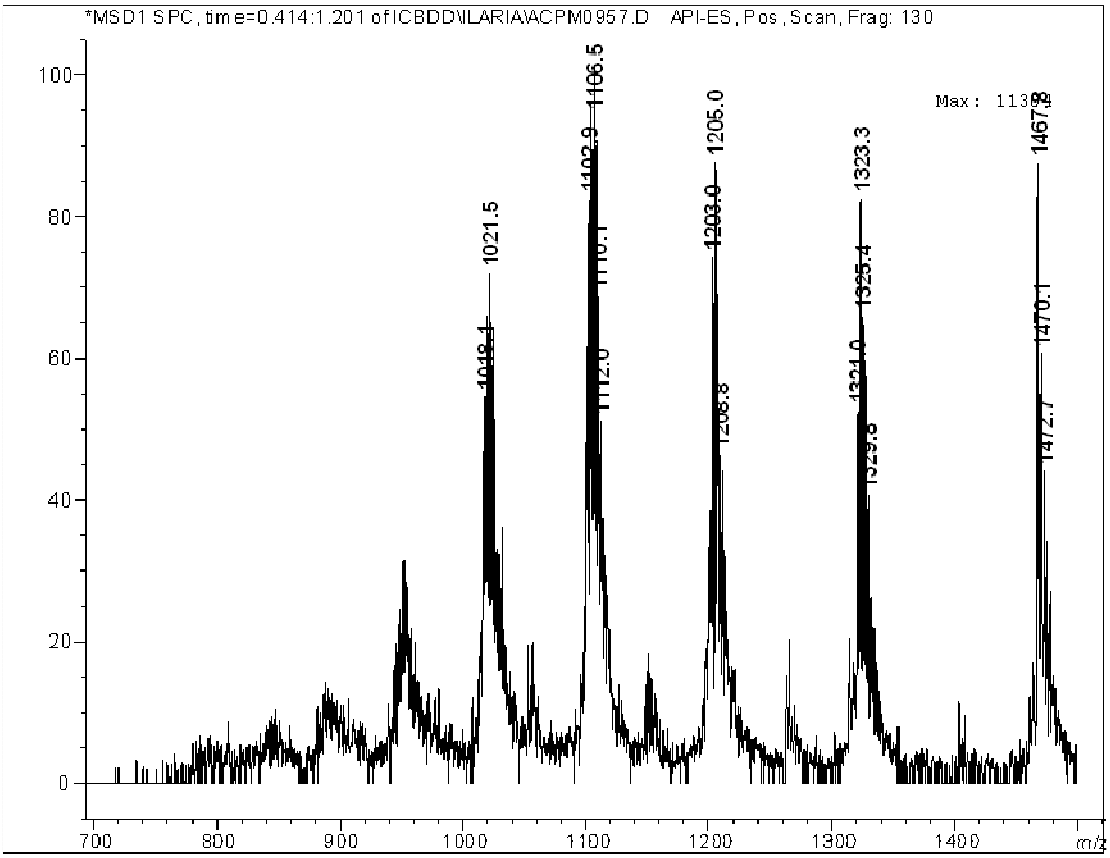

ESI spectrum deconvolutes to 13,200 Da the exact mass of palmitoyl-AcpM

Holo-ACP synthase

Holo-ACP synthase (ACPS) was cloned expressed and purified as described previously(*38, 42*). Briefly, transformants containing pET-AcpS were selected on solid LB-ampicilin (200 µg/ml) media and individual colonies were grown to an OD_{600} 0.8-1.0 on a 1L scale in YT media (1L H_2O, 16g Tryptone, 10g Yeast, 5g (85mM) NaCl, 2.4g (20mM) sodium phosphate). Cells were induced with 0.1 mM IPTG at 30°C for 3 hours. Cultures were harvested by centrifugation, resuspended in 50 mM Tris HCl pH 8.0 and lysed

by sonication. Cell free extract was gently mixed with 1 g DE-52 resin to form a slurry at 4°C for 15 minutes. DE-52 was removed by centrifugation and this step was repeated. Supernatant was adjusted to pH 6.5 with a saturated MES solution. This crude protein mixture was loaded onto an 8 ml SP-separose column (8cm X 1cm) equilibrated with 50mM Tris HCl pH 6.5. Pure ACPS protein was eluted with a linear gradient of NaCl and concentrated using a YM-10 centricon concentrator. Protein was stored at -20 °C or -80 °C with 10-50% glycerol. All samples retained Holo-AcpS transfer activity for over 2 years.

KasA Mutagenesis

The C171Q mutant of KasA was prepared using the Quikchange mutagenesis kit and with the forward and reverse primers shown in Table 2. After verifying the sequence of the plasmid by ABI sequencing, the C171Q KasA was expressed and purified as described above for the wild-type protein.

Table 2: *C171Q Mutagenesis Primers*

Forward	5'-ACCCCGGTGTCGGCCCAGTCGTCGGGCTCGGAA-3’
Reverse	5'-TCCCGAGCCCGACGACTGGGCCGACACCGGGGT-3’

KasA Assay

KasA activity was monitored using a continuous assay by coupling the reaction to the reduction of the product by MabA, the FAS-II β-ketoacyl-ACP reductase. MabA (purified as previously described(*43, 44*)) utilizes NADPH as the reductant enabling the reaction to be followed at 340 nm. MabA was expressed and purified from *E. coli* strain BL21-DE3 and purified by Ni affinity chromatography. Excess MabA (6μM) was used in the coupled assays to insure that this enzyme was not rate limiting. Reactions were performed in 50 mM Tris HCl, 1 mM DTT, at pH 8.5.

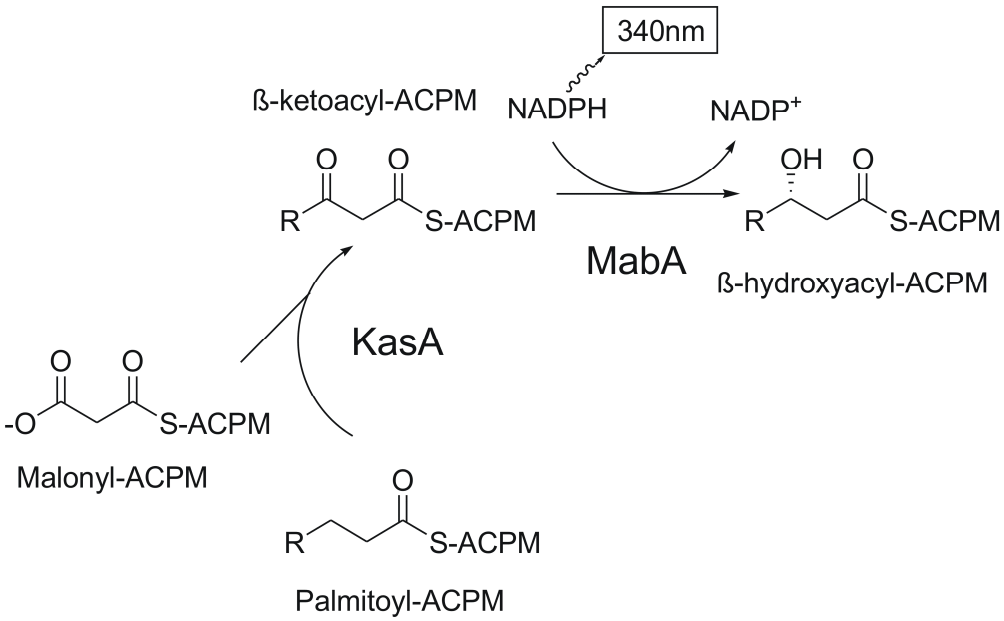

Figure 9: *Coupled assay for KasA activity. Oxidation of NADPH cofactor by coupling enzyme MabA is monitored at 340nm*

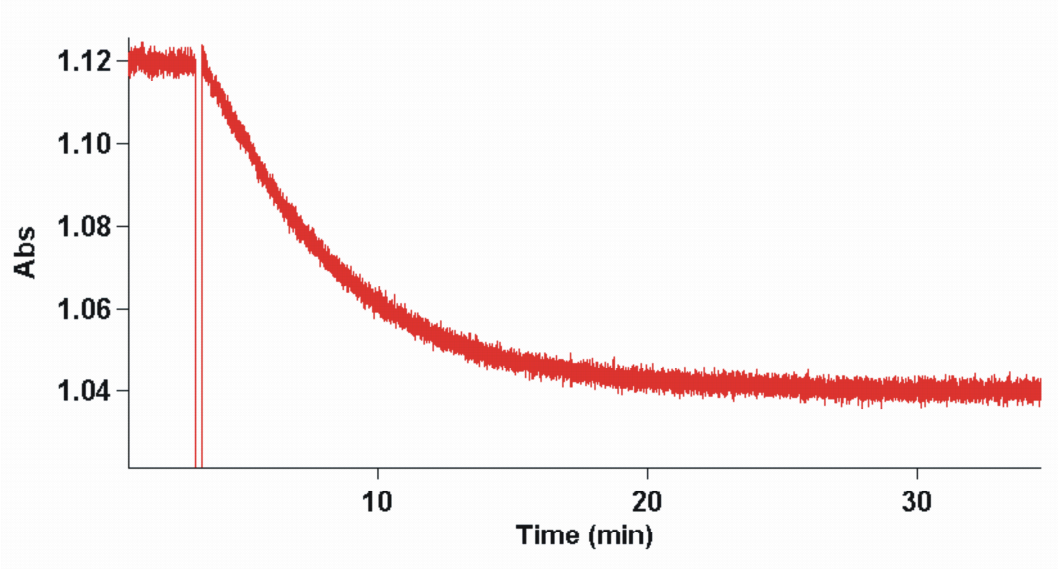

Figure 10: *340nm UV trace of the oxidation of NADPH by MabA coupling enzyme in the KasA kinetic assay; linear portion of curve used to calculate the initial velocity*

Thiolactomycin Inhibiton Assays

The IC_{50} values for KasA inhibition by TLM were determined using the above assay. Reactions mixtures contained 250 μM NADPH, 6 μM MabA, 15 μM of each substrate, and 90 nM KasA. Reactions were initiated by addition of one substrate to a cuvette containing the other components of the assay. In some cases, reactions were initiated immediately after adding TLM to the cuvette, whereas experiments were also performed having first preincubated TLM in the reaction mixture. Preincubation time was set to 15 minutes based

on the observation that TLM potency did not increase after 10 and 15 minute preincubation times. Data fitting was achieved using IC_{50} software in the enzyme kinetics program Grafit 4.0.

Direct Binding Fluorescence Experiments

A photon technology international (PTI) quanta master fluorimeter was used to monitor the intrinsic tryptophan fluorescence of KasA, acyl-KasA and C171Q mutant. Excitation and emission wavelengths were 280 and 337nm respectively with an excitation slit width of 4.0 nm and an emission slit width of 8.0 nm. TLM solutions in buffer (50 mM Tris pH 8.5, 1mM DTT) were titrated into 1 μM enzyme in the same buffer. All solutions were filtered and equilibrated to 25 ºC. Titration curves were corrected for inner filter effects and K_d values were calculated using the Scatchard equation (Grafit 4.0).

Slow Binding Kinetic Measurements

The fluorescence emission at 337 nm was monitored as a function of time in order to quantitate the slow-onset binding of TLM to acyl-KasA and the C171Q KasA mutant. Aliquots of TLM were added to 1 μM KasA in filtered buffer (50 mM Tris pH 8.5, 1 mM DTT) at 25 ºC and the fluorescence signal

was monitored for 35 minutes. Fluorescence intensities were fit to a double exponential to account for a slight decrease in background (Equation 1) (*45*).

$$y = Ae^{-k_{(obs)}t} + Be^{-k_{(2)}t} \quad (1)$$

The values of k_{obs} obtained from the exponential fitting were dependent on the concentration of TLM and were subsequently fit to equation 2 to extract values for K_i, the dissociation constant of the initial enzyme-inhibitor complex (EI), as well as k_1 and k_2, the forward and reverse rate constants for conversion of EI to the final enzyme-inhibitor complex (EI*) (Scheme 1)(*18, 46, 47*).

$$k_{obs} = k_2 + k_1 [I] / (K_i + [I]) \quad (2)$$

Subsequently, K_i*, the overall dissociation constant of the final EI* complex, was calculated using equation 3(*18, 46, 47*).

$$K_i^* = K_i / (1 + (k_1/k_2)) \quad (3)$$

Holo-ACP Phosphodiesterase ACPH

The *E. coli* holo-ACP phosphodiesterase (ACPH) was cloned expressed and purified in order to increase the efficiency of AcpM substrate production, that is the ACPM mixture (apo, holo, acyl) could be converted to one form increasing the yield of apo-ACPM. The recently discovered AcpH (*43, 44*)(annotated *yajB*) was PCR amplified from *E. coli* genomic DNA using forward and reverse primers shown in Table 3.

Table 3: *AcpH Cloning Primers*

Forward	5'-CTAGCTAGCATGAATTTTTTAGCTCACCTGCA-3'
Reverse	5'-CGGGGATCCTTATAACGCCTTGCGTGACGCC-3'

The PCR amplified gene was subcloned into NheI and BamHI restriction sites resulting in an in frame N-terminally His-tagged *AcpH* gene. The protein was over-expressed using *E. coli* pLysS and purified using standard Nickel affinity chromatography. The purified protein showed an R_f values on an SDS-PAGE gel consistent with a calculated mass of 22,961Da (data not shown). The AcpH gene product was tested for activity using holo-AcpM in previously reported reaction conditions and assayed with the above described SDS-PAGE gel shift assay. The enzyme was repeatedly shown to be

inactive. The project was abandoned after attempts to change the enzyme reaction conditions were unsuccessful.

MALDI-MS peptide fragment analysis with KasA

Recombinant KasA was digested overnight with trypsin using standard in gel digestion. Protein tryptic digest was analyzed with a Bruker Autoflex II MALDI-TOF mass spectrometer. Protein fragment sample was mixed with α-hydroxycinnamic acid as matrix and peptide masses were determined in the reflectron mode with external calibration. The mass spectrum is displayed below.

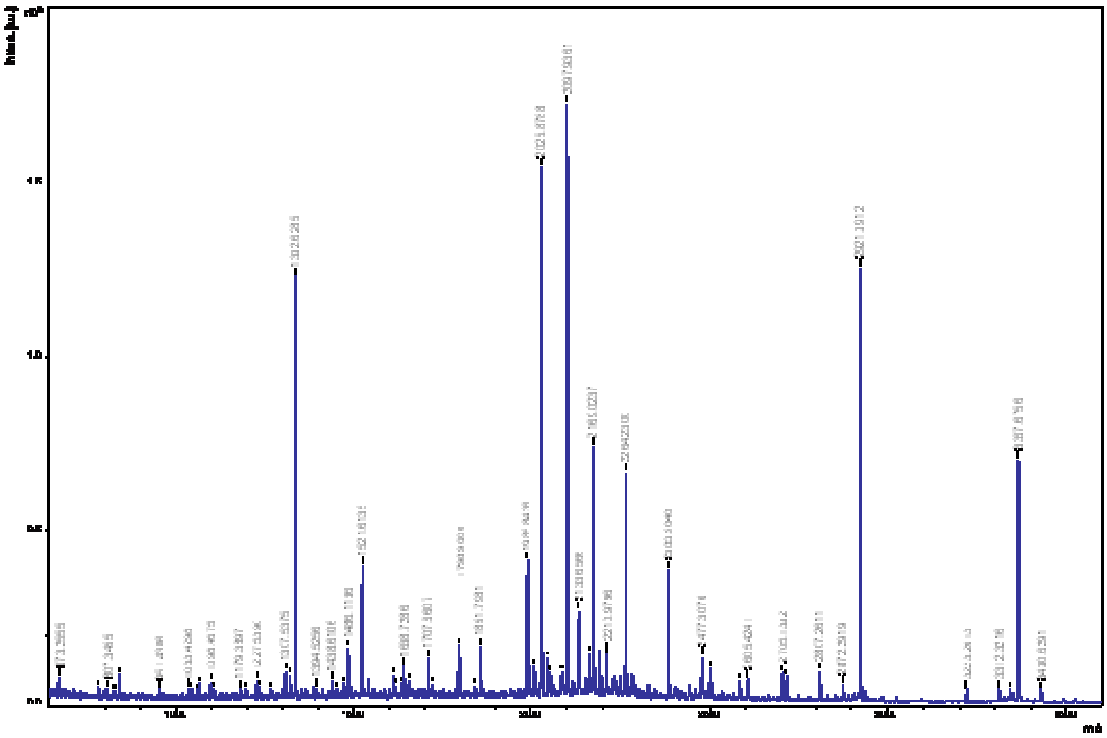

Sequence of recombinant KasA is shown below; peptide coverage shown in red. Blue peptide sequence falls outside of the MS tolerance of 120ppm. Sequencing results identify protein as KasA.

MGSSHHHHHHSSGLVPRGSHMSQPSTANGGFPSVVVTAVTATTSISPDIESTWK**GLLAGES**
GIHALEDEFVTKWDLAVKIGGHLKDPVDSHMGRLDMRR**MSYVQR**MGK**LLGGQLWESAGS**
PEVDPDRFAVVVGTGLGGAERIVESYDLMNAGGPRKVSPLAVQMIMPNGAAAVIGLQLGA
RAGVMTPVSACSSGSEAIAHAWRQIVMGDADVAVCGGVEGPIEALPIAAFSMMRAMSTRN
DEPER**ASRPFDK**DR**DGFVFGEAGALMLIETEEHAKARGAKPLARLLGAGITSDAFHMVAP**
AADGVRAGRAMTR**SLELAGLSPADIDHVNAHGTATPIGDAAEANAIR***VAGCDQAAVYAPK***
SALGHSIGAVGALESVLTVLTLRDGVIPPTLNYETPDPEIDLDVVAGEPRYGDYRYAVNNSF
GFGGHNVALAFGRYN

LC-MS analysis of KasA

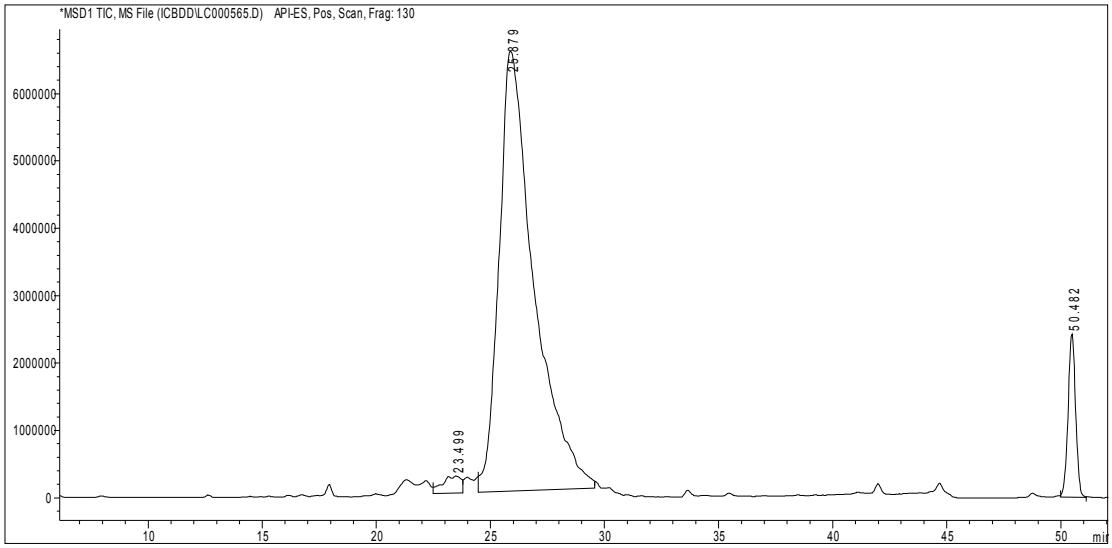

LC/MS chromatogram with TIC (m/*z* =300-1500) detection

Averaged mass spectra for the peak at R_t = 25.8min

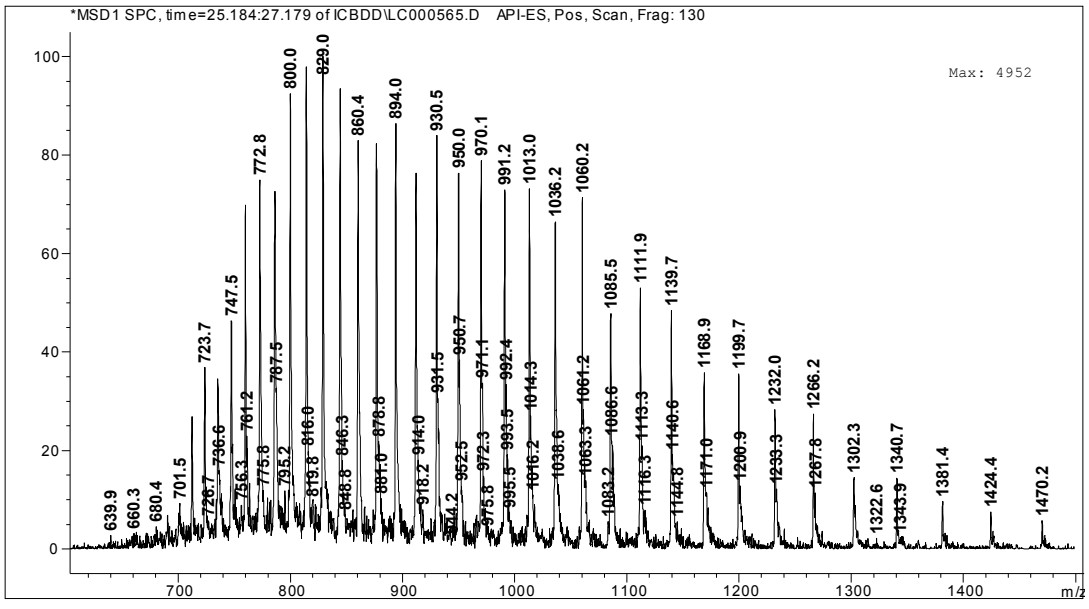

The spectral deconvolution of this data gives a MW = 45548 ± 2 Da similar to the calculated MW for recombinant his-tagged KasA of 45561.

RESULTS:

KasA from an M. smegmatis host and AcpM substrates

Solubility issues with heterologously expressed proteins are common, especially among mycobacterial proteins and KasA overexpression in *E.coli* was no exception(*38*). Multiple methods commonly used to increase the yield of soluble protein were used with the expression of KasA in *E. coli*. Among them were reduced induction temperatures, multiple inducer concentrations, fusion protein constructs, co-expression with proteins that share the kas operon, and osmotic stress. Despite our extensive efforts, soluble KasA remained elusive. We therefore expressed KasA as an N-terminally His tagged construct in *Mycobacterium smegmatis*, a non-pathogenic, relatively fast growing soil mycobacterium. Our working hypothesis was that the similarity between *M. tuberculosis* and *M. smegmatis* (93% among KAS enzymes) may make *M. smegmatis* a more suitable host for heterologous expression of KasA(*48*). Additionally the bacteria share a similar cell wall structure and overall morphology (Figure 11)(*15, 17*).

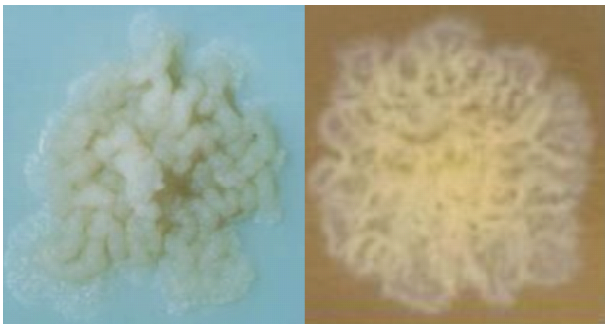

Figure 11: *M. tuberculosis (blue) and M. smegmatis (brown) showing similar mycobacterial morphology*

The purified product gave a band on an SDS-PAGE gel consistent with the calculated molecular weight of recombinant KasA of 45 kDa. The peptide sequence of the recombinant product was also confirmed by trypsin digestion, MALDI-MS and peptide fragment analysis. LC-MS analysis showed a MW= 45548. This value compares well to the calculated MW of 45561.

Coenzyme-A based substrates used for activity assays with other FAS-II enzymes are inactive with KasA (data not shown) and rather than using a discontinuous radiolabeling assay, which is both costly and less sensitive, we turned to an assay system based on the natural mycobacterial acyl carrier protein (AcpM) substrate described previously(*38*). A continuous spectrophotometric coupled assay was used with the NADPH dependent β-ketoacyl-Acp reductase enzyme MabA utilized as a coupling partner. The

natural malonyl-AcpM and palmitoyl-AcpM substrates were synthesized from apo-AcpM using the *E. coli* holo-ACP synthase enzyme and the appropriate CoA substrate as previously described(*38*).

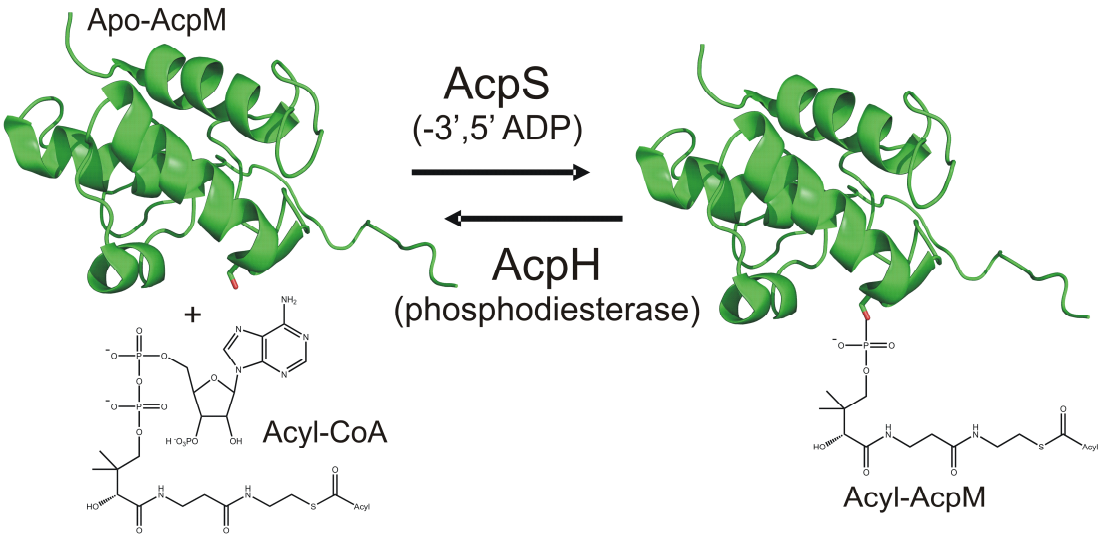

Figure 12: *Reaction catalyzed by AcpS used to synthesize AcpM based substrates from apo-AcpM and CoA for KAS activity assays.*

Kinetic values for KasA compare well to previously reported data (Table 4) with a modest 6 fold increase in k_{cat}. This increase may be explained by the use of AcpM rather than the more easily obtainable *E. coli* Acp substrates which are less active with KasA(*38*).

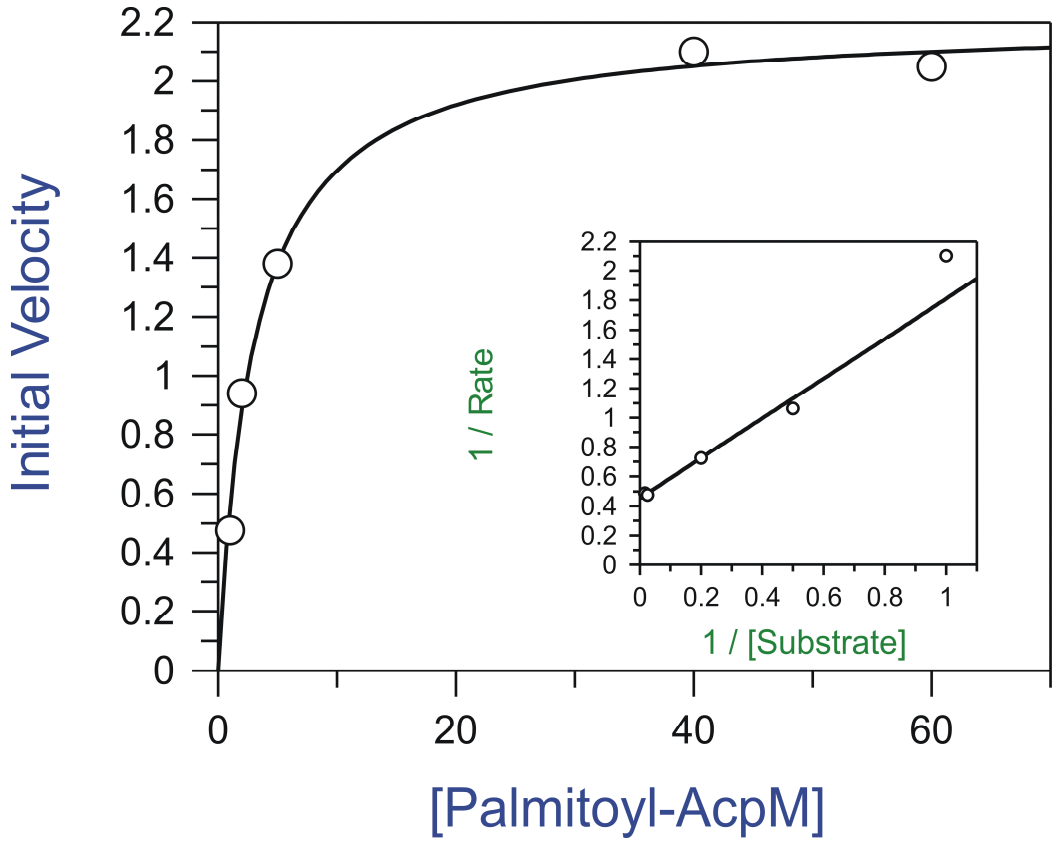

Figure 13: *Kinetic data for KasA activity varying Palmitoyl-AcpM with respect to 54 µM Malonyl-AcpM*

Table 4: *Kinetic Parameters for the KAS activity of M. tuberculosis KasA*

	K_m (µM)	k_{cat} (min^{-1})	k_{cat}/K_m (M^{-1} min^{-1})
Palmitoyl-$Acp_{(E.Coli)}$[a]	3.2 ± 0.3[b]	5.3 ± 0.1	1.7 X 10^6
Palmitoyl-AcpM	2.9 ± 0.6[c]	32 ± 2.0	1.1 X 10^7

a: Previously reported data (*38*)

b: with respect to 54 µM Malonyl-$Acp_{(E. coli)}$

c: with respect to 54 µM Malonyl-AcpM

With a working kinetic assay, we set out to determine the IC_{50} value for TLM with KasA. This experiment revealed that pre-incubation with the acyl form of the enzyme was required for TLM potency. When the reaction is initiated with KasA an IC_{50} value greater than 200 μM is observed with our kinetic assay. This value is not consistent with the values of 14 μM(*24*) and 20 μM (*38*) published previously. The IC_{50} values were then determined following pre-incubation of TLM and KasA followed by initiation of the reaction with one or other of the two substrates. The IC_{50} value determined when palmitoyl-AcpM was added to an incubation mixture containing KasA, TLM and malonyl-AcpM was 242 μM. However, when the reaction was initiated with malonyl-AcpM following preincubation with palmitoyl-AcpM, the observed IC_{50} value was 19 μM. These data suggest that TLM is binding with a higher affinity to the acyl-enzyme form of KasA. A similar result was reported recently with platencimycin, a potent and selective natural product inhibitor of the acyl intermediate form of FabF (KASII *E. coli*). (*11*)

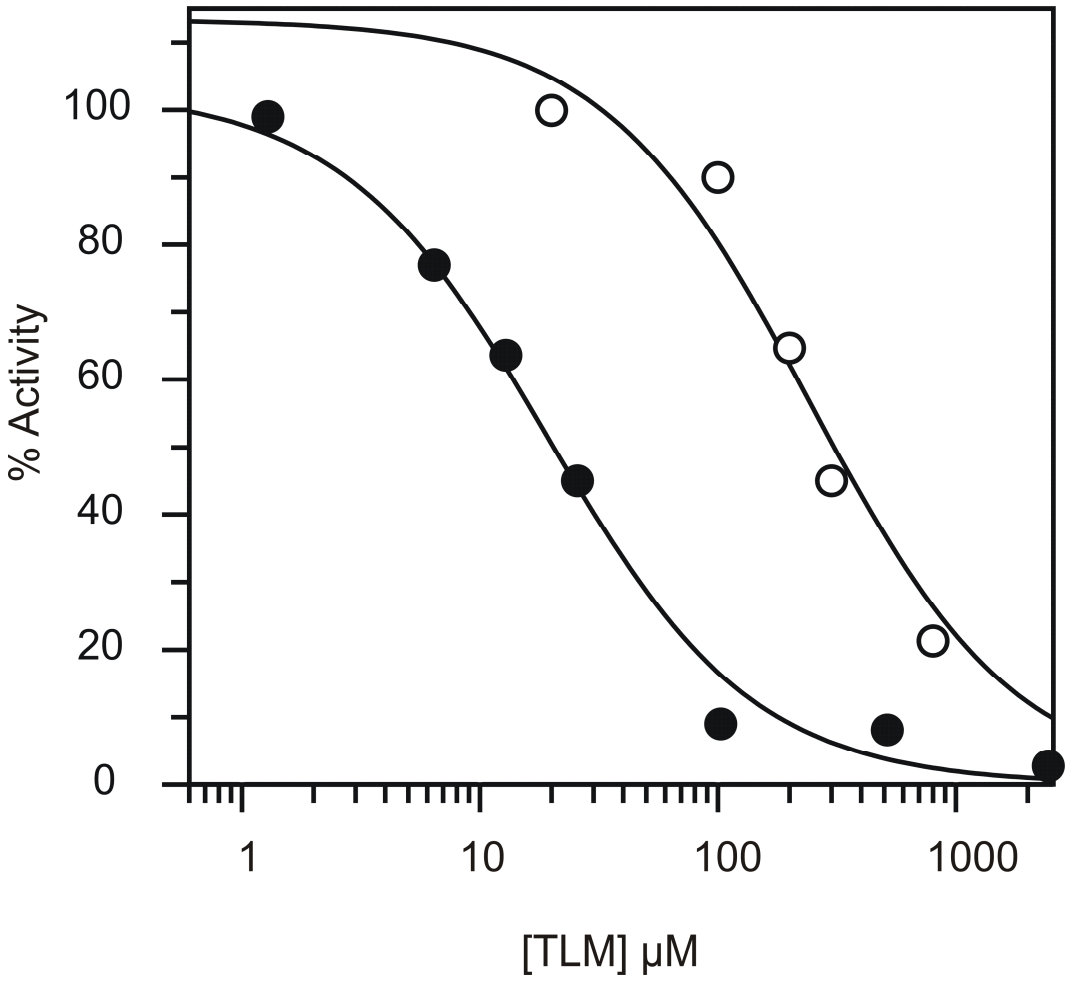

Figure 14: *Overlay of IC_{50} data for TLM. Filled circles; reaction initiated with Malonyl-AcpM IC_{50}=19 ± 2 µM. Open circles; reaction initiated with Palmitoyl-AcpM IC_{50}= 242 ± 60 µM.*

Direct Binding Experiments

The effect of palmitoyl-AcpM on the IC_{50} value for enzyme inhibition was only observed when TLM was preincubated with the enzyme. Since the palmitoyl-KasA acyl-enzyme is expected to form rapidly, this observation suggests that there is a slow-onset component to the interaction of TLM with acyl-KasA. This phenomenon was further examined using a direct binding experiment in which the intrinsic tryptophan fluorescence of KasA was used to measure the affinity and slow rate of binding of TLM to KasA. Interaction of TLM with KasA results in a decrease in fluorescence which we speculate is due to alterations in the environment of W182, a tryptophan residue that lies at the base of the active site α-helix in KasA, according to a comparison of the KasA sequence to the KasB crystal structure(*6, 49*).

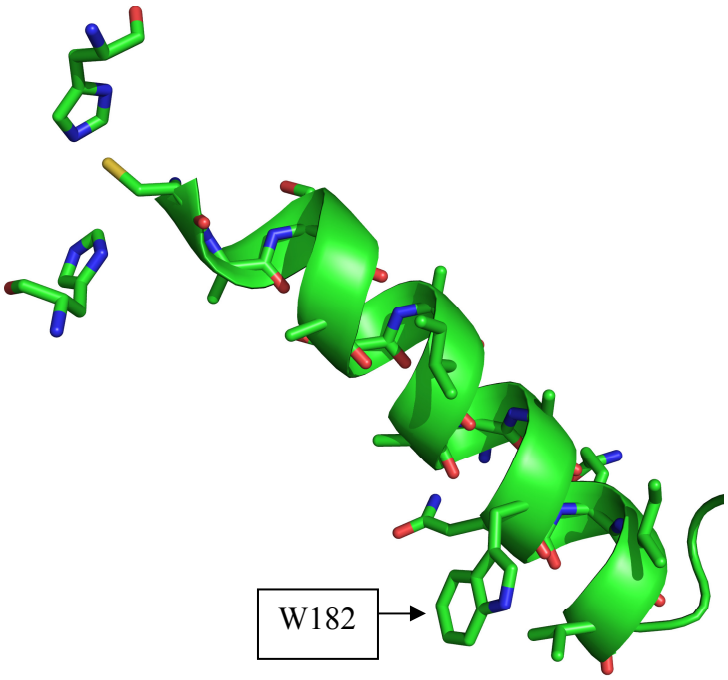

Figure 15: *KasB active site triad and active site α-helix Nα3 showing tryptophan 182*

After correction of the data for the inner filter effect, the fluorescence titrations yielded a K_d value of 226 μM for the interaction of TLM with the free enzyme. This K_d value is similar to the IC_{50} value obtained when TLM was not preincubated with the reaction mixture (see above).

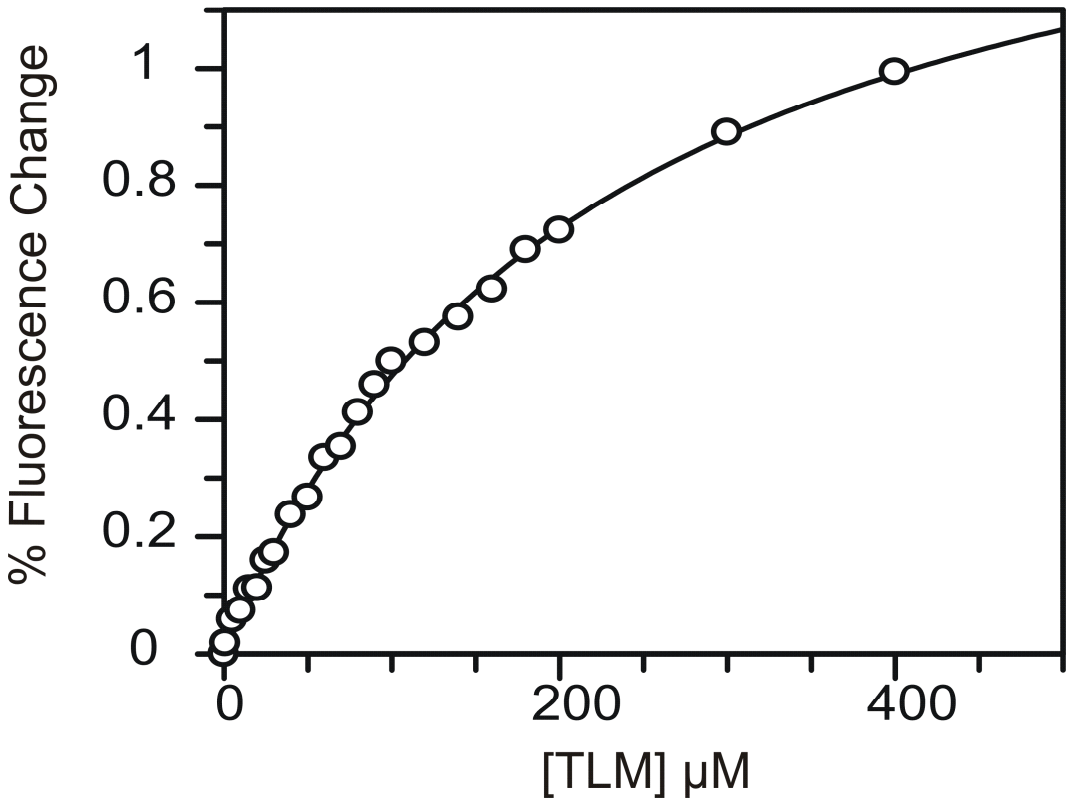

Figure 16: *Fluorescence titration of TLM with apo-KasA. The best fit curve to the scatchard equation is shown.* K_d *= 226* $\pm$ *9 µM*

Based on the decrease in IC_{50} value observed when TLM was preincubated with palmitoyl-ACP and KasA, we set out to quantitate the interaction of TLM with acyl-KasA. We synthesized the acyl-KasA intermediate by incubation of palmitoyl-CoA with KasA for 10 min as previously described(*11*). When the titration was repeated with the acylated form of KasA, addition of TLM to the enzyme solution resulted in a much slower decrease in the fluorescence signal than the instantaneous change

observed for the free enzyme. The rate of decay of the fluorescence signal was dependent on the concentration of TLM and the data were fit to a double exponential to correct for a slight background decrease in intensity and to obtain k_{obs}, the rate of TLM binding(*18, 45*). The k_{obs} values obtained at different TLM concentrations were then fit to equation 2 which describes the interaction of TLM with KasA using a 2 step binding model (Scheme 1).

$$E + I \underset{}{\overset{K_i}{\rightleftharpoons}} EI \underset{k_2}{\overset{k_1}{\rightleftharpoons}} EI^*$$

Scheme 1: *Two step binding model*

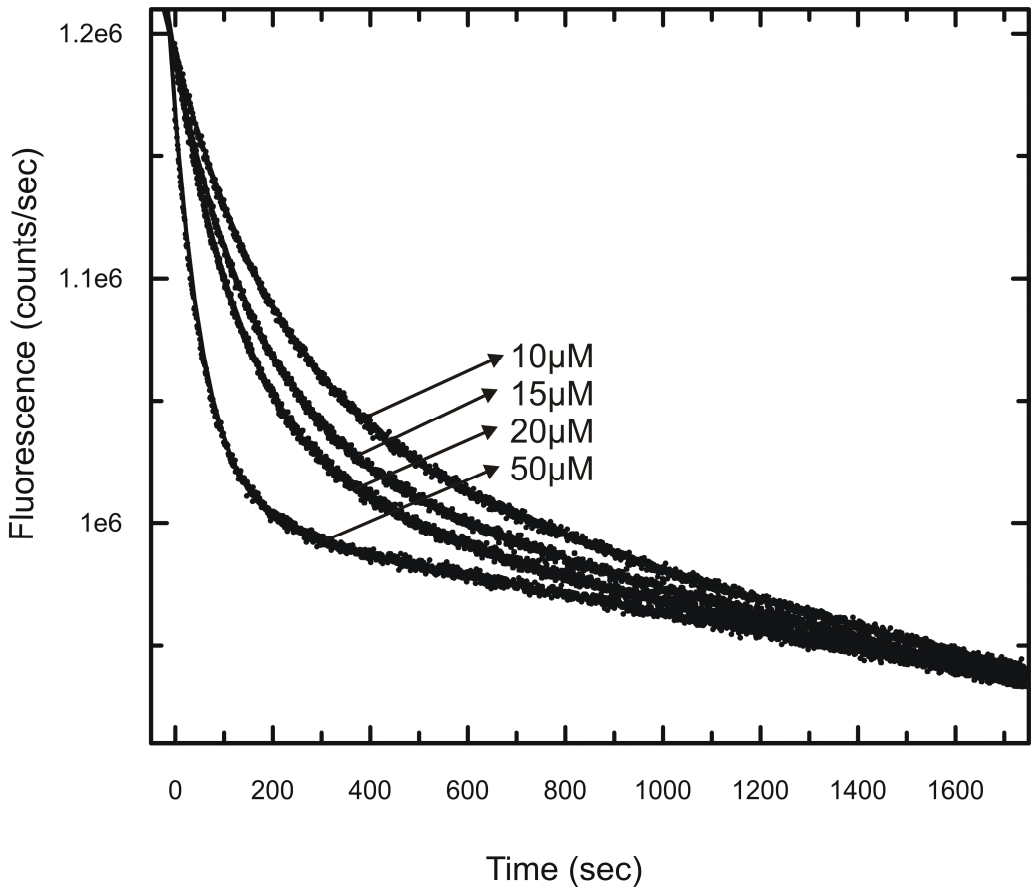

Figure 17: *Representative fluorescence decay curves for different concentrations of TLM with C171Q KasA. Curves were fit to equation 1 to obtain k_{obs}.*

$$y = Ae^{-k_{(obs)}t} + Be^{-k_{(2)}t} \quad \textbf{1}$$

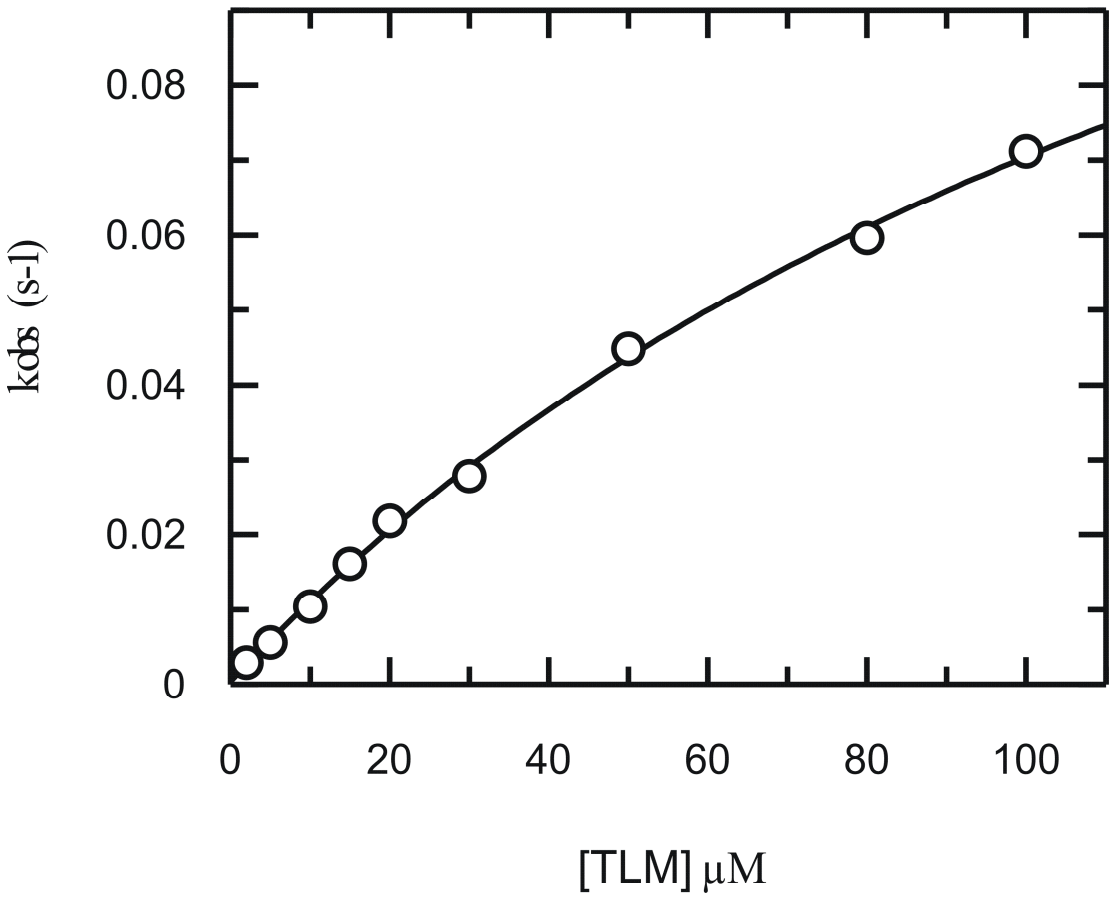

Figure 18: *Secondary Plot of k_{obs} vs. concentration of TLM with Acyl-KasA. Best fit curve to equation 2 is shown.*

$$k_{obs} = k_2 + k_1 [I] / (K_i + [I]) \qquad \textbf{2}$$

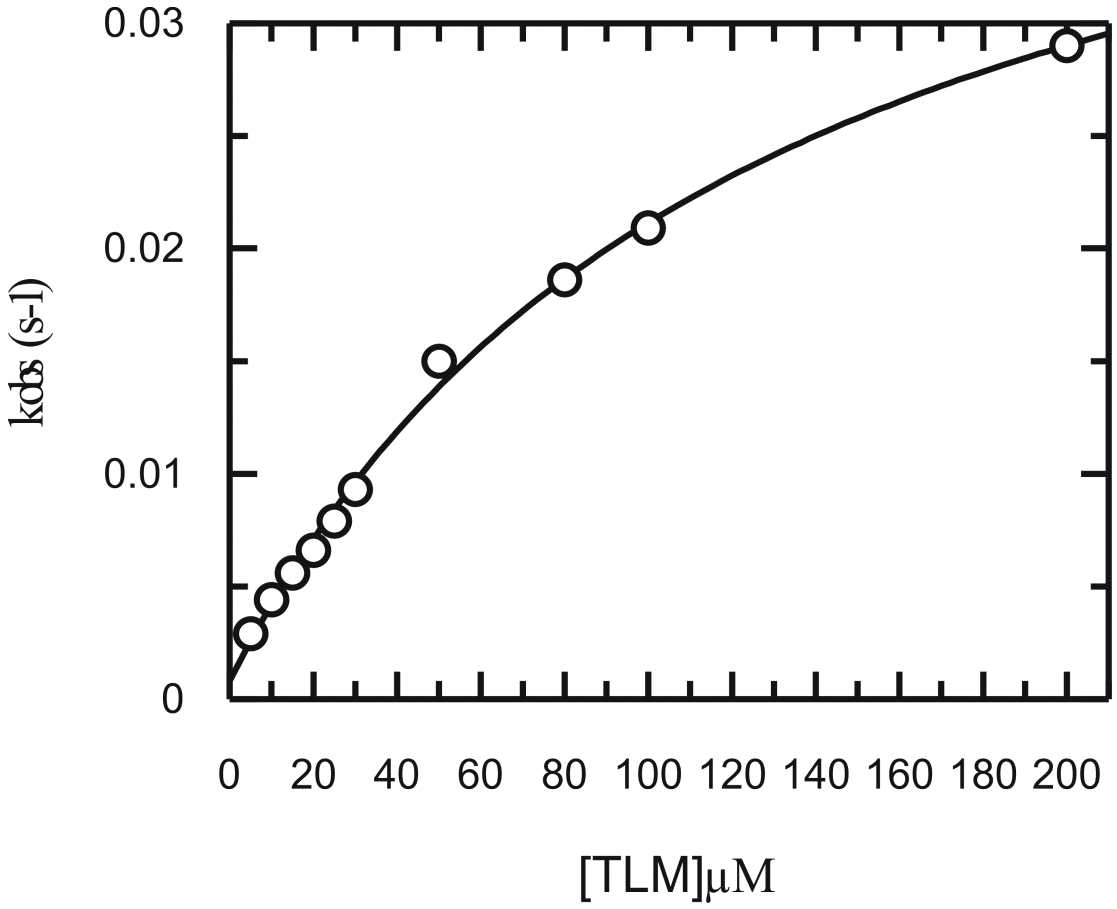

Figure 19: *Secondary Plot of k_{obs} vs. concentration of TLM with C171Q KasA. Best fit curve to equation 2 is shown.*

Table 5: *Kinetic and Thermodynamic Parameters for the Interaction of TLM with KasA*

Enzyme	IC_{50} (μM)	K_d (μM)[c]	K_i (μM)[d]	$k_1(s^{-1})$[d]	k_2 (s-1)[d]	K_i*(μM)[e]
KasA	242 ± 60[a]	226 ± 9	ND	ND	ND	ND
Acyl-KasA	19.0 + 2.3[a, b]	ND	163 + 28	0.19 ± 0.02	0.0004 ± 0.0009	0.3 ± 0.8
C171Q KasA	ND[f]	ND	126 + 16	0.046 + .002	0.0008 ± 0.0005	2.2 ± 1.6

a: IC_{50} value was determined by preincubating TLM with KasA and malonyl-AcpM and initiating the reaction by addition of palmitoyl-AcpM.

b: IC_{50} value was determined by preincubating TLM with KasA and palmitoyl-AcpM and initiating the reaction by addition of malonyl-AcpM.

c: Kd values were determined by fluorescence titration and fitting the data to the Scatchard equation.

d: Parameters were determined by fitting the k_{obs} data for the slow binding of TLM to acyl-KasA of the C171Q mutant using equation 2.

e: K_i* was calculated using equation 3.

f: ND, not determined.

This analysis yielded estimates for K_i* of 0.3 ± 0.8 μM for the formation of the final enzyme inhibitor complex EI*. Variation in the calculated K_i* values was due primarily to significant errors in the observed values for $k_{(rev)}$. Based on the report that the C163Q mutant of FabF mimicked the structural change accompanying acyl-FabF formation(*11*), we repeated the fluorescence titration using C171Q KasA mutant and obtained a K_i* value of 2.2 ± 1.6 μM.

DISCUSSION :

We have shown through kinetic analysis and direct binding experiments that TLM has 10-fold more potent binding to the acyl-KasA covalent enzyme intermediate and C171Q mutant than to the apo form of the enzyme. Additionally, TLM is a slow binding inhibitor of the acyl-enzyme intermediate and acyl mimic mutant. Differential binding affinities for TLM with the two forms of the keto-acyl synthase enzyme along the reaction coordinate are not reported in the literature. In a study involving FabF the *E. coli* KAS II enzyme however it has been reported that platencimycin, a natural product inhibitor, exhibits differential binding affinities for the apo and acyl forms. In that study binding of TLM to lauroyl-FabF is reported to be 1 μM. This value is less than previously reported(*7*) but an acyl/apo comparison is not reported.

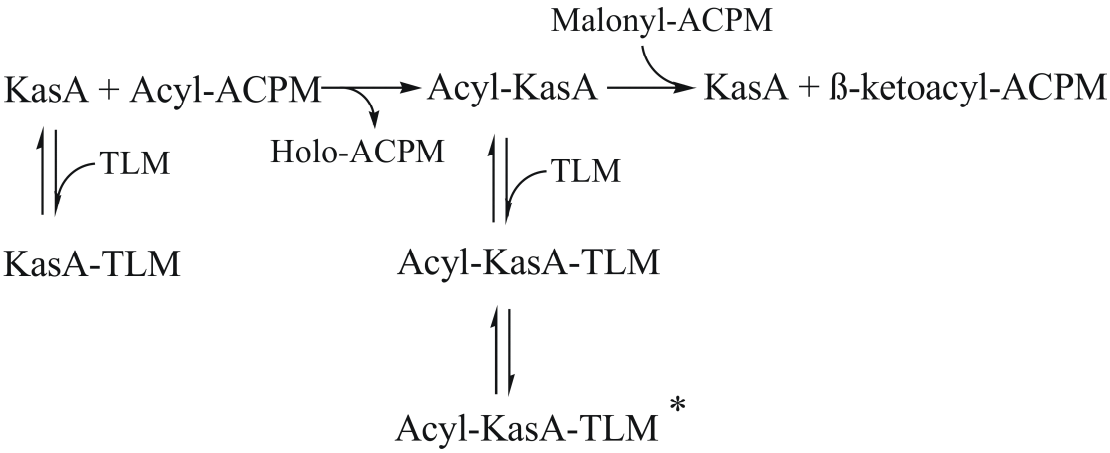

Scheme 2: *TLM KasA differential binding model. TLM acts as both a low affinity uncompetitive inhibitor as well as a high affinity slow onset competitive inhibitor*

TLM binding data have been reported with the KASIII purified from pea *(Pisum Sativum L.*)(*32*). In this paper Jones *et al* report TLM inhibition kinetics where TLM is an uncompetitve inhibitor at high concentrations and a competive inhibitor at low concentrations with respect to malonyl-Acp. The authors attribute these complexities to a loose fit of TLM in the active site (IC_{50}=0.7 mM). Price *et al* (*7*) report a K_d for FabF which is much higher than would be extrapolated based on IC_{50} data (IC_{50} =6 μM vs. K_d =60 μM), however a K_d with the acyl form is not reported. A differential binding affinity between the acyl and apo forms of these KAS enzymes could explain these complexities.

Despite considerable efforts in the field, a structure for KasA remains elusive. The structural basis for the time-dependent binding is therefore not yet clear. Analysis of homologous proteins structural data has not explained the time dependent rearrangement or the differential binding affinity. Our work toward structural corroboration of these data is discussed in Chapter 3.

Mechanistic Insights for Lead Optimization

The insights gained from the TLM mechanistic study discussed above will aid in the development of TLM as a lead molecule. We now understand that

there is a fundamental difference between the apo-enzyme and acyl-enzyme that is reflected in TLM potency and that there is an additional slow binding component to acyl-enzyme binding. Understanding the exact molecular interactions that allow TLM to bind more tightly to the acyl form is now a fundamental question that underscores TLM optimization. To this end we have invested extensive effort focused on obtaining structural data for the mutant acyl-KasA mimic. We believe that this structure would help explain the slow binding phenomenon and in addition would aid in drug discovery efforts by elucidating differences in the TLM active site interactions between the weak apo-form and the more strongly inhibited acyl-enzyme form. Structural data for this tightly bound acyl-enzyme complex could reveal why structure based inhibitor design based on the TLM apo-enzyme bound structure have had limited success(*24*). Additionally, these data significantly contribute to the importance of TLM as a lead molecule for anti-TB drug development for two reasons. Firstly; The *in vitro* inhibition mechanism and binding mode are now well understood and Secondly; the previously unknown slow-onset component to the inhibition mechanism increases the residence time of the inhibitor on the enzyme which will contribute to its *in vivo* efficacy and therefore its appeal as a lead molecule(*50*).

References:

1. Heath, R. J., and Rock, C. O. (2002) The Claisen condensation in biology, *Nat Prod Rep 19*, 581-596.
2. Haapalainen, A. M., Merilainen, G., and Wierenga, R. K. (2006) The thiolase superfamily: condensing enzymes with diverse reaction specificities, *Trends in biochemical sciences 31*, 64-71.
3. Mathieu, M., Zeelen, J. P., Pauptit, R. A., Erdmann, R., Kunau, W. H., and Wierenga, R. K. (1994) The 2.8 A crystal structure of peroxisomal 3-ketoacyl-CoA thiolase of Saccharomyces cerevisiae: a five-layered alpha beta alpha beta alpha structure constructed from two core domains of identical topology, *Structure 2*, 797-808.
4. Mathieu, M., Modis, Y., Zeelen, J. P., Engel, C. K., Abagyan, R. A., Ahlberg, A., Rasmussen, B., Lamzin, V. S., Kunau, W. H., and Wierenga, R. K. (1997) The 1.8 A crystal structure of the dimeric peroxisomal 3-ketoacyl-CoA thiolase of Saccharomyces cerevisiae: implications for substrate binding and reaction mechanism, *Journal of molecular biology 273*, 714-728.
5. Modis, Y., and Wierenga, R. K. (1999) A biosynthetic thiolase in complex with a reaction intermediate: the crystal structure provides new insights into the catalytic mechanism, *Structure 7*, 1279-1290.
6. White, S. W., Zheng, J., Zhang, Y. M., and Rock. (2005) The structural biology of type II fatty acid biosynthesis, *Annu Rev Biochem 74*, 791-831.
7. Price, A. C., Choi, K. H., Heath, R. J., Li, Z., White, S. W., and Rock, C. O. (2001) Inhibition of beta-ketoacyl-acyl carrier protein synthases by thiolactomycin and cerulenin. Structure and mechanism, *The Journal of biological chemistry 276*, 6551-6559.
8. von Wettstein-Knowles, P., Olsen, J. G., McGuire, K. A., and Henriksen, A. (2006) Fatty acid synthesis. Role of active site histidines and lysine in Cys-His-His-type beta-ketoacyl-acyl carrier protein synthases, *The FEBS journal 273*, 695-710.

9. von Wettstein-Knowles, P., Olsen, J., Arnvig Mcguire, K., and Larsen, S. (2000) Molecular aspects of beta-ketoacyl synthase (KAS) catalysis, *Biochem Soc Trans 28*, 601-607.

10. Khandekar, S. S., Gentry, D. R., Van Aller, G. S., Warren, P., Xiang, H., Silverman, C., Doyle, M. L., Chambers, P. A., Konstantinidis, A. K., Brandt, M., Daines, R. A., and Lonsdale, J. T. (2001) Identification, substrate specificity, and inhibition of the Streptococcus pneumoniae beta-ketoacyl-acyl carrier protein synthase III (FabH), *The Journal of biological chemistry 276*, 30024-30030.

11. Wang, J., Soisson, S. M., Young, K., Shoop, W., Kodali, S., Galgoci, A., Painter, R., Parthasarathy, G., Tang, Y. S., Cummings, R., Ha, S., Dorso, K., Motyl, M., Jayasuriya, H., Ondeyka, J., Herath, K., Zhang, C., Hernandez, L., Allocco, J., Basilio, A., Tormo, J. R., Genilloud, O., Vicente, F., Pelaez, F., Colwell, L., Lee, S. H., Michael, B., Felcetto, T., Gill, C., Silver, L. L., Hermes, J. D., Bartizal, K., Barrett, J., Schmatz, D., Becker, J. W., Cully, D., and Singh, S. B. (2006) Platensimycin is a selective FabF inhibitor with potent antibiotic properties, *Nature 441*, 358-361.

12. Young, K., Jayasuriya, H., Ondeyka, J. G., Herath, K., Zhang, C., Kodali, S., Galgoci, A., Painter, R., Brown-Driver, V., Yamamoto, R., Silver, L. L., Zheng, Y., Ventura, J. I., Sigmund, J., Ha, S., Basilio, A., Vicente, F., Tormo, J. R., Pelaez, F., Youngman, P., Cully, D., Barrett, J. F., Schmatz, D., Singh, S. B., and Wang, J. (2006) Discovery of FabH/FabF inhibitors from natural products, *Antimicrobial agents and chemotherapy 50*, 519-526.

13. Surolia, A., Ramya, T. N., Ramya, V., and Surolia, N. (2004) 'FAS't inhibition of malaria, *The Biochemical journal 383*, 401-412.

14. Barry, C. E., 3rd, Slayden, R. A., and Mdluli, K. (1998) Mechanisms of isoniazid resistance in Mycobacterium tuberculosis, *Drug Resist Updat 1*, 128-134.

15. Mdluli, K., Slayden, R. A., Zhu, Y., Ramaswamy, S., Pan, X., Mead, D., Crane, D. D., Musser, J. M., and Barry, C. E., 3rd. (1998) Inhibition of a

Mycobacterium tuberculosis beta-ketoacyl ACP synthase by isoniazid, *Science (New York, N.Y 280*, 1607-1610.

16. Bhatt, A., Kremer, L., Dai, A. Z., Sacchettini, J. C., and Jacobs, W. R., Jr. (2005) Conditional depletion of KasA, a key enzyme of mycolic acid biosynthesis, leads to mycobacterial cell lysis, *Journal of bacteriology 187*, 7596-7606.
17. Slayden, R. A., Lee, R. E., Armour, J. W., Cooper, A. M., Orme, I. M., Brennan, P. J., and Besra, G. S. (1996) Antimycobacterial action of thiolactomycin: an inhibitor of fatty acid and mycolic acid synthesis, *Antimicrobial agents and chemotherapy 40*, 2813-2819.
18. Rawat, R., Whitty, A., and Tonge, P. J. (2003) The isoniazid-NAD adduct is a slow, tight-binding inhibitor of InhA, the Mycobacterium tuberculosis enoyl reductase: adduct affinity and drug resistance, *Proceedings of the National Academy of Sciences of the United States of America 100*, 13881-13886.
19. Odriozola, J. M., and Bloch, K. (1977) Effects of phosphatidylcholine liposomes on the fatty acid synthetase complex from Mycobacterium smegmatis, *Biochimica et biophysica acta 488*, 198-206.
20. Veyron-Churlet, R., Guerrini, O., Mourey, L., Daffe, M., and Zerbib, D. (2004) Protein-protein interactions within the Fatty Acid Synthase-II system of Mycobacterium tuberculosis are essential for mycobacterial viability, *Molecular microbiology 54*, 1161-1172.
21. Oishi, H., Noto, T., Sasaki, H., Suzuki, K., Hayashi, T., Okazaki, H., Ando, K., and Sawada, M. (1982) Thiolactomycin, a new antibiotic. I. Taxonomy of the producing organism, fermentation and biological properties, *J Antibiot (Tokyo) 35*, 391-395.
22. Hamada, S., Fujiwara, T., Shimauchi, H., Ogawa, T., Nishihara, T., Koga, T., Nehashi, T., and Matsuno, T. (1990) Antimicrobial activities of thiolactomycin against gram-negative anaerobes associated with periodontal disease. f1, *Oral Microbiol Immunol 5*, 340-345.

23. Noto, T., Miyakawa, S., Oishi, H., Endo, H., and Okazaki, H. (1982) Thiolactomycin, a new antibiotic. III. In vitro antibacterial activity, *J Antibiot. (Tokyo) 35*, 401-410.

24. Kim, P., Zhang, Y. M., Shenoy, G., Nguyen, Q. A., Boshoff, H. I., Manjunatha, U. H., Goodwin, M. B., Lonsdale, J., Price, A. C., Miller, D. J., Duncan, K., White, S. W., Rock, C. O., Barry, C. E., 3rd, and Dowd, C. S. (2006) Structure-activity relationships at the 5-position of thiolactomycin: an intact (5R)-isoprene unit is required for activity against the condensing enzymes from Mycobacterium tuberculosis and Escherichia coli, *J Med Chem 49*, 159-171.

25. Hayashi, T., Yamamoto, O., Sasaki, H., Kawaguchi, A., and Okazaki, H. (1983) Mechanism of action of the antibiotic thiolactomycin inhibition of fatty acid synthesis of Escherichia coli, *Biochemical and biophysical research communications 115*, 1108-1113.

26. Miyakawa, S., Suzuki, K., Noto, T., Harada, Y., and Okazaki, H. (1982) Thiolactomycin, a new antibiotic. IV. Biological properties and chemotherapeutic activity in mice, *J Antibiot (Tokyo) 35*, 411-419.

27. Jackowski, S., Zhang, Y. M., Price, A. C., White, S. W., and Rock, C. O. (2002) A missense mutation in the fabB (beta-ketoacyl-acyl carrier protein synthase I) gene confers tiolactomycin resistance to Escherichia coli, *Antimicrobial agents and chemotherapy 46*, 1246-1252.

28. Tsay, J. T., Rock, C. O., and Jackowski, S. (1992) Overproduction of beta-ketoacyl-acyl carrier protein synthase I imparts thiolactomycin resistance to Escherichia coli K-12, *Journal of bacteriology 174*, 508-513.

29. Nishida, I., Kawaguchi, A., and Yamada, M. (1986) Effect of thiolactomycin on the individual enzymes of the fatty acid synthase system in Escherichia coli, *J Biochem (Tokyo) 99*, 1447-1454.

30. He, X., Mueller, J. P., and Reynolds, K. A. (2000) Development of a scintillation proximity assay for beta-ketoacyl-acyl carrier protein synthase III, *Anal Biochem 282*, 107-114.

31. Schaeffer, M. L., Carson, J. D., Kallender, H., and Lonsdale, J. T. (2004) Development of a scintillation proximity assay for the Mycobacterium tuberculosis KasA and KasB enzymes involved in mycolic acid biosynthesis, *Tuberculosis (Edinb) 84*, 353-360.

32. Jones, A. L., Gane, A. M., Herbert, D., Willey, D. L., Rutter, A. J., Kille, P., Dancer, J. E., and Harwood, J. L. (2003) Beta-ketoacyl-acyl carrier protein synthase III from pea (Pisum sativum L.): properties, inhibition by a novel thiolactomycin analogue and isolation of a cDNA clone encoding the enzyme, *Planta 216*, 752-761.

33. Kim, P., Barry, C. E., and Dowd, C. S. (2006) Novel route to 5-position vinyl derivatives of thiolactomycin: Olefination vs. deformylation, *Tetrahedron Lett 47*, 3447-3451.

34. McFadden, J. M., Frehywot, G. L., and Townsend, C. A. (2002) A flexible route to (5R)-thiolactomycin, a naturally occurring inhibitor of fatty acid synthesis, *Org Lett 4*, 3859-3862.

35. McFadden, J. M., Medghalchi, S. M., Thupari, J. N., Pinn, M. L., Vadlamudi, A., Miller, K. I., Kuhajda, F. P., and Townsend, C. A. (2005) Application of a flexible synthesis of (5R)-thiolactomycin to develop new inhibitors of type I fatty acid synthase, *J Med Chem 48*, 946-961.

36. Witkowski, A., Joshi, A. K., Lindqvist, Y., and Smith, S. (1999) Conversion of a beta-ketoacyl synthase to a malonyl decarboxylase by replacement of the active-site cysteine with glutamine, *Biochemistry 38*, 11643-11650.

37. Nomura, S., Horiuchi, T., Omura, S., and Hata, T. (1972) The action mechanism of cerulenin. I. Effect of cerulenin on sterol and fatty acid biosynthesis in yeast, *J Biochem (Tokyo) 71*, 783-796.

38. Schaeffer, M. L., Agnihotri, G., Volker, C., Kallender, H., Brennan, P. J., and Lonsdale, J. T. (2001) Purification and biochemical characterization of the Mycobacterium tuberculosis beta-ketoacyl-acyl carrier protein synthases KasA and KasB, *The Journal of biological chemistry 276*, 47029-47037.

39. Changsen, C., Franzblau, S. G., and Palittapongarnpim, P. (2003) Improved green fluorescent protein reporter gene-based microplate screening for

antituberculosis compounds by utilizing an acetamidase promoter, *Antimicrobial agents and chemotherapy 47*, 3682-3687.

40. Hackbarth, C. J., Unsal, I., and Chambers, H. F. (1997) Cloning and sequence analysis of a class A beta-lactamase from Mycobacterium tuberculosis H37Ra, *Antimicrobial agents and chemotherapy 41*, 1182-1185.
41. Newton, G. L., Unson, M. D., Anderberg, S. J., Aguilera, J. A., Oh, N. N., delCardayre, S. B., Av-Gay, Y., and Fahey, R. C. (1999) Characterization of Mycobacterium smegmatis mutants defective in 1-d-myo-inosityl-2-amino-2-deoxy-alpha-d-glucopyranoside and mycothiol biosynthesis, *Biochemical and biophysical research communications 255*, 239-244.
42. Lambalot, R. H., and Walsh, C. T. (1995) Cloning, overproduction, and characterization of the Escherichia coli holo-acyl carrier protein synthase, *The Journal of biological chemistry 270*, 24658-24661.
43. Thomas, J., and Cronan, J. E. (2005) The enigmatic acyl carrier protein phosphodiesterase of Escherichia coli: genetic and enzymological characterization, *The Journal of biological chemistry 280*, 34675-34683.
44. Thomas, J., Rigden, D. J., and Cronan, J. E. (2007) Acyl carrier protein phosphodiesterase (AcpH) of Escherichia coli is a non-canonical member of the HD phosphatase/phosphodiesterase family, *Biochemistry 46*, 129-136.
45. Tsai, Y. C., and Johnson, K. A. (2006) A new paradigm for DNA polymerase specificity, *Biochemistry 45*, 9675-9687.
46. Copeland, R. A., Williams, J. M., Giannaras, J., Nurnberg, S., Covington, M., Pinto, D., Pick, S., and Trzaskos, J. M. (1994) Mechanism of selective inhibition of the inducible isoform of prostaglandin G/H synthase, *Proceedings of the National Academy of Sciences of the United States of America 91*, 11202-11206.
47. Houtzager, V., Ouellet, M., Falgueyret, J. P., Passmore, L. A., Bayly, C., and Percival, M. D. (1996) Inhibitor-induced changes in the intrinsic fluorescence of human cyclooxygenase-2, *Biochemistry 35*, 10974-10984.
48. Gey Van Pittius, N. C., Gamieldien, J., Hide, W., Brown, G. D., Siezen, R. J., and Beyers, A. D. (2001) The ESAT-6 gene cluster of Mycobacterium

tuberculosis and other high G+C Gram-positive bacteria, *Genome biology 2*, RESEARCH0044.

49. Sridharan, S., Wang, L., Brown, A. K., Dover, L. G., Kremer, L., Besra, G. S., and Sacchettini, J. C. (2007) X-ray crystal structure of Mycobacterium tuberculosis beta-ketoacyl acyl carrier protein synthase II (mtKasB), *Journal of molecular biology 366*, 469-480.

50. Copeland, R. A., Pompliano, D. L., and Meek, T. D. (2006) Drug-target residence time and its implications for lead optimization, *Nat Rev Drug Discov 5*, 730-739.

Chapter 3

Structural Corroboration of KAS inhibition by TLM

Extension of Studies in Chapter 2 with FabF and a General Binding Model for TLM

Structural Studies

Materials and Methods

Results & Discussion

References

Extension of Studies in Chapter 2 with FabF and a General Binding Model for TLM

As an extension of the studies discussed in Chapter 2, we sought to corroborate our TLM differential binding model (10 fold higher binding affinity to the acyl-enzyme intermediate) as well as TLM slow onset inhibition with structural evidence. Additionally we sought to test if our binding models do in fact serve to explain discrepancies found in the literature with other KAS enzymes(*1-3*). That is, can the enigmatic TLM inhibition data with KASIII from the Pea plant showing uncompetitive inhibition at high concentration and competitive inhibition at low concentration be rationalized with our model? Additionally, can our model explain why the K_d measured for TLM (60 μM) with FabF is higher than would be expected based on the IC_{50} (6 μM)? Studies with FabF similar to our studies with KasA could answer these questions as well as aid in our structural discussions. A FabB X-ray structure is reported in the literature however no KasA X-ray structure has been reported, nor has an apo to acyl-enzyme comparision been made with any TLM complex. To this end, we proceeded in parallel with studies including both *E. coli* FabF (one of the most well characterized KAS enzymes) (*3-6*) and KasA.

Firstly, we considered that our development of an efficient source of recombinant and soluble KasA from an *M. smegmatis* expression host

afforded us an advantage over other groups who considered screens for the elusive KasA crystal conditions too venturesome for their investment ((*7*) and personal communication with Laurent Kremer, Gurdyal Besra). We therefore proceeded, in collaboration with Prof. Caroline Kisker (Würzburg University), to structurally examine TLM binding to our recombinant KasA directly. Crystal condition screens and subsequent structural studies were immediately undertaken (below).

Crystallization conditions as well as X-ray structural data for FabF are present throughout the literature(*1, 4*). The studies with the FabB-TLM complex show the active site interactions to the apo enzyme. However, a comparison of the TLM bound to apo and acyl-enzyme structures is not reported. These data are required to understand the higher binding affinity to the acyl-enzyme. We therefore sought to exploit the reported crystal conditions with FabF (*3*) for our own studies in parallel to experiments involving KasA in order to ensure a greater chance of successfully obtaining structural data. In order to solidify any structural corroboration made using structural comparisons with KAS enzymes from *E. coli* we needed to first examine *E. coli* FabF directly to test the hypothesis that our differential and slow binding models are in fact general TLM binding phenomena for this class of enzymes.

To this end, we cloned, expressed, purified and characterized *E. coli* (wt)-FabF and C164Q-FabF using both enzyme assays (in the case of wt-FabF) and direct binding experiments. Additionally, we synthesized and purified a hexadecyl-chloromethyl-ketone (C16) (Figure 1) as a reagent for acyl-enzyme studies that require a stable acylated active site cysteine (crystallization and mass spectrometry). Such a reagent, used in structural studies, will reveal active site interactions in the acyl-enzyme intermediate. In parallel, we have exploited our efficient source of heterologously expressed KasA to conduct extensive crystal trials and X-ray structural characterization of apo wt-KasA and apo C171Q-KasA as well as studies with binary TLM complexes (below).

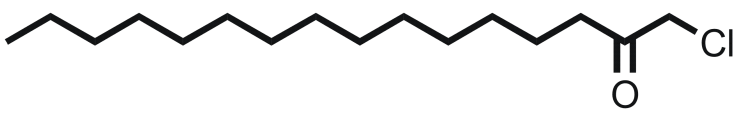

Figure 1: *C16 Chloromethylketone (CMK)*

Structural Studies

KasA belongs to a superfamily of enzymes, the thiolase superfamily, that share a common 3-dimentional fold despite a lack of sequence identity. The thiolase fold consists of a βαβαβαββ topology as described in previous Chapters. The catalytic triad consists of 2 histidine residues and a cysteine whose active site sulfhydryl group sits at the N-terminus of a long α-helix.

The cysteine interacts with the adjacent backbone amides of A170 and G174 making the sulfur ideally positioned to receive the full benefit of the half unit of positive charge generated by the helical dipole moment(*4*) lowering the pK_a by as much as 1.6 units(*8*).

The binding mode for TLM has been determined with *E. coli* FabB and is discussed in greater detail in Chapter 4(*1*). Briefly, TLM is thought to mimic malonyl-Acp binding and has specific H-bond partners within the active site. The TLM isoprene is stacked between 2 conserved loops, the hydroxyl group interacts with a network of water molecules that in turn interact with the FabB backbone and two conserved threonine residues (T313/T315, KasA numbering). The carbonyl carbon forms H-bonds to each of the active site histidines while the sulfur heteroatom has no clear H-bond partner. The structure of TLM and IUPAC numbering is shown in Figure 2.

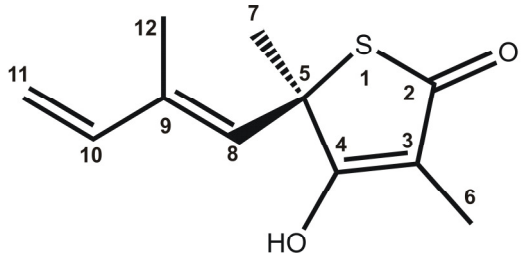

Thiolactomycin

Figure 2: *Thiolactomycin structure showing IUPAC numbering*

Materials and Methods:

WT-FabF and C164Q FabF preparation:

E. coli FabF was PCR amplified from *E. coli* genomic DNA using forward and reverse primers listed in Table 1 and subcloned into NheI and XhoI sites in pET28a to yield an in frame N-terminally hexahistadine tagged *fabF* gene.

Table 1: *PCR Primers for FabF cloning*

Forward	5'-CTA GCT AGC GTG TCT AAG CGT CGT GTA GTT-3'
Reverse	5'CCG CTC GAG TTA TTA GAT CTT TTT AAA GAT CAA AGA-3'

The C164Q mutant clone was prepared using Quikchange mutagenesis with forward and reverse primers listed in Table 2. The sequencing of both plasmids was achieved by standard ABI sequencing. Wild type and mutant recombinant protein was expressed in the *E.coli pLysS* cell line and purified using Ni affinity chromatography as described previously (*3*). Purified protein was analyzed by SDS-PAGE and LC/MS analysis (below).

Table 2: *C164Q Primers used for Mutagenesis*

Forward	5'-TCT ATC GCG ACT GCC CAG ACT TCC GGC GTG CAC-3'
Reverse	5'-GTG CAC GCC GGA AGT CTG GGC AGT CGC GAT AGA-3'

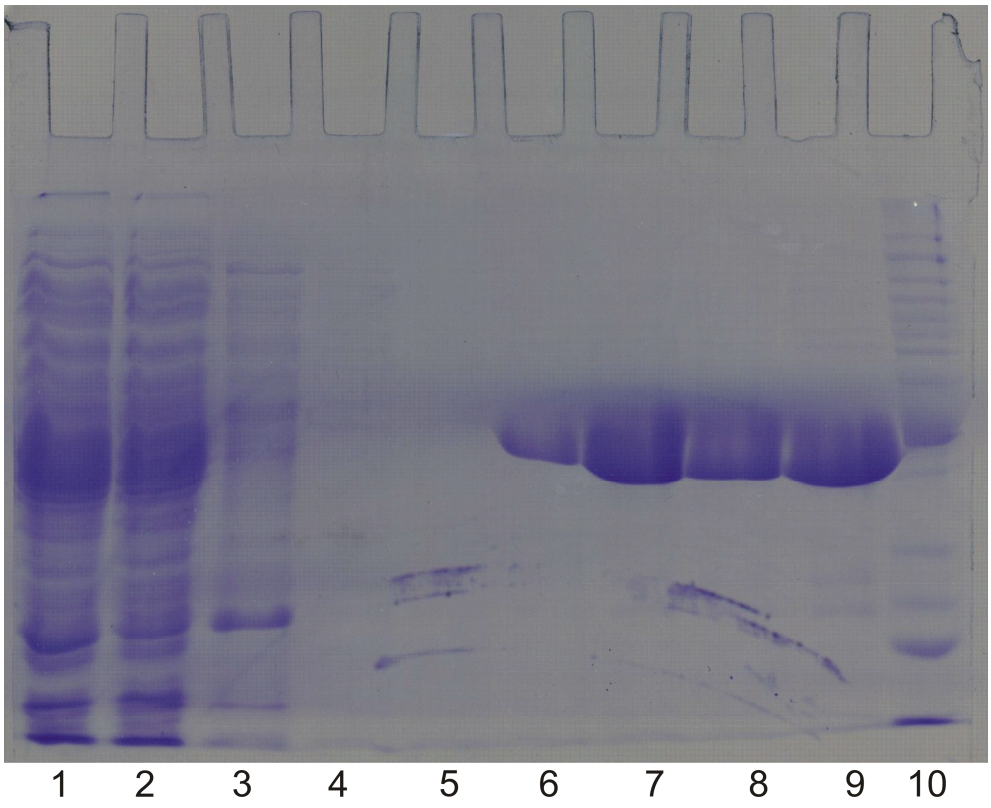

Figure 3: *12% SDS-PAGE Analysis of wt-FabF Purification Profile*

Table 3: *Legend for Samples Shown in Figure 3*	
Lane	Sample Description
1	overexpressed FabF in *E. coli* pLysS cell free extract
2	Column Flow-through (5mM imidazole, 0.5M NaCl, 20mM Tris pH 7.9)
3	Column wash (60mM imidazole, 0.5M NaCl, 20mM Tris pH 7.9)
4	Elution Fraction 1 (linear gradient from 5mM to 1M imidazole)
5	Elution Fraction 2 (linear gradient from 5mM to 1M imidazole)
6	Elution Fraction 3 (linear gradient from 5mM to 1M imidazole)
7	Elution Fraction 4 (linear gradient from 5mM to 1M imidazole)
8	Elution Fraction 5 (linear gradient from 5mM to 1M imidazole)
9	Elution Fraction 6 (linear gradient from 5mM to 1M imidazole)
10	Invitrogen Benchmark Protein Standard

LC/MS Characterization of Purified FabF Sample

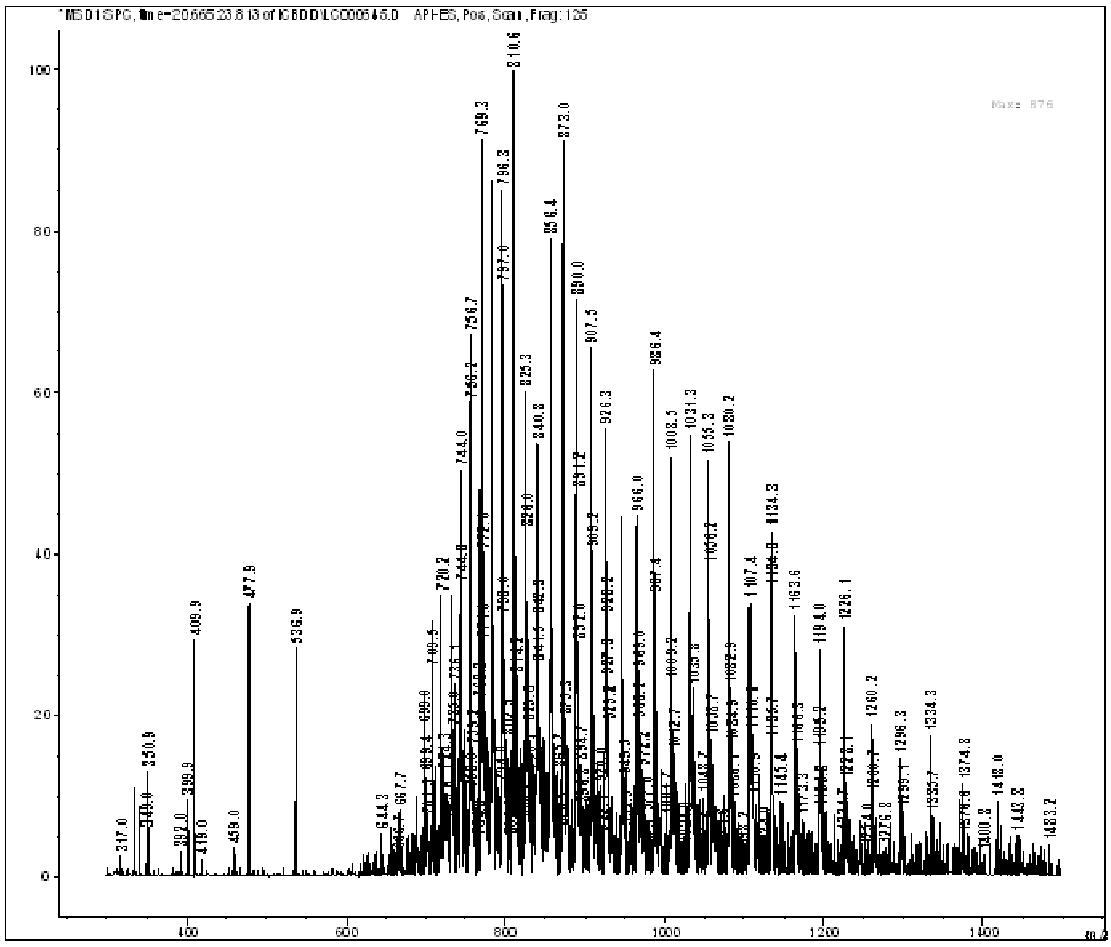

LC/MS analysis of FabF utilized a Phenomenex Jupiter C4 Column, 5 µm, 300 Å, 4.6 x 250 mm. A linear gradient 20-80% B from 5 to 30 min with solvent A; 0.4 % formic acid in water and solvent B; 100 % acetonitrile was used to elute FabB at R_t = 22.2 min. This spectral deconvolution gives a molecular weight (MW) = 45334 ± 4 Da which is consistent with the calculated MW for recombinant FabF = 45340 Da.

FabF Continuous Coupled Activity Assay

An activity assay similar to one discussed in Chapter 2 for KasA was used with FabF. Oxidation of NADPH by MabA (Chapter 2) was again coupled to the production to β-ketoacyl product. Significantly, we found FabF to be active with malonyl-CoA (Sigma) and lauroyl-CoA (Sigma) (12 carbon chain length) avoiding the need to purify Acp based substrates for activity testing. Kinetic data for FabF was analyzed using Grafit 4.0 software and kinetic parameters are reported in Table 4. The K_m values we obtained with CoA based substrates are greater than those reported in studies with FabF from *S. aureus* using Acp based substrates(*9*). To our knowledge this is the only reported kinetic data for any FabF.

WT-FabF and C164Q FabF direct binding experiments

Similar to KasA (Chapter 2), a photon technology international (PTI) quanta master fluorimeter was used to monitor the intrinsic tryptophan fluorescence of FabF and mutant FabF. Excitation and emission wavelengths were 280 and 340nm respectively with an excitation slit width of 4.0 nm and an emission slit width of 8.0 nm. TLM solutions in buffer (50 mM KPO_4 pH 6.5, 50mM NaCl) were titrated into 1.0 μM enzyme in the same buffer. All solutions were filtered and equilibrated to 25 ºC. Titration curves were

corrected for inner filter effects and K_d values were calculated using the Scatchard equation (Grafit 4.0).

KasA Crystallization

Crystallization screens were conducted solely by Sylvia Lückner, a Doctoral Candidate in the laboratory of Prof. Caroline Kisker (University of Würzburg). Sylvia worked for 3 months as a visiting student in the Tonge Group. She learned to manipulate M. Smegmatis and to purify KasA and was able to return to The University of Würzburg to conduct crystallization screens independently.

WT-KasA was crystallized by the hanging drop vapour diffusion technique. 1 µL of protein solution was added to 1 µL of precipitant solution (10 % Isopropanol, 0.2 M NaCl, 0.1 M Hepes pH 7.5) and suspended over 1 mL of precipitant solution. After two days of incubation at 20 °C diffraction quality crystals grew at an air bubble that was trapped in the hanging drop.

KasA-C171Q crystals grew within one day in a drop containing equal amounts of protein and precipitant solution (20 % PEG 3350, 0.2 M potassium formate) at 20 °C. For the formation of the KasA-C171Q Inhibitor complex, TLM was dissolved in isopropanol and added to the concentrated protein solution as a solid powder in a molar ratio of 30:1 prior to

crystallization. The co-crystals grew in the same conditions as the apo-crystals.

Data collection structure solution and refinement

The diffraction data set of the WT-KasA was collected at a Rigaku MicroMax™-007HF with a Raxis HTC Detector. Before cryocooling, the crystal was transferred into a cryoprotectant solution containing the mother liquor with 30 % Glycerol.

The datasets were indexed, integrated and scaled using xxx (des program von crystal clear). The structure was solved by molecular replacement using phaser. As a search model, a monomer was derived from the protein data bank entry 2gp6. Molecular replacement yielded one monomer in the asymmetric unit that forms half of a dimer with the symmetry related molecules. Model building and refinement was carried out using alternating rounds of Coot for manual model building and Refmac for maximum likelihood refinement. Five percent of all reflections were omitted throughout the refinement for the calculation of R_{free}.

Diffraction data sets of apo KasA-C171Q and TLM-KasA-C171Q were collected at the protein structure factory beamline BL14.2 of the free University of Berlin at BESSY Synchrotron, Berlin. Before cryocooling, the

crystals of the KasA-C171Q protein were transferred into a cryoprotectant solution containing the mother liquor and 30 % ethylene glycol. In case of the TLM KasA-C171Q co-crystals, the cryosolution contained the mother liquor with 30 % ethylene glycol and TLM.

The two structures were solved by molecular replacement using phaser. For the TLM-KasA-C171Q structure, the monomer of the refined wt-KasA structure was used as a search model and for the apo KasA-C171Q structure one monomer of the refined TLM-KasA-C171Q structure was used. Molecular replacement yielded in eight molecules in the asymmetric unit that form four dimers. Model building and refinement was carried out using alternating rounds of Coot for manual model building and Refmac for maximum likelihood refinement. Five percent of all reflections were omitted throughout the refinement for the calculation of R_{free}. In the initial refinement rounds of the TLM KasAC171Q structure, the density improved significantly and allowed the unambiguous modeling of the TLM molecule into the electron density with Coot.

Model analysis and comparisons

Protein structure validation was done using Procheck. Superpositions were done with the Program Superpose SSM Lsqkab (ccp4). All model illustrations were prepared with Pymol.

Chloromethyl Ketone Synthesis (in collaboration with Florian Diwischek)

In collaboration with an organic chemistry graduate student at the University of Würzburg we synthesized a chloromethylketone (CMK) fatty acid analog in an attempt to make a stable acyl enzyme mimic. We hypothesized that the active site sulfhydryl group of KasA would nucleophilically attack the methylene adjacent to the carbonyl displacing a chlorine leaving group and forming a stable carbon sulfur bond. The use of this class of molecules as irreversible inhibitors of proteases is common (*10*). We sought a C16 acyl-CMK derivative for our purposes based on the chain length specificity of KasA(*11*). After multiple attempts to quantify the reaction between CMK and enzyme with mass spectrometry, we have not yet shown that this molecule modifies the enzyme as we hypothesized. Additionally, given the utility of the C to Q mutation as an acyl-enzyme mimic this reagent was not widely used in our studies. Nonetheless an examination of the utility of CMK is still underway.

Reaction scheme 1:

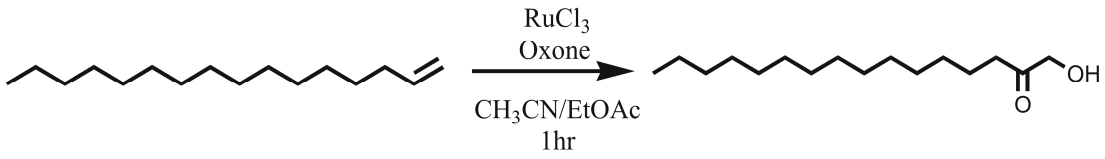

1-Hydroxyhexadecan-2-one

The experimental procedure used for reaction Scheme 1 was similar to that of Plietker(*12*). A round bottom flask was charged with 0.94 g (11.19 mmol) $NaHCO_3$, 0.45 ml (0.05 mmol) of a 0.1 M aqueous solution of $RuCl_3$, 5 ml distilled H_2O, 25 ml acetonitrile and 25 ml ethyl acetate. The suspension was stirred vigorously and 13.60 g (22.30 mmol) Oxone® was added in a single aliquot (gas↑). After the mixture turned yellow, 1.00 g (4.46 mmol) commercially available 1-hexadecene was added and the mixture was stirred for 40 min at RT and analyzed by TLC. When no starting material could be observed, the suspension was extracted with 60 ml saturated aqueous $NaHCO_3$ solution and 60 ml sat. aq. Na_2SO_3 solution. The aqueous layers were combined and extracted with 50 ml ethyl acetate. Ethyl acetate layers were combined, dried over anhydrous Na_2SO_4 and evaporated. The crude product was purified by column chromatography and analyzed by ^1H NMR and ESI/MS

1-Hydroxyhexadecan-2-one

Formula	$C_{16}H_{32}O_2$
Molecular weight	256.42
Yield	32 %
Column chromatography solvent:	CH_2Cl_2
R_f (solvent)	0.92
R_f (product)	0.49

^{1}H NMR (300 MHz, $CDCl_3$, δ = ppm, *J* = Hz): 4.24 (s, 2H, C*H*$_2$OH), 3.11 (s, 1H, CH_2*OH*), 2.40 (t, 2H, *J* 7.2, C*H*$_2$CO), 1.63 (m, 2H, C*H*$_2$CH$_2$CO), 1.25 (s, 22H, CH_3[C*H*$_2$]$_{11}$CH$_2$CH$_2$CO), 0.88 (t, 3H, *J* 6.3, C*H*$_3$)

Reaction scheme 2:

1-Chlorohexadecan-2-one

The experimental procedure used for reaction Scheme 2 was similar to that of Sampson *et. al.* (*13*). A mixture of 250 mg (0.98 mmol) 1-Hydroxyhexadecan-2-one and 0.65 ml *s*-collidine (4.93 mmol) was treated under nitrogen with 0.21 g (4.93 mmol) LiCl dissolved in 5 ml anhydrous THF.

The mixture was cooled to 0 °C and treated dropwise with 0.40 ml (5.09 mmol) methanesulfonyl chloride. The solution became thick and stirring was continued for 2h. Afterwards, the mixture was warmed to RT and 30 ml H_2O was added. The solution was washed with ether (3x 30 ml) and the ether extracts were combined and washed with saturated aqueous $Cu(NO_3)_2$ solution (3x 30 ml). The organic layer was dried over anhydrous Na_2SO_4 and evaporated. The residue was purified by column chromatography to yield pure 1-Chlorohexadecan-2-one.

1-Chlorohexadecan-2-one

Formula	$C_{16}H_{31}ClO$
Molecular weight	274.87
Yield	51 %
Melting point	51-52°C [Lit.: 53-54°C](*14*)
Column chromatography solvent:	CH_2Cl_2
R_f (solvent)	0.49
R_f (product)	0.86

^{1}H NMR (300 MHz, $CDCl_3$, δ = ppm, *J* = Hz): 4.06 (s, 2H, C*H*$_2$Cl), 2.57 (t, 2H, *J* 7.5, C*H*$_2$CO), 1.61 (m, 2H, C*H*$_2$CH$_2$CO), 1.25-1.28 (m, 22H, $CH_3[CH_2]_{11}CH_2CH_2CO$), 0.87 (m, 3H, C*H*$_3$) **m/z** 275

Results and Discussion

FabF Characterization

FabF was cloned, expressed, purified and characterized as described in materials and methods. Significantly, we found FabF to be active with high concentrations of CoA based substrates eliminating the need to use the Acp carrier. Apparent K_m values were determined for each of the two substrates, lauroyl-CoA (C12) and malonyl-CoA and kinetic plots are shown in Figures 4 and 5. These kinetic parameters are summarized in Table 4 and are considerably higher than previously reported values. In a study using FabF from *S. aureus* with octanoyl-Acp and malonyl-Acp Schaeffer *et al* (*9*) report K_m values for each substrate of less than 1 μM. The difference between the reported values and our values undoubtedly arises from the use of the natural Acp based substrate, whereas we use the commercially available CoA based carrier.

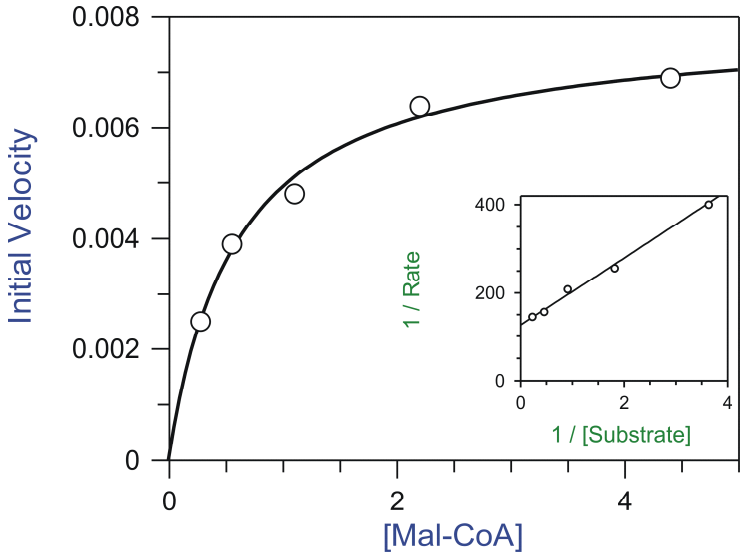

Figure 4: *K_m determination for malonyl-CoA with respect to 100 µM lauroyl-CoA*

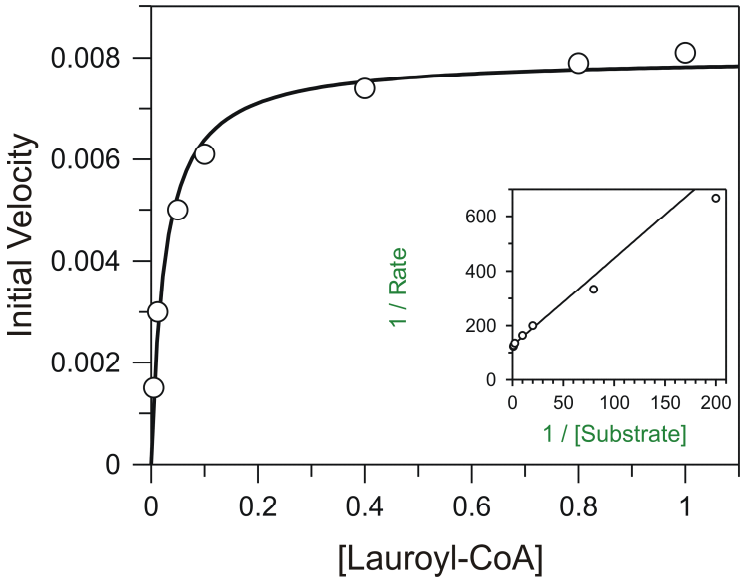

Figure 5: *Km determination for lauroyl-CoA with respect to 2mM malonyl-CoA*

Table 4: *Kinetic Parameters for E. coli FabF*

Substrate	$^{App}K_m$ (μM)	k_{cat} (min^{-1})	$k_{cat}/ {}^{App}K_m$ (M^{-1}, min^{-1})
Malonyl-CoA[a]	602 ± 74 μM	2.5 ± 0.1	4.2 X 10^3
Lauroyl-CoA[b]	25.6 ± 0.3 μM	2.5 ± 0.1	1.0 X 10^5

a. with respect to 100 μM lauroyl-CoA
b. with respect to 2 mM malonyl-CoA

With a working kinetic assay and characterized enzyme we set out to test if the TLM inhibition mechanism of FabF was similar to KasA. The IC_{50} for TLM with FabF was determined using the above described assay and gave an IC_{50} = 5.3 ± 0.6 μM consistent with a previous report of 6 μM(*1*). In separate assays we varied the pre-incubation time with free enzyme and with acyl-enzyme similar to our experiments with KasA. We observed no effect on IC_{50} (TLM potency) with apo or acyl-enzyme, using preincubation times of 3, 10, and 30 min. We therefore concluded that there is no slow binding component to the inhibition mechanism of TLM with *E. coli* FabF.

As we highlighted, a previously reported K_d for TLM with FabF (60 μM) is higher than would be extrapolated based on the measured IC_{50} (6 μM) but an acyl-enzyme direct binding experiment is not reported (*1*). We therefore set out to conduct our own set of direct binding experiments to correlate with our IC_{50} data and to test if the TLM differential binding phenomenon exists with FabF. A fluorescence titration with TLM and apo-FabF or C164Q- FabF was conducted and the overlaid results are shown in Figure 6. As we expect, the

direct binding experiment showed that TLM has a greater affinity for the acyl-enzyme mimic than for the apo-enzyme (K_d = 1.7 $\pm$ 0.3 μM vs. K_d = 76 $\pm$ 16 μM). This data serves to better explain previous data and suggests that TLM is a specific inhibitor of the acyl-enzyme intermediate of bacterial KAS's.

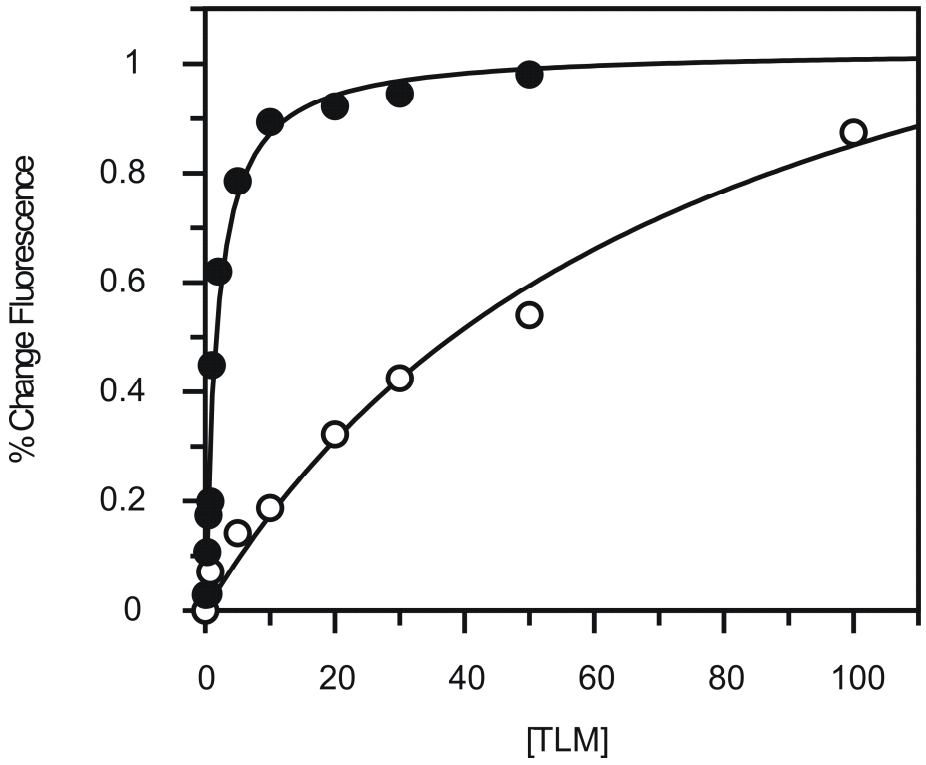

Figure 6: *Fluorescence Titrations of TLM with C164Q-FabF (filled circles) and wt-FabF (open circles) K_d values are listed in Table 5*

Table 5: *TLM Binding Data for E. coli FabF*

Protein	K_d (μM)	IC_{50} (μM)
wt-FabF	76 ± 16 μM	5.3 ± 0.3 μM[a]
C164Q	1.7 ± 0.3 μM	N/A

a. Preincubation did not effect potency

Once obtained we can now compare TLM-wt-FabF and TLM-C164Q-FabF structures in an attempt to explain the specific difference in TLM interactions within the two active sites that underscore the differential binding model.

From these kinetic experiments, we also learned that slow-onset inhibition could not be explained from an examination of FabF structures. Since we proceeded in a parallel manner with these projects (KasA and FabF) we came to the end of our FabF characterization at the same time as our KasA crystal screens came to fruition. We then realized that KasA binding could be observed directly and we focused primarily on KasA leaving FabF for our future studies. Significantly, as shown below, FabF structural comparisons with apo-C164Q-FabF and TLM-C164Q-FabF will serve as a negative control for any structural conclusions made with regard to slow binding to KasA. Ultimately, we have shown that the differential binding model is applicable to another KAS, while slow onset inhibition is not.

KasA Crystallization

During our cloning and characterization of FabF, KasA crystallization condition screens were underway at the University of Würzberg and conditions for four complexes of interest were determined (Figure 7).

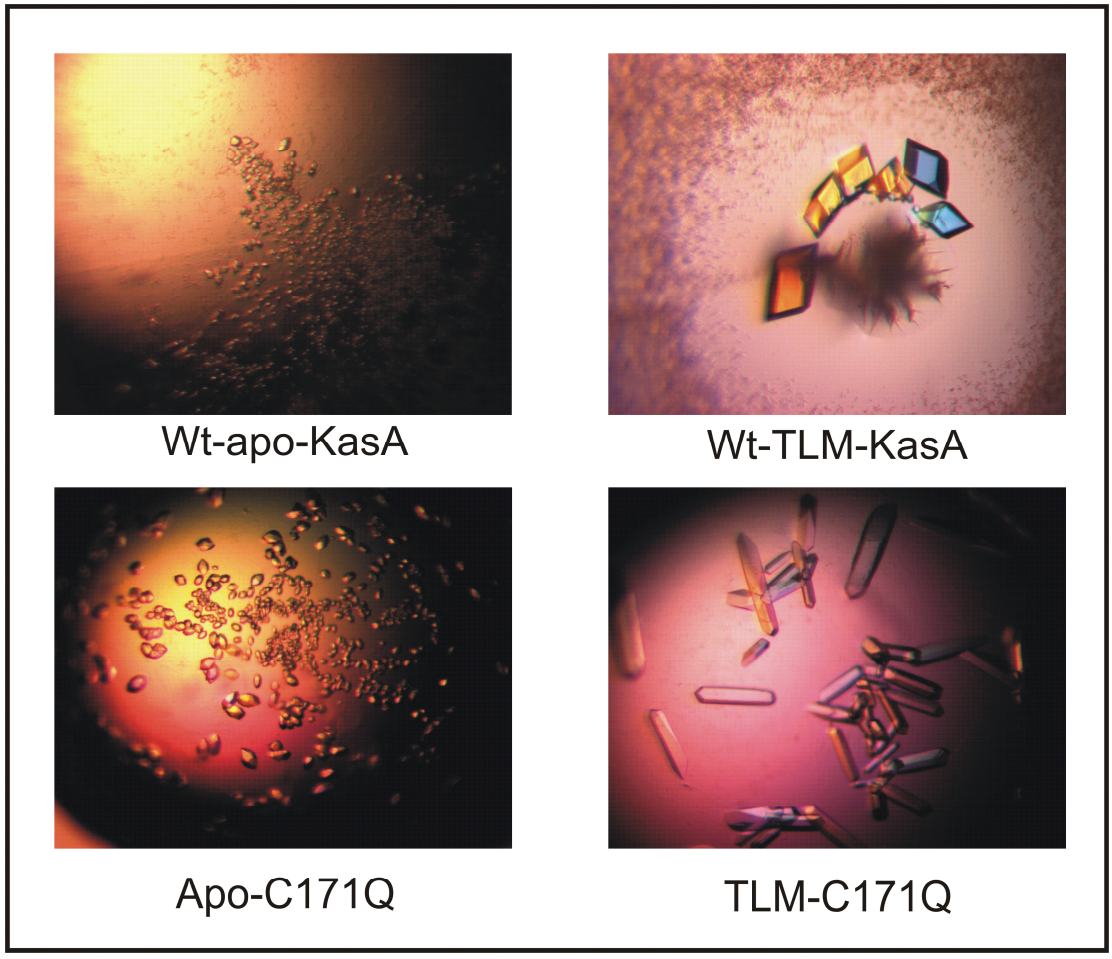

Figure 7: *Protein crystals used for the first reported structural determination of KasA and C171Q-KasA with and without TLM bound.*

Crystals obtained in condition optimization experiments were diffraction quality and used to determine the structure of KasA as well as C171Q-KasA and TLM bound C171Q-KasA by the molecular replacement technique. Recently, we have obtained preliminary refinement data for 3 of the four structures of interests (all but the WT-KasA-TLM data).

As these structures are one of our most recent developments, some additional structural refinements are currently underway. Nonetheless, we proceeded with the comparison of the TLM-C171Q and the apo-C171Q. As one would predict the overall fold of the structures are very similar when the bound and unbound data are compared (Figure 8).

Figure 8: *Overlay of TLM bound (gray) and unbound (magenta) C171Q-KasA showing a very similar global fit.*

Despite these global similarities, subtle differences between the bound and unbound structures can be observed upon close examination. Firstly, in one of the TLM bound structures the TLM isoprene (Figure 9B, green) adopts a different conformation than previously reported(*1*). This conformation also differs from the conformation found in other monomers in our own data (Figure 9A).

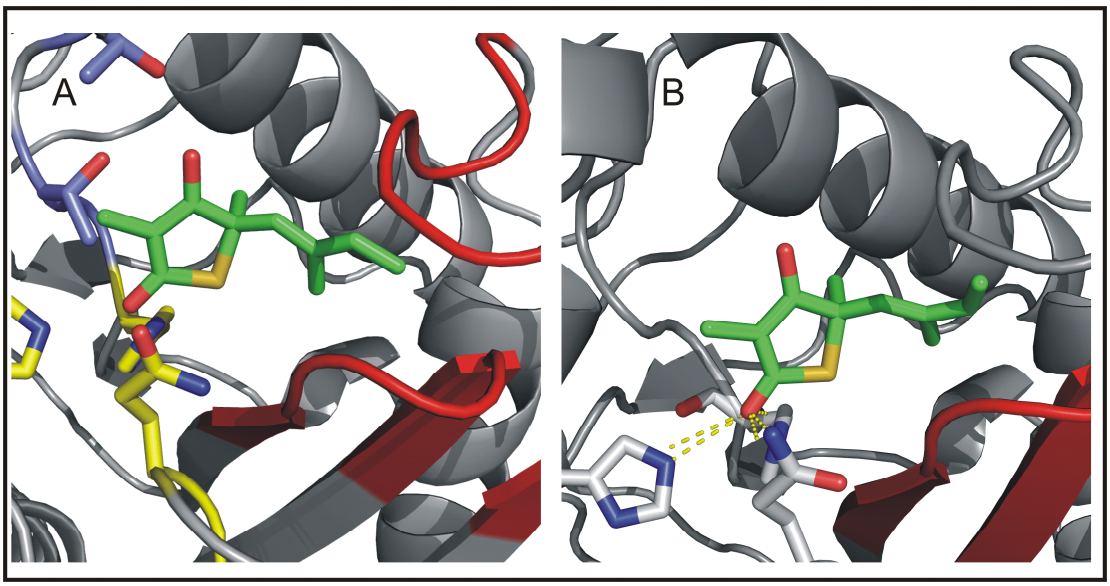

Figure 9: A. *TLM conformer bound to C171Q-KasA, similar to reported data.* **B**. *TLM bound to C171Q-KasA showing unique isoprene conformation*

Additionally, we observe other subtle changes in the structure of C171Q-KasA upon TLM binding. One such change is a rotation of the active site glutamine (Q171) to form or break an H-bond with the 4 position carbonyl (Figure 9A Q171-yellow and 9B Q171-light gray). Additional conformations of this residue are observable (Figure 10 apo-Q171 shown in cyan, TLM-Q171 shown in yellow) and further model refinement is needed to confirm these data. Such refinement may simplify these data revealing more concrete models to correlate with biochemical data.

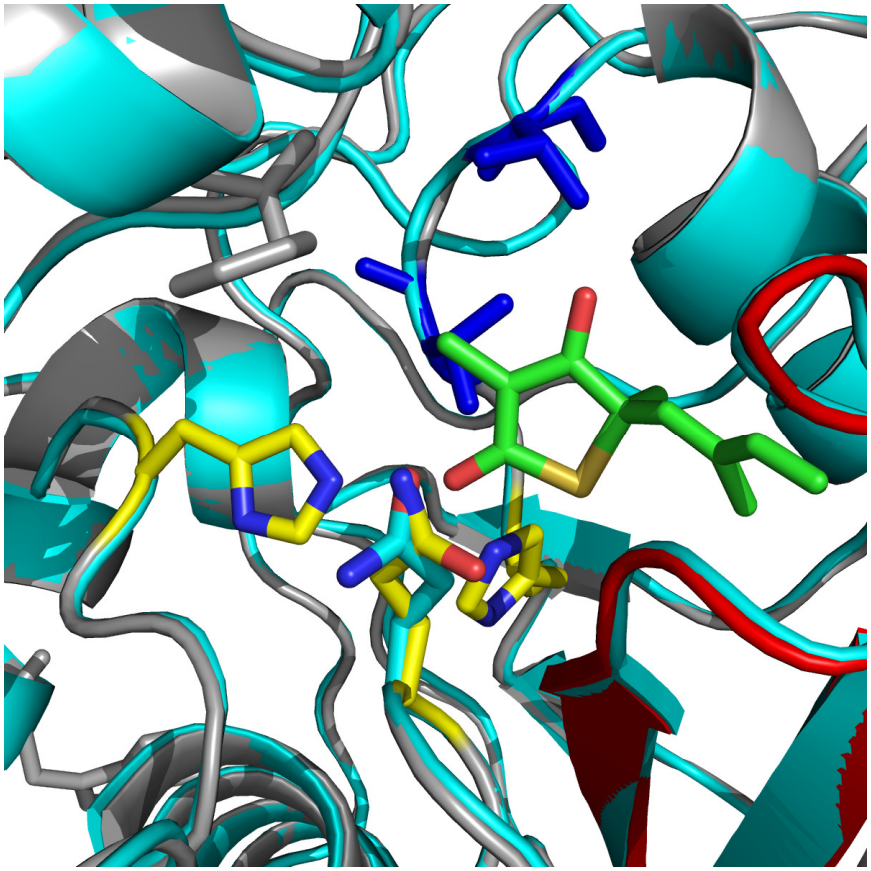

Figure 10: *Overlay of C171Q KasA bound (silver with yellow active site triad) and unbound (cyan)*

Intriguingly, ordering of a β-sheet is correlated with TLM binding. Active site helix Nα3 stacks adjacent to three β-strand structures and one of these becomes ordered upon TLM binding. When the TLM bound and unbound C171Q structures are compared, a loop structure (labeled in yellow; Figure 11 left) becomes ordered upon TLM binding to form a β-sheet (labeled gray; Figure 11 right).

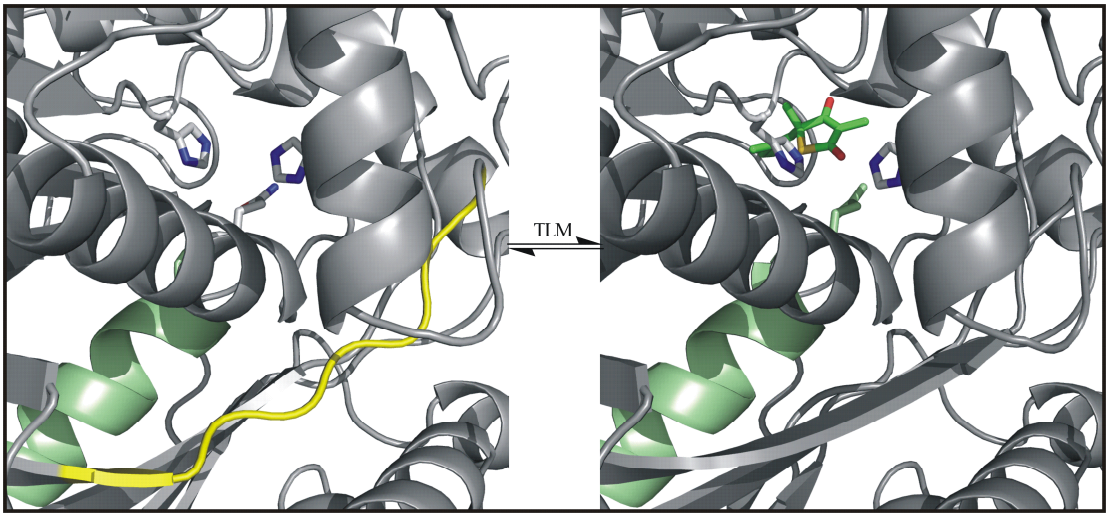

Figure 11: *β-sheet ordering upon TLM binding (yellow vs. gray); active site helix (Nα3) shown in pale green*

Finally, we observe shifts in the active site loops of approximately 1 to 1.2 Å upon TLM binding to the mutant. These preliminary models do show structural changes that correlate with TLM binding but further model refinement as well as negative control experiments with FabF must be conducted before solid conclusions are made with respect to corroborating our differential and slow binding models. Nonetheless this is an exciting and compelling structural project with its roots tied directly to our efficient expression source of soluble, active KasA.

Wild type KasA and Differential Binding

Subsequent structural comparisons were conducted in order to understand the fundamental difference in the active sites of the wild-type and mutant proteins that leads to an increase in TLM binding affinity. Unfortunately, a key piece of data (the wt-KasA-TLM structure) is still under refinement and a comparison of wild-type and mutant complexes is not yet possible. However, we did compare the apo structures of wild-type and mutant KasA (Figure 12).

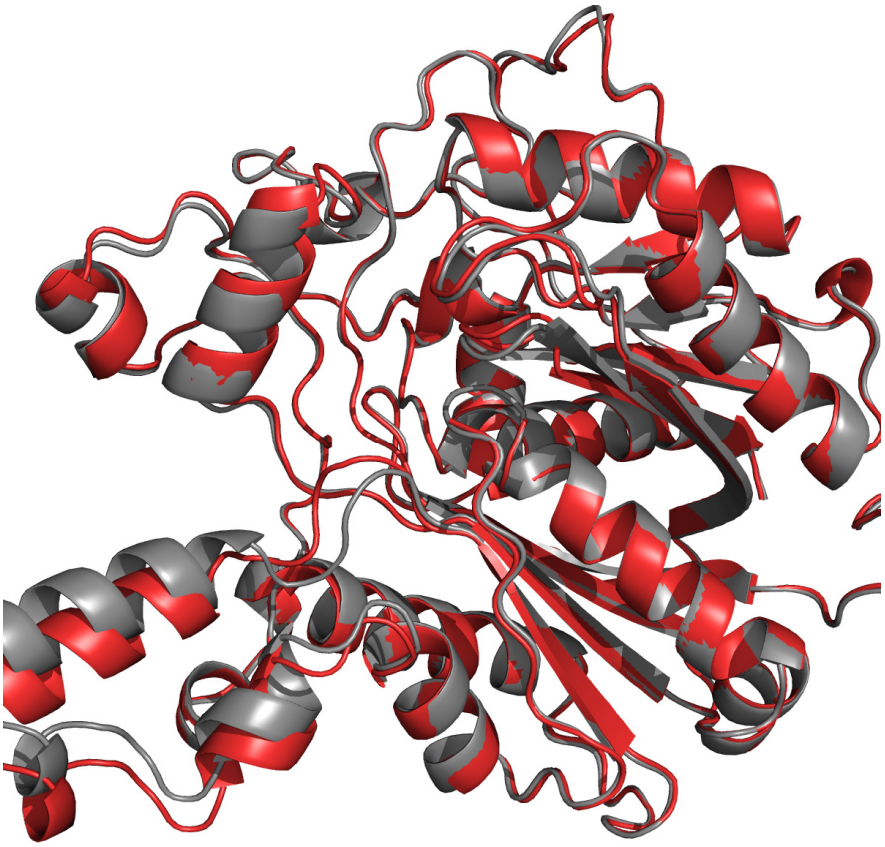

Figure 12: *Global comparison of wt-KasA (red) and Acyl-mimic C171Q (gray) showing significant conformational changes*

As shown in Figure 12 there are significant conformational differences between the WT-KasA (red) and acyl-mimic C171Q (gray). One might predict such conformational changes based solely on the switch in enzyme activity from a transferase to a decarboxylase. Upon closer examination of the active site rearrangements we observe changes similar to those previously reported by Wang *et al*(*3*).

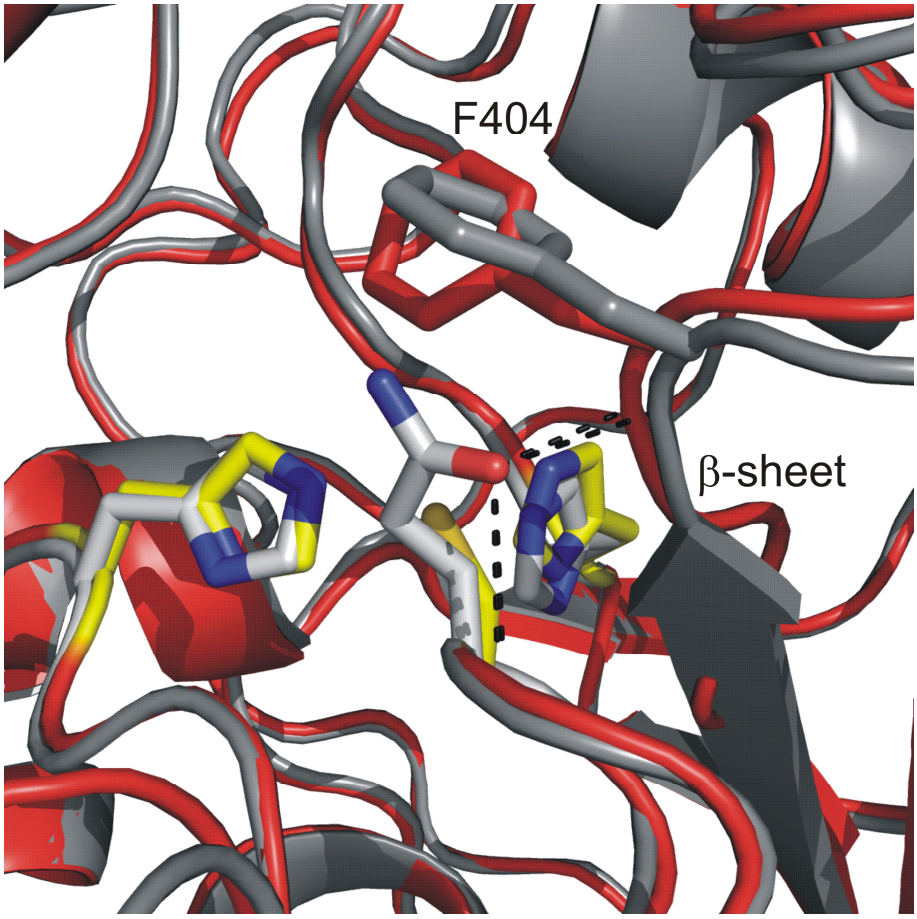

Figure 13: *WT/C171Q active site overlay showing structural changes. Q171-light gray, C171-yellow; WT-KasA backbone (red) becomes ordered β-sheet (gray)in C171Q*

Wang *et al* structurally characterized the difference between WT-FabF and C164Q-FabF. Consistent with this report we observe a rotation in F404

(Figure 13). This residue is considered by Wang to be the “gatekeeper” residue converting FabF from the closed (transferase) conformation to the open (decarboxylase) conformation. Additionally, the backbone amide of F404 is thought to stabilize the negative charge build up at the carbonyl oxygen of the acyl-enzyme thioester as part of the oxyanion hole(*3, 15, 16*). This is consistent with the H-bond from the carbonyl oxygen of Q171 to the backbone amide shown as a black dashed line in Figure 13. The backbone amide of C171 (Q171) also forms an H-bond to this oxygen in the oxyanion hole contributing to catalysis (again shown as a black dashed line). Finally, we observe another β-sheet ordering event (labeled in Figure 13) distinct from the ordering event described above. As shown in red, the WT-KasA structure has a less ordered region at the N-terminal side of F404. The formation of H-bonds between the thioester mimic and the oxyanion hole (black dashed lines) apparently contribute to the stability of this β-sheet substructure.

Although these structural determinations are preliminary, they create an intriguing and exciting platform for the discussion of our extensive biochemical characterization of the complex KasA TLM interaction. Additionally, as we will see in Chapter 4 the structural and biochemical characterization of KasA inhibition by TLM will not only significantly contribute to the literature but will aid in our own structure based drug design and synthesis.

References:

(1) Price, A. C., Choi, K. H., Heath, R. J., Li, Z., White, S. W., and Rock, C. O. (2001) Inhibition of beta-ketoacyl-acyl carrier protein synthases by thiolactomycin and cerulenin. Structure and mechanism. *J Biol Chem 276*, 6551-9.

(2) Jones, A. L., Gane, A. M., Herbert, D., Willey, D. L., Rutter, A. J., Kille, P., Dancer, J. E., and Harwood, J. L. (2003) Beta-ketoacyl-acyl carrier protein synthase III from pea (Pisum sativum L.): properties, inhibition by a novel thiolactomycin analogue and isolation of a cDNA clone encoding the enzyme. *Planta 216*, 752-61.

(3) Wang, J., Soisson, S. M., Young, K., Shoop, W., Kodali, S., Galgoci, A., Painter, R., Parthasarathy, G., Tang, Y. S., Cummings, R., Ha, S., Dorso, K., Motyl, M., Jayasuriya, H., Ondeyka, J., Herath, K., Zhang, C., Hernandez, L., Allocco, J., Basilio, A., Tormo, J. R., Genilloud, O., Vicente, F., Pelaez, F., Colwell, L., Lee, S. H., Michael, B., Felcetto, T., Gill, C., Silver, L. L., Hermes, J. D., Bartizal, K., Barrett, J., Schmatz, D., Becker, J. W., Cully, D., and Singh, S. B. (2006) Platensimycin is a selective FabF inhibitor with potent antibiotic properties. *Nature 441*, 358-61.

(4) White, S. W., Zheng, J., Zhang, Y. M., and Rock. (2005) The structural biology of type II fatty acid biosynthesis. *Annu Rev Biochem 74*, 791-831.

(5) Young, K., Jayasuriya, H., Ondeyka, J. G., Herath, K., Zhang, C., Kodali, S., Galgoci, A., Painter, R., Brown-Driver, V., Yamamoto, R., Silver, L. L., Zheng, Y., Ventura, J. I., Sigmund, J., Ha, S., Basilio, A., Vicente, F., Tormo, J. R., Pelaez, F., Youngman, P., Cully, D., Barrett, J. F., Schmatz, D., Singh, S. B., and Wang, J. (2006) Discovery of FabH/FabF inhibitors from natural products. *Antimicrob Agents Chemother 50*, 519-26.

(6) Wang, J., Kodali, S., Lee, S. H., Galgoci, A., Painter, R., Dorso, K., Racine, F., Motyl, M., Hernandez, L., Tinney, E., Colletti, S. L., Herath, K., Cummings, R., Salazar, O., Gonzalez, I., Basilio, A., Vicente, F., Genilloud, O., Pelaez, F., Jayasuriya, H., Young, K., Cully, D. F., and Singh, S. B. (2007) Discovery of platencin, a dual FabF and FabH inhibitor with in vivo antibiotic properties. *Proc Natl Acad Sci U S A 104*, 7612-6.

(7) Sridharan, S., Wang, L., Brown, A. K., Dover, L. G., Kremer, L., Besra, G. S., and Sacchettini, J. C. (2007) X-ray crystal structure of Mycobacterium tuberculosis beta-ketoacyl acyl carrier protein synthase II (mtKasB). *J Mol Biol 366*, 469-80.

(8) Kortemme, T., and Creighton, T. E. (1995) Ionisation of cysteine residues at the termini of model alpha-helical peptides. Relevance to unusual thiol pKa values in proteins of the thioredoxin family. *J Mol Biol 253*, 799-812.

(9) Schaeffer, M. L., Carson, J. D., Kallender, H., and Lonsdale, J. T. (2004) Development of a scintillation proximity assay for the Mycobacterium tuberculosis KasA and KasB enzymes involved in mycolic acid biosynthesis. *Tuberculosis (Edinb) 84*, 353-60.

(10) Frydrych, I., and Mlejnek, P. (2007) Serine protease inhibitors N-alpha-Tosyl-L-Lysinyl-Chloromethylketone (TLCK) and N-Tosyl-L-Phenylalaninyl-Chloromethylketone (TPCK) are potent inhibitors of activated caspase proteases. *J Cell Biochem*.

(11) Schaeffer, M. L., Agnihotri, G., Volker, C., Kallender, H., Brennan, P. J., and Lonsdale, J. T. (2001) Purification and biochemical characterization of the Mycobacterium tuberculosis beta-ketoacyl-acyl carrier protein synthases KasA and KasB. *J Biol Chem 276*, 47029-37.

(12) Plietker, B. (2003) RuO4-catalyzed ketohydroxylation of olefins. *J Org Chem 68*, 7123-5.

(13) Karim, M. R., and Sampson, P. (1990) pp 598-605.

(14) Ogawa, K., Terada, T., Muranaka, Y., Hamakawa, T., Hashimoto, S., and Fujii, S. (1986) Studies of hypolipidemic agents. I. Syntheses and hypolipidemic activities of 1-substituted 2-alkanone derivatives. *Chem Pharm Bull (Tokyo) 34*, 1118-27.

(15) Heath, R. J., and Rock, C. O. (2002) The Claisen condensation in biology. *Nat Prod Rep 19*, 581-96.

(16) Haapalainen, A. M., Merilainen, G., and Wierenga, R. K. (2006) The thiolase superfamily: condensing enzymes with diverse reaction specificities. *Trends Biochem Sci 31*, 64-71.

Chapter 4

Fragment Based Design of TLM Analogues Guided by Structural Models and ILOE-NMR

Thiolactomycin; Background and Discovery

Modern Synthetic Routes to TLM

SAR studies of TLM

TLM Patent Literature

Structural Insights

Introduction to ILOE-NMR

Materials and Methods

Results & Discussion

Thiolactomycin background and discovery

Thiolactomycin (TLM) is a natural product thiolactone first isolated from *Nocardia* sp., a bacterial strain identified by a group of scientists at a Japanese pharmaceutical company (Chugai Pharmaceuticals) in 1981. The actinomycetes strain, belonging to the genus *Norcardia* based on genomic studies, was identified from a soil sample collected in Sayama City, Saitama Prefecture, Japan(*1*). An assay for antibiotic activity against *Pseudomonas aeruginosa* in fermentation broth was first used to detect the activity of TLM. Ultimately the producing strain was identified and TLM was purified and structurally characterized(*1, 2*). The purification from fermentation broth that had been used to grow *Nocardia* utilized a simple extraction with chloroform and a silica gel column eluted with benzene:acetone 95:5. The initial characterization of TLM included UV, IR, ^{1}H NMR, and ^{13}C NMR spectroscopy correctly solving the structure shown in Figure 1.

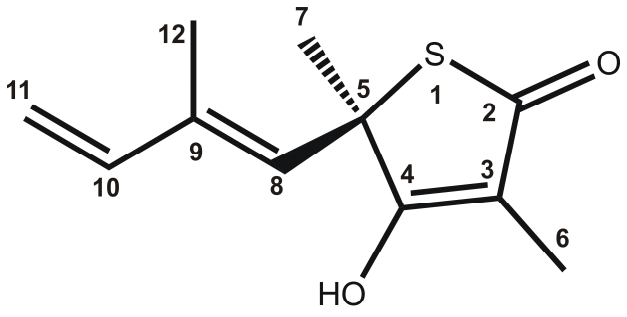

Thiolactomycin

Figure 1: *Labeled carbons show IUPAC numbering*

The ^{13}C NMR spectra were later (2003) shown by Reynolds *et al* (*3*) to have two carbon peak assignments reversed when compared to the original report. These later assignments were reconfirmed by our own gradient HMQC and HMBC experiments as described in materials and methods (below) and the chemical shifts, IUPAC numbering and assignments are summarized in Table 1.

Table 1: *^{13}C assignments for Thiolactomycin*

Carbon	^{13}C Chemical Shift[a] (ppm) ($CHCl_3$)	^{13}C Chemical Shift[b] (ppm) ($CDCl_3$)	^{13}C Chemical Shift[c] (ppm) (D_2O)
C-2	197.3	197.7	198.6
C-3	110.9	*140.0*[d]	104.4[e]
C-4	180.2	180.7	201.0[e]
C-5	55.8	55.7	58.7
C-6	8.1	7.7	8.5
C-7	30.2	29.5	29.5
C-8	129.5	129.3	133.6
C-9	140.8	*110.3*[d]	141.0
C-10	141.0	140.7	141.3
C-11	114.5	113.8	113.5
C-12	12.5	12.1	12.5

a. Previously reported by Reynolds *et al* 2003 (*3*)
b. Original assignment by Sasaki *et al* 1982 (*2*)
c. Assignments based on studies conducted at SBU (Machutta, Picart)
d. Peak assignments shown to be incorrectly reversed
e. Solvent (D_2O) effect on resonance

In conjunction with the initial identification and characterization of TLM(*1, 2*), two additional papers describing the *in vitro* antimicrobial activity(*4*) as well as reports on the toxicity and bioavailability(*5*) can be found in four seminal back to back papers in the April 1982 issue of *J. Biochem.* (Tokyo). The minimum inhibitory concentration (MIC) values for TLM against a wide variety of both Gram positive and Gram negative bacteria are reported in this initial study as well as in many subsequent studies. These data are summarized in Table 2 and illustrate TLM's broad spectrum of antimicrobial activity and utility as a lead molecule.

Table 2: *Broad spectrum In vitro Biological data for Thiolactomycin*

Organism	MIC (µg/ml)	Ref	Organism	MIC (µg/ml)	Ref
B. subtilis PCI-219	100	(*4*)	*H. influenzae* 1014-33	3.1	(*4*)
B. cereus T-1	200		*H. influenzae* 1076-48	6.3	
M. luteus B	25		*H. influenzae* 764-69	3.1	
S. pyogenes SV	37.5		*Ps. aeruginosa* J272	800	
S. epidermidis TO-3	50		*Ps. aeruginosa* M-57740[g]	1.6	
S. aureus 209-P	25		*M. tuberculosis* H_{37}RV	25	
S. aureus JU-5	50		*M. tuberculosis* H_{37}RV-SMr[a]	25	
S. aureus A-5	50		*M. tuberculosis*H_{37}RV-INHr[b]	25	
E. coli NIHJ	50		*M. tuberculosis*H_{37}RVPASr[c]	12.5	
E. coli NO-9	50		*M. tuberculosis* H_{37}RV	25	(*6*)
E. coli 11	25		*M. smegmatis*	75	(*6*)
S. enteritidis	12.5		*M. tuberculosis* H_{37}RV	13	(*7*)
S. typhi	12.5		*E. coli* ANS1	1	(*7*)
K. pneumoniae 3K25	200		*S. aureus*[e]	128	(*8*)
K. pneumoniae 15C	100		*M. catarrhalis*	0.25	(*8*)
Sh. flexneri 2b T-1	6.3		*H. influenzae*	2	(*8*)
Sh. sonnei T-1	100		*B. fragilis*	1	(*8*)
S. marcescens FU111	50		*S. aureus*	64	(*9*)
S. marcescens T-50	50		*S. aureus* (MRSA)	64	(*9*)
B. fragilis	3.12		*P.falciparum*[e,f]	143	(*10*)

M. tuberculosis H_{37}RV[d]	MIC $_{(PAS)}$	MIC $_{(RIF)}$
	12-25 µg/ml (*11*)	32 µg/ml (*12*)

a. Streptomycin resistant
b. Isoniazid (INH) resistant
c. Pyrazinamide (PAS) resistant
d. MIC data for Rifampacin (RIF) and PAS
e. Racemic TLM used in measurement
f. Reported as IC_{50} value in whole cell viability assay
g. Ampicillin sensitive mutant

The potency of growth inhibition for TLM was generally moderate and bacteriostatic for most bacteria. Significantly, the MIC value for TLM against MTB is comparable to frontline drugs pyrazinamide (PAS) and rifampicin (RIF) (Table 2) and TLM activity was observed under anaerobic conditions in assays against *B. fragilis* (Table 2)(4). Recalling the anaerobic environment found within an infected macrophage, these data combine to make TLM an appealing pharmacophore for anti-TB chemotherapy development.

Despite TLM's moderate *in vitro* activity it is rapidly absorbed in rats when administered both orally and by intramuscular injection (20 mg/kg) with the peak serum concentration (49μg/ml) reached within 15 minutes(*5*). This allows TLM to protect rats against both systemic and urinary tract infections. Rats were challenged systemically and transurethrally with several strains of *S. marcescens, K. pneumoniae* and *E. coli* and TLM showed a marked protective effect against infection(*5*). Finally the excretion of TLM was quantified by an HPLC assay and shown to have a 52.8% urinary clearance after 24 hours with only 0.42% biliary excretion suggesting that TLM is not suseptable to first pass glucuronidation in the liver as a primary mode of excretion.

TLM has also shown activity in a murine macrophage model of *M. tuberculosis* infection(*6*). Bone marrow macrophages purified from mice were infected with MTB and treated with TLM. TLM decreased the number of

viable MTB in a dose dependent manner in this model as well as in culture. These data show that TLM is not only active *in vitro* against MTB but also efficiently penetrates murine macrophages. This report also presents supporting data for the *in vitro* molecular target of TLM; the fatty acid biosynthesis (FASII) cycle (below). The incorporation of [^{14}C]-acetate into mycolic acids in *M. smegmatis* was monitored by reverse phase TLC to show that TLM inhibits the synthesis of these long chain FASII products. The activity of TLM in a mouse model of MTB infection is not yet reported in the literature however given the above summarized data one could hypothesize that TLM would show *in vivo* efficacy in such a model.

The appeal of TLM as a lead molecule extends beyond these *in vitro* data when one considers the physical properties of TLM. TLM satisfies the entire set of Lipinski's "Rule of 5" (Table 3), a set of rules that describe a compounds drug-likeness based on the physio-chemical properties of the 90th percentile of drug candidates that reached Phase-II clinical trials(*13*). According to Lipinski, a 30 year drug discovery veteran at Pfizer, to be a drug-like molecule the candidate should have less than 5 hydrogen bond (H-bond) donors, less than 10 H-bond acceptors, a molecular weight of less than 500 and a calculated partition coefficient (clogP) of less than 5. These four rules of 5 are not only satisfied by TLM (Table 3) but leave significant room for modification of the pharmacophore.

Table 3: *Thiolactomycin and Lipinski's Rule of 5*

Rule	Thiolactomycin
Less than 5 H-Bond donors	0-1[a]
Less than 10 H-Bond acceptors	2-3[a]
Molecular weight less than 500 g/mol	210 g/mol
clogP[b] of less than 5.0	2.1-3.0[c]

a. Dependent on pH (protonation state of 4 position hydroxyl)
b. Calculated partition coefficient
c. Calculated using Chemdraw (*2.8*), ChemAxon (*2.1*), and as previously reported (*3.0*) (*7*)

TLM is a selective and reversible FAS-II inhibitor that is known to inhibit KAS enzymes(*1, 6, 14*), but does not inhibit the mammalian FAS-I enzyme(*15*). TLM resistant *E. coli* strains contain mutations in the *fabB* gene(*16*) and overproduction of FabB confers TLM resistance *in vivo* (*17*) suggesting that FabB is the major cellular target. Additionally over-expression of KasA in MTB confers resistance reaffirming that KAS inhibition is the dominant molecular mechanism(*18*). Based on kinetic and structural data, TLM is thought to be a competitive inhibitor of malonyl-Acp (*14, 19*). Similar to the selectivity of platencimycin, our studies have shown that TLM binds preferentially to the covalently modified KAS acyl-enzyme intermediate (Machutta *et al* unpublished data) (Chapter 2). We have also observed compelling data that suggests that the differential binding model proposed in Chapter 2 is a general TLM binding model for KAS enzymes (Chapter 3). These data solidify assumptions we make about the similarity of structural models made using KAS enzymes from other bacteria (*E. coli* FabF) and explicitly used for our own rational inhibitor design efforts (presented below).

Additionally, our differential and slow binding models discussed in Chapter 2 revitalize the interest in TLM as a lead molecule. In a recent Nature Drug Discovery paper (*20*), Copeland *et al* highlight the implications of inhibitor residence time on lead optimization and *in vivo* efficacy. Copeland discusses an intuitively simple principle first conceptualized by Paul Ehrlich at the turn of the twentieth century; *corpora non agunt nisi fixate* or "a substance will not work unless it is bound"(*21*). The residence time or length of time an inhibitor is bound to a target is influenced by both the rate of association (k_{on}) and the rate of dissociation (k_{off}). Ultimately, an inhibitor with a rapid reversible binding mode can produce residence times on the order of seconds while slow onset inhibitors can remain bound to their target for hours or even days. A variety of drugs owe their clinical efficacy to extraordinarily long residence times and are summarized by Copeland and others(*20, 22, 23*). The discovery of the slow binding mechanism of TLM to the acyl-enzyme intermediate of KasA will serve to increase its appeal over rapid reversible inhibitors because of this principle of residence time.

Given our extensive work with FAS enzymes and in particular with *M. tuberculosis* KasA, we chose the TLM-KasA system as a platform for anti-bacterial drug discovery efforts. Our goal to this end is to make structural modifications to the TLM pharmacaphore that retain high absorption and bioavailability in animals while optimizing target binding affinity.

Modern synthetic Routes to TLM

Several synthetic and semi-synthetic (*24*) strategies for TLM and TLM analogues have been developed, but significant synthetic challenges remain with respect mostly to yield and difficulty. The first synthesis of racemic TLM was reported in 1984(*25*). Subsequently, an asymmetric synthesis of the (5*S*) isomer was reported(*26*), however this isomer is now thought be inactive against KAS(*7*). The advent of an asymmetric synthesis of (5*R*) TLM from D-alanine in 2002 is efficient and flexible, allowing for the incorporation of variability on the thiolactone ring (Figure 2). Recently, an additional synthetic approach to the natural (5*R*) TLM has been reported(*27*). More recently, Kumal *et al* reported a partial enzymatic synthesis involving a lipase-mediated alcoholysis(*24*). In this report a commercially available *Carica papaya* lipase was utilized in a transesterification reaction to generate an intermediate in the synthesis of TLM(*24*). This synthetic strategy, though interesting, has not been used to generate TLM analogues for biological evaluation.

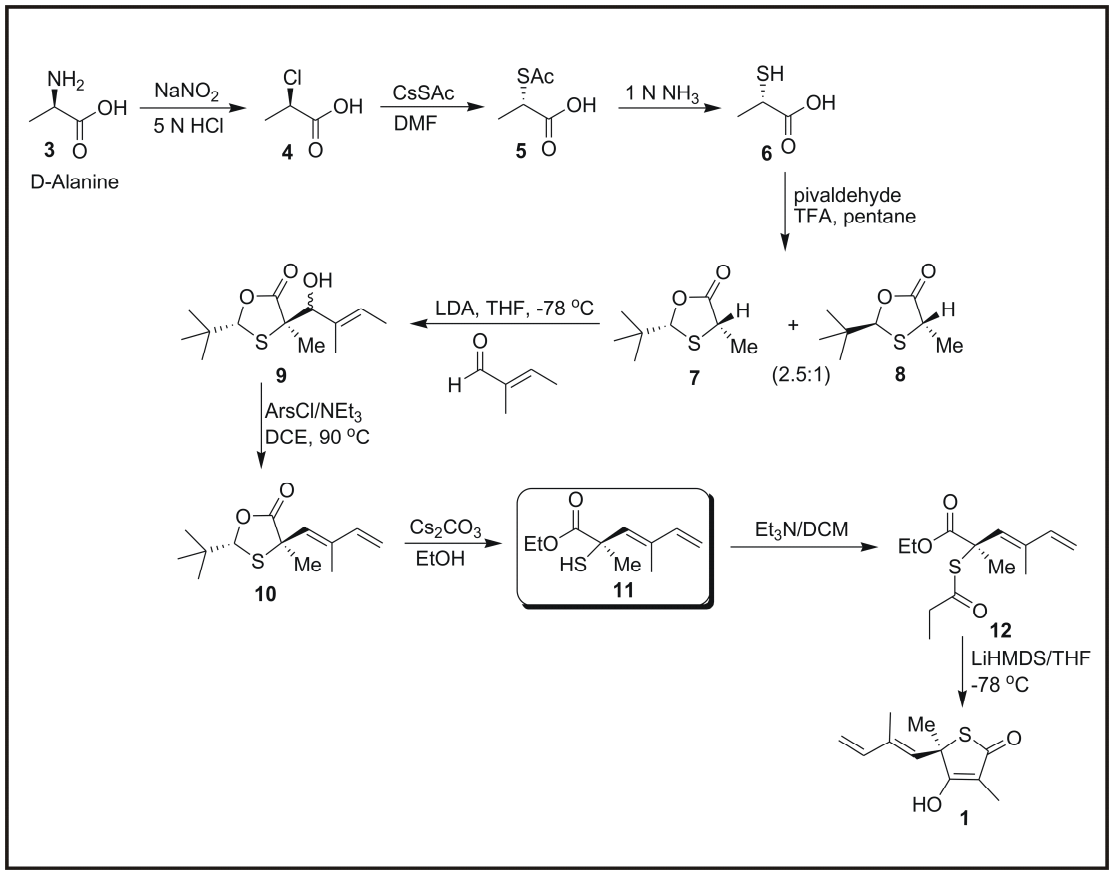

Figure 2: *Synthesis of (5R) Thiolactomycin (28)*

SAR studies of TLM

Synthetic accessibility at the 5 position has driven the bulk of the currently reported structural modifications to the TLM phamacophore(*7, 29-31*). While reports of TLM analogues with increased activity are presented in the literature many of these compounds are tested in whole cell assays against *P. falciparum, E. coli, S. aureus,* and MTB making conclusions about target

binding optimization and rigorous structure activity relationships (SAR) impossible. Besra and colleagues report 5 position biphenyl compounds with increased affinity for *mtb*FabH, the KASIII from MTB, but whole cell data is never reported(*32-34*). Interpretation of these studies is further complicated by the fact that FabH is not thought to be essential to MTB(*35*) and that multiple KAS activities (KAS I, II and III as well as polyketide synthases (PKS)) exist within the cell. TLM, with moderate affinity for these other KAS domains, could conceivably be optimized by structural modifications, making conclusions from whole cell assays difficult to interpret.

Nonetheless a report on 5 position TLM analogs with both IC_{50} and MIC data does provide some insight into rigorous SAR with *E. coli* FabB and KasA(*7*). This report clearly shows that the 5 position isoprene is essential for binding using *in vitro* enzyme assays. TLM binding is mostly intolerable to substitution. For instance, saturation of the terminal double bond of the 5 position isoprene abrogates binding. Modifications that were tolerated at the 5 position were groups containing long aliphatic chains consistent with the binding mode of the TLM isoprene. Based on TLM-FabB X-ray structures the isoprene is clearly stacked between two active site loops that are thought to be involved in fatty acid substrate binding(*14*). This binding mode is consistent with our own observations of the TLM-KasA X-ray crystal structure (Chapter 3).

In an SAR study using *P. falciparum*, the causative agent of malaria, and pure recombinant pfKasIII, Jones and colleagues showed that modifications at the 3 and 4 position, pointing toward the unoccupied pantetheine binding site, were tolerated and in some cases showed increased potency(*10*). These data however are complicated by a weak correlation between the *in vitro* activity against the pure enzyme and the whole cell MIC suggesting possible off target effects(*10*). Again, one could rationalize these results by hypothesizing that TLM binding has been optimized to one of the other KAS domains present in the cellular milieu.

Despite the utility of rigorous SAR studies with TLM, (involving pure enzyme and whole cell assays) such reports are lacking in the literature. As highlighted by the synthetic scheme in Figure 2, modifications at the 3 position are synthetically accessible (below). The synthetic accessibility and absence of 3 position SAR work in the literature combine to provide a niche suitable for the potential development of more potent compounds. 3 position analogs of TLM become even more appealing following a discussion of our own structural and NMR studies (below).

Patent Literature

As one would predict, the patent literature has greater than twenty entries for TLM and TLM analogs. Our understanding of the scope of TLM utility is

further broadened upon examination of these patent fillings. TLM is of course patented for a variety of anti-microbial applications from an anti-*Moraxella* surface sterilizing agents to anti-endoparasitic agents. TLM is also patented for use as an inhibitor of pigmentation by inhibition of FAS, inhibition of neuropeptide Y and analogs of TLM inhibit the eukaryotic FAS-I which is a target for the development of anti-tumor agents. In our search for TLM and thiotetronic acids in the patents literature we found no patent filings for TLM utility as an anti-TB agent. A more complete understanding of these patent filings will require the consultation of experts in patent law, but our preliminary examination is encouraging in the context of our TLM based anti-TB drug development program.

Structural Insights

A general binding mode for TLM has been structurally elucidated by studies reported by Price *et al* using co-crystallization conditions with *E. coli* FabB(*14*). These structural insights with TLM have been extended by our own studies using co-crystals of KasA as well as the more tightly bound mutant C171Q-KasA discussed in Chapter 3. In general the binding mode and active site interactions are similar when the TLM-FabB and TLM-KasA structures are compared.

The KAS active site can be considered in two halves; the acyl transfer half (transferase) and the malonyl-Acp decarboxylation half (decarboxylase) (*7, 14*). TLM binds to the malonyl-Acp binding half and is thought to mimic this substrate (Figure 3) via hydrogen bonding interactions between the active site histidines and the 2-position carbonyl oxygen of TLM. The 4-position hydroxyl (oxygen anion) forms hydrogen bonds with a series of water molecules that in turn form hydrogen bonds with backbone amides lining the pantetheine binding channel. The sulfur heteroatom in TLM does not have a clear H-bond partner in any reported X-ray structure. This is consistent with experiments where substitution of the heteroatom in TLM did not significantly effect binding affinity(*10*). Finally, the 5 position isoprene moiety is stacked between two hydrophobic substrate binding loops. These data are summarized schematically in Figure 3 and an X-ray structural model of TLM in complex with C171Q KasA is shown in Figure 4.

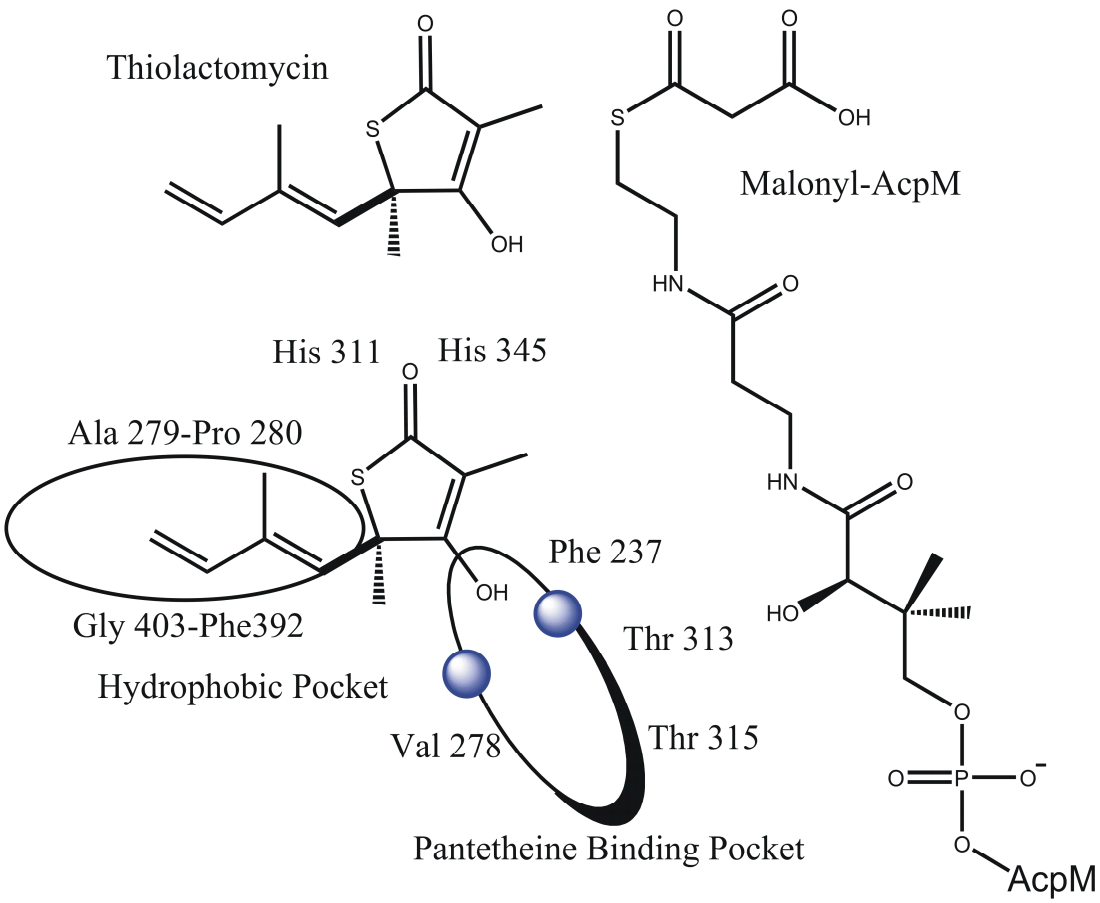

Figure 3: *Comparison of TLM and Malonyl-AcpM; Schematic representation of active site occupancy by TLM (36) Blue dots represent water molecules*

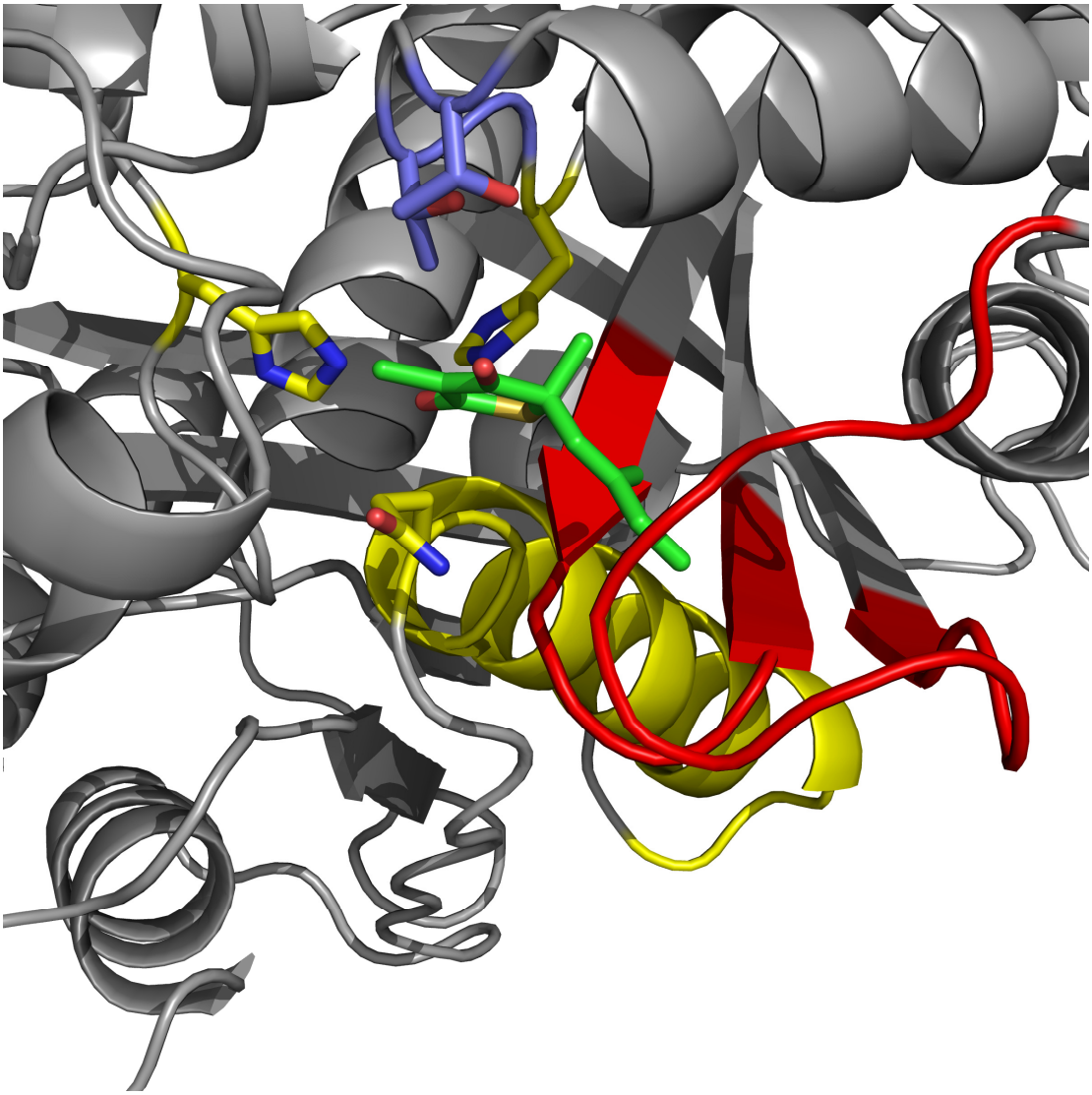

Figure 4: *C171Q-KasA-TLM X-ray Structure. Active site helix and triad labeled in yellow, Conserved threonines (313 and 315) labeled blue, Active site loops labeled red, TLM shown in green.*

Introduction to ILOE-NMR

Given the highlighted TLM analog synthetic challenges, we set out to rationally modify the TLM pharmacophore while reducing the amount of chemical synthesis required for obtaining a more potent inhibitor. This, being the shared goal of the bulk of drug discovery science, there is no shortage of techniques for inhibitor optimization. However, at the onset of this project a detailed molecular mechanism and an X-ray crystal structure for the TLM-KasA complex was not yet known. We therefore sought, in parallel, to obtain both X-ray structural information (Chapter 3) and to probe specific interactions within the active site in the absence of structural data.

The inter-ligand Nuclear Overhauser Effect (ILOE-NMR) technique, similar to SAR by NMR, is an efficient and powerful way to screen for small molecule fragments that bind to adjacent sub-sites on a drug target. The ILOE technique is distinct from SAR by NMR in that ^{15}N labeled protein is not needed and signals from the protein (amide chemical shift changes) are not observed. This fragment based concept, illustrated in Figure 5, was pioneered more than ten years ago by Hajduk *et al*. (*37-39*) working as a post-doctoral scientist at Abbott Pharmaceuticals and extended to the ILOE technique by the work of Maurizio Pellecchia(*40*). The ILOE technique utilizes through space NOE effects to report on proximity interactions between small molecule fragments while they are bound to adjacent sites on a protein.

The NOEs that are developed during the bound state transfer to the unbound state as long as the rate of ligand dissociation is more rapid than the relaxation time of the NOE(*40*). These NOE imprints give essential and potentially detailed information about the relative binding orientation and relative distances between the bound fragments. The technique is most often employed to screen a mixture of compound for ligands (fragments) bound to adjacent sites. This so called fragment based drug design approach has gained popularity in drug discovery science since its advent in the early 1990's. Our work employs the ILOE-NMR technique; however fragment library screens have not yet been added to our inhibitor development toolbox. Rather; the context that ILOE-NMR was used in our studies was simply to determine the relative orientation of two ligands within the active site of KasA.

We hypothesized that the TLM binding site and the adjacent pantetheine binding site would bind their respective ligands simultaneously. Additionally we hypothesized that the relative orientation of the molecules within the active site could be probed using established ILOE-NMR technology. In order to probe the relative binding mode of the ligands within the active site a series of pantetheine analogs (pantoylamides) with increasing aliphatic chains lengths were synthesized (materials and methods). These analogs were characterized using ^{1}H NMR and ^{13}C NMR (below).

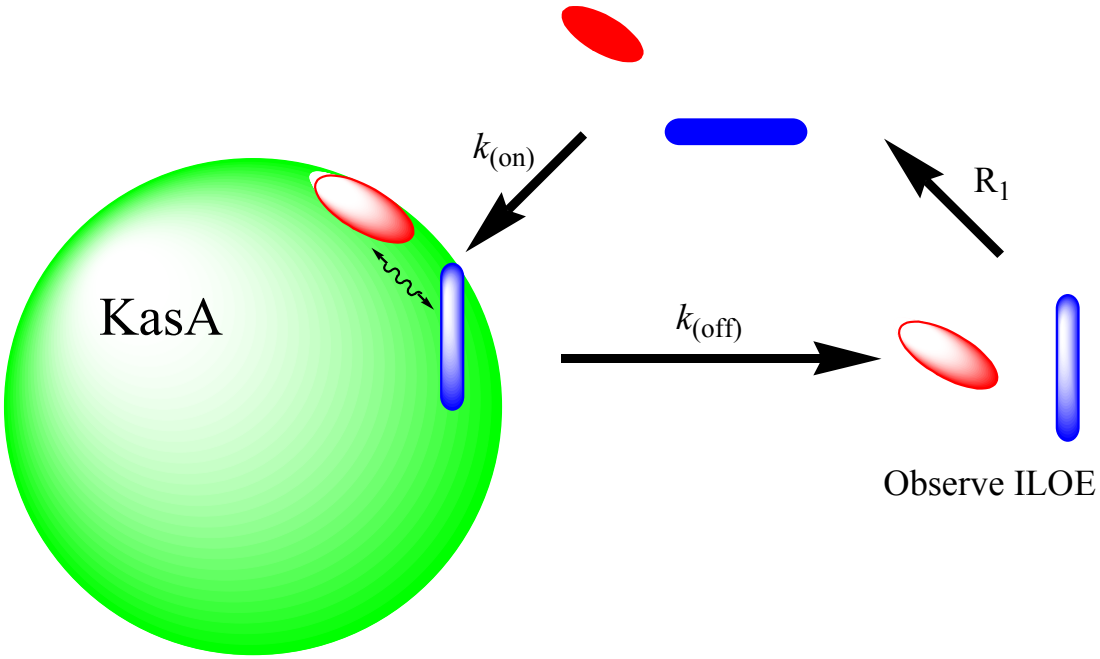

Figure 5: *Schematic Representation of ILOE-NMR*

Extension of the ILOE-NMR technique

During our initial characterization of the TLM-pantoylamide-KasA ternary complex using two dimensional NOESY, it became apparent that a significant increase in NOE intensities would be required to properly understand the relative binding orientation of the two ligands. Significantly, the continued contributions of Francis Picart (Director of NMR Instrumentation, Dept. of Chemistry, Stony Brook University) lead us to an extension of the SAR by NMR technique that yields the needed increase in NOE intensity. The technique allows for the selective inversion of NOE such that specific questions about these interactions can be asked.

The basis of our extension to the ILOE-NMR technique is a 1D NOE experiment that employs pulsed field gradients and selective excitations. The method was first developed to detect enhanced NOE intensities and suppress all other background signals by Shaka *et al(41, 42)*. In this technique a double pulsed field gradient spin echo (DPFGSE) experiment was employed to achieve greater sensitivity and resolution once the initial 2D NOESY signal was observed. In these studies single ^{1}H peaks are observable (1D spectrum) after selective inversion of target peaks corresponding to the though space NOE interactions with the single inverted proton peak. The utility of these studies is apparent not only in the increased signal strength but in the simplification of the spectral de-convolution. The drawback of the Shaka method is that complete NOE build up experiments must be performed to estimate distances within the 10 Å upper limit of this technique.

Materials and Methods

Materials

TLM purified from Nocardia was generously provided by Cynthia Dowd and Clifton Barry III at the National Institute for Allergy and Infectious Diseases (NIAID). Buffers and other reagents were purchased from Fisher Scientific. Deuterium Oxide (D_2O) was purchased from Cambridge Isotope Laboratories Inc. (CIL).

Protein Purification and Preparation

KasA and *E. coli* FabF were cloned expressed and purified as described in Chapters 2 and 3 respectively. Pure protein samples were exchanged into D_2O buffer (50mM $NaPO_4$, 0.3M NaCl, pD 8.0) using a micro-con (10MW cut off) concentrator. This served to exchange the TrisHCl buffer, which gives an ^1H NMR signal, with phosphate buffer (no signal) and to remove excess H_2O. Protein samples were generally concentrated to 50-60 μM and diluted by half into D_2O buffer containing varied concentrations of TLM and pantoylamides to a final volume of 600 μl.

Synthesis and Characterization of Pantoylamides

The series of pantoylamides shown in Figure 6 and 7 were synthesized by Pilho Kim, a post-doctoral scientist in Clifton Barry's lab at the NIH, hence the "PK" annotation of the series.

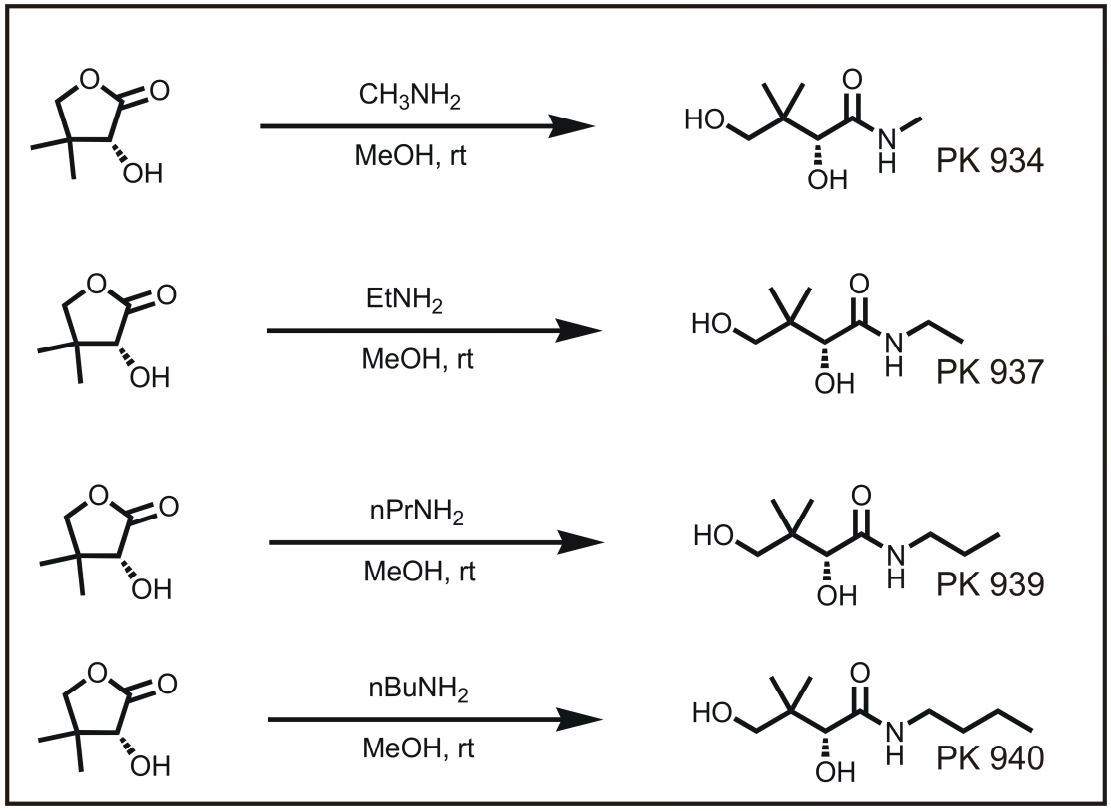

Figure 6: *Scheme for the synthesis of the pantoylamide series, Pilho Kim (NIAID)*

The pantoylamide PK940 was characterized using ^{1}H NMR (Figure 10) COSY (Figure 11) and ^{13}C NMR and the ^{13}C NMR assignments are presented in Table 4. These data were consistent across the pantoylamide series.

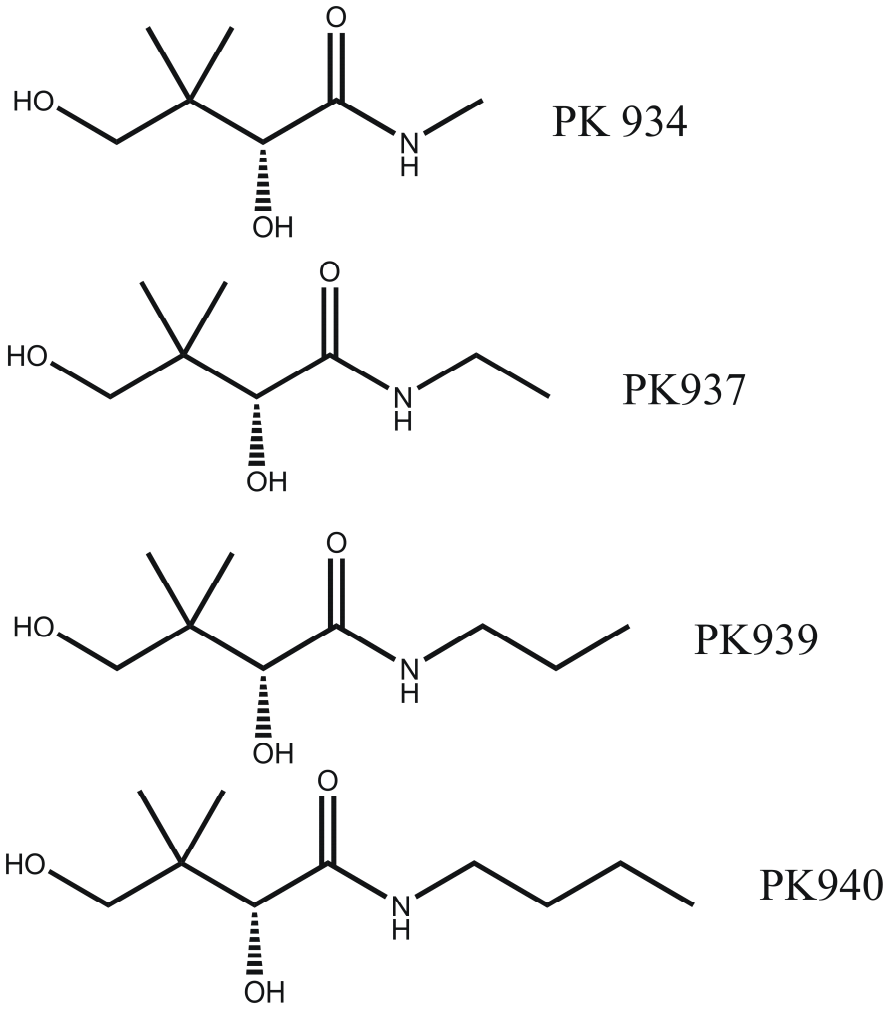

Figure 7: *Pantoylamide Series*

NMR Methods (Francis Picart)

All NMR data were acquired at 600 MHz and 500 MHz on Varian Inova NMR instruments in D_2O solvents at 25 °C and 15 °C (enzyme present) and all data processing was done with Varian software. ^{1}H chemical shifts for TLM and PK940 are reported relative to an internal DSS reference standard, for a combined sample of TLM and PK940 at 25 °C, and these shift assignments were carried over to all subsequent spectra. ^{13}C chemical shift scales for the indirect dimensions of the gradient-referenced HMQC and gradient HMBC spectra were calculated from the ^{1}H scale (standard). 1-dimensional ^{1}H and DPFGSE NOE data were collected at 6000 Hz spectral width using 24000 complex data points for 2.0 second acquisition times and 1 second recycle delays. The DPFGSE NOE experiments were performed for the indicated mixing times as previously reported by Shaka *et al* (*41, 42*). Standard 2-dimensional NOESY experiments were collected at 600 MHz over a range of mixing times from 300 msec to 900 msec using 0.155 sec acquisition times, 1.00 sec recycle delays with 6600 Hz spectral widths in F1 and F2 respectively, collected with 2048 complex 128 real data points. NOESY data were processed with Varian software to final data sizes of 2048 X 512 using forward linear prediction and shifted sine bell apodization parameters of sb = 0.109 sec and ssb = -0.050 sec. Standard gradient phase-insensitive COSY and phase-sensitive double quantum filtered (DQF) COSY data were collected at 600 MHz using 6000 Hz spectral widths in F1 and F2. 2040

complex points were collected in F2 and 128 and 200 indirect points were collected for the COSY and DQF-COSY experiments respectively. COSY data were processed to 2048 X 2048 final data sizes using forward linear prediction and similar shifted sine bell parameters as used for the NOESY data. These COSY spectra are presented below. Standard gradient HMQC data were collected phase sensitive at 600 MHz using a 6000 Hz spectral width in the ^{1}H dimension and 25141 Hz in the indirect ^{13}C dimension. Standard gradient HMBC data were collected (phase insensitive) with a 6000 Hz spectral width in the ^{1}H dimension and 36199 Hz in the indirect ^{13}C dimension. HMQC and HMBC data were processed to 2048 X 2048 final data sizes using linear prediction and Gaussian apodization of 0.052 and 0.003 was used to process both HMQC and HMBC data. F1 phase sensitivity was achieved by the States-Habercorn method for all phase sensitive experiments. The final peak assignments and spectra are reported herein.

Structural Models

All structural models and figures were created and manipulated with Pymol structural visualization software. FabH-CoA and FabB-TLM were overlaid using a 12 atom pair fitting using PDB files 1hnd and 1fj4 respectively.

Table 4: *PK940 ^{13}C NMR Assignments*	
Carbon	^{13}C Chemical Shift (ppm)(D_2O)
1	13.2
2	19.7
3	31.1
4	38.7
5	175.7
6	75.8
7	20.5
8	68.9
9[a]	20.5, 19.2
10[a]	19.2, 20.5
a. no pro-chiral assignment	

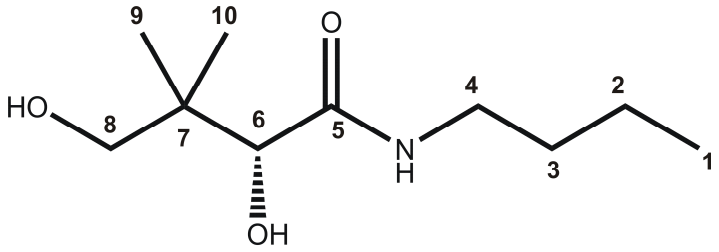

Figure 8: *PK940 Structure and Numbering*

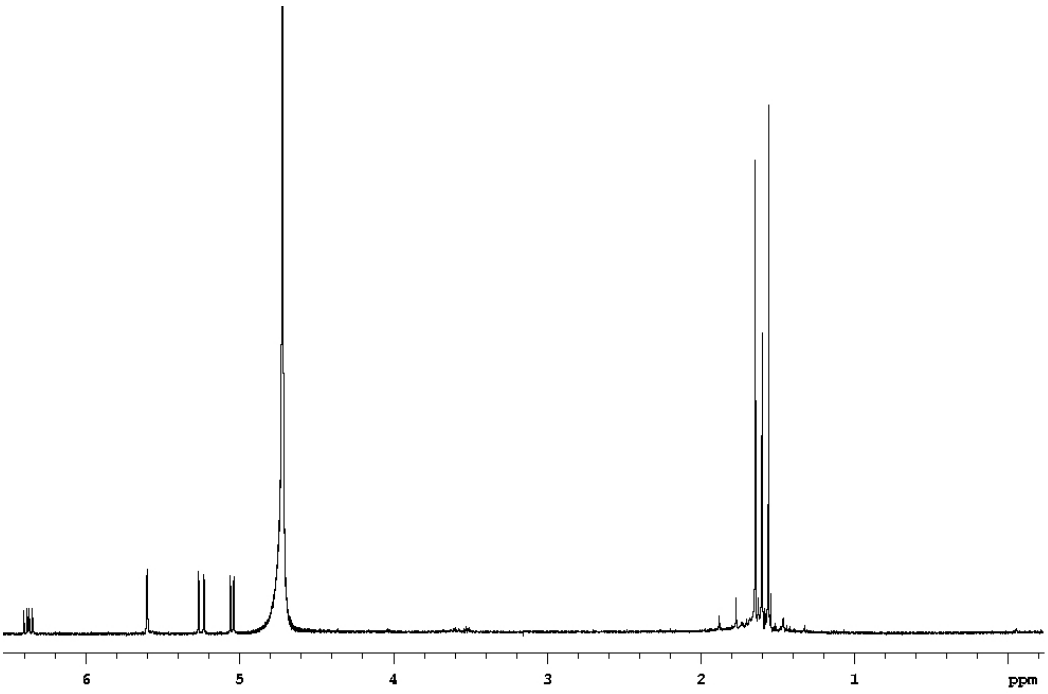

Figure 9: *TLM 1D ^{1}H NMR Spectrum*

(5*R*)Thiolactomycin. ^{1}H NMR (D_2O) 6.39ppm (dd, 1H), 5.63ppm (s, 1H), 5.07ppm (d, 1H, *J* = 18Hz), 5.07ppm (d, 1H *J* = 10.4 Hz), 4.68ppm (H_2O), 1.65ppm (s, 3H), 1.61ppm (s, 3H), 1.57ppm (s, 3H).

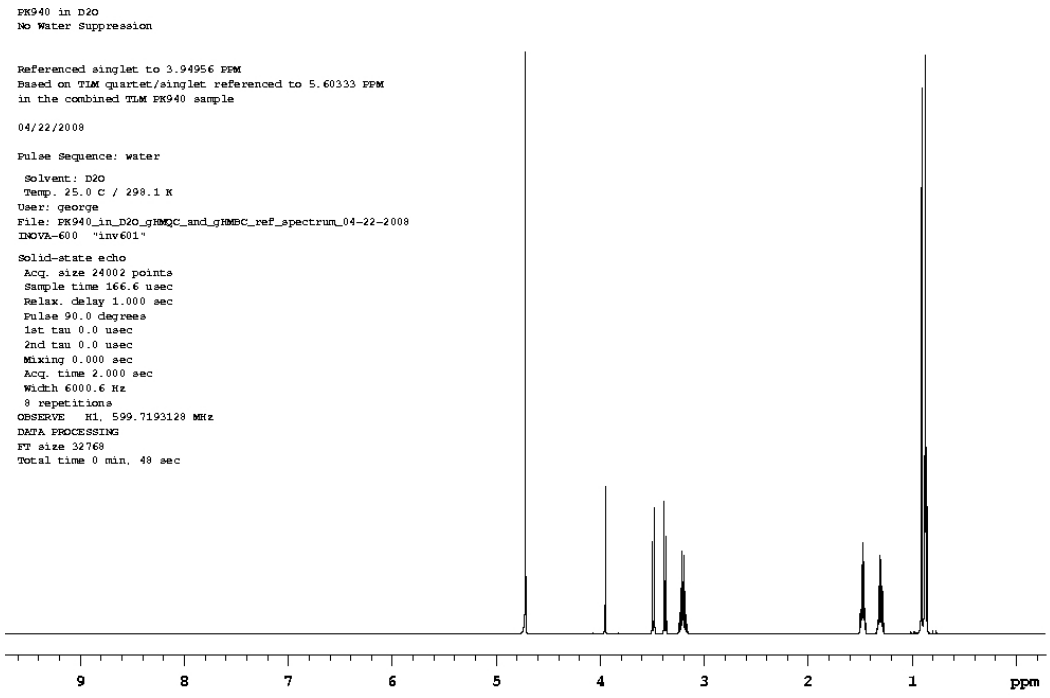

Figure 10: *PK 940 1D ^{1}H NMR Spectrum*

Pantoylamide (PK 940). ^{1}H NMR (D_2O) 4.68ppm (H_2O), 3.97 (s, 1H), 3.50ppm (d, 1H), 3.38ppm (d, 1H), 3.21ppm (dd, 2H), 1.49ppm (dd, 2H), 1.31ppm (dd, 2H), 0.92ppm (s, 3H), 0.88ppm (s, 3H), 0.88ppm (dd, 3H). Stacked doublet of doublets (C1, .88ppm) were resolved from geminal methyl singlet peaks (C9 and C10, .92-.88ppm) using the DPFGSE technique (Figures 13 and 14).

Figure 11: *PK940 COSY*

Figure 12: *TLM COSY*

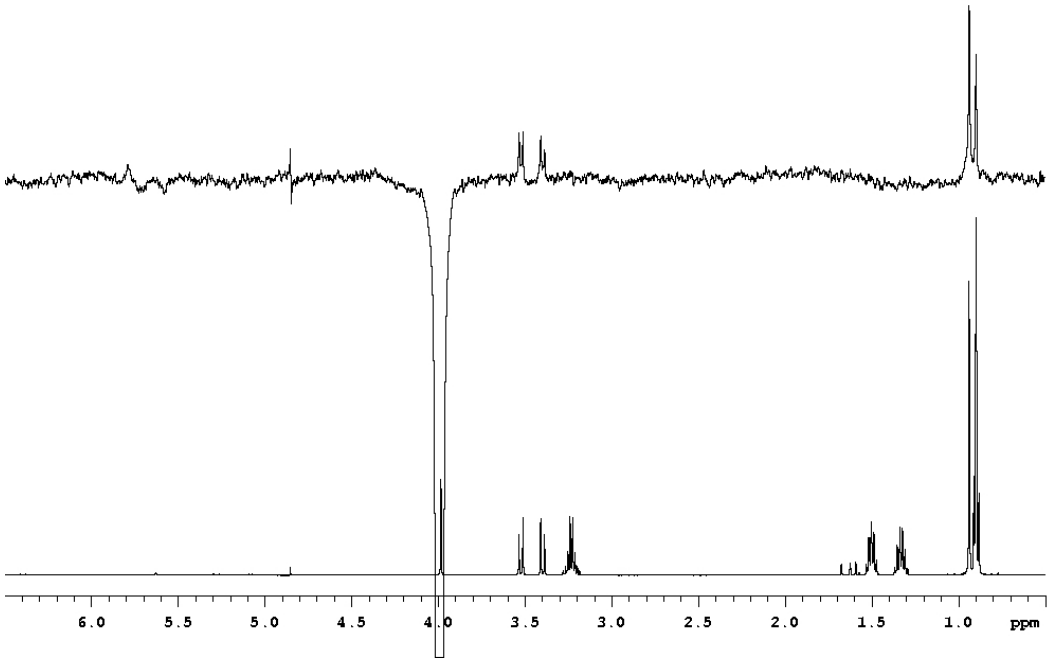

Figure 13: *Selective inversion of PK940 singlet (on C6) and resultant intra-ligand NOE to PK940 geminal methyls (C9, C10). As expected the appearance of these NOE signals is mutually inclusive.*

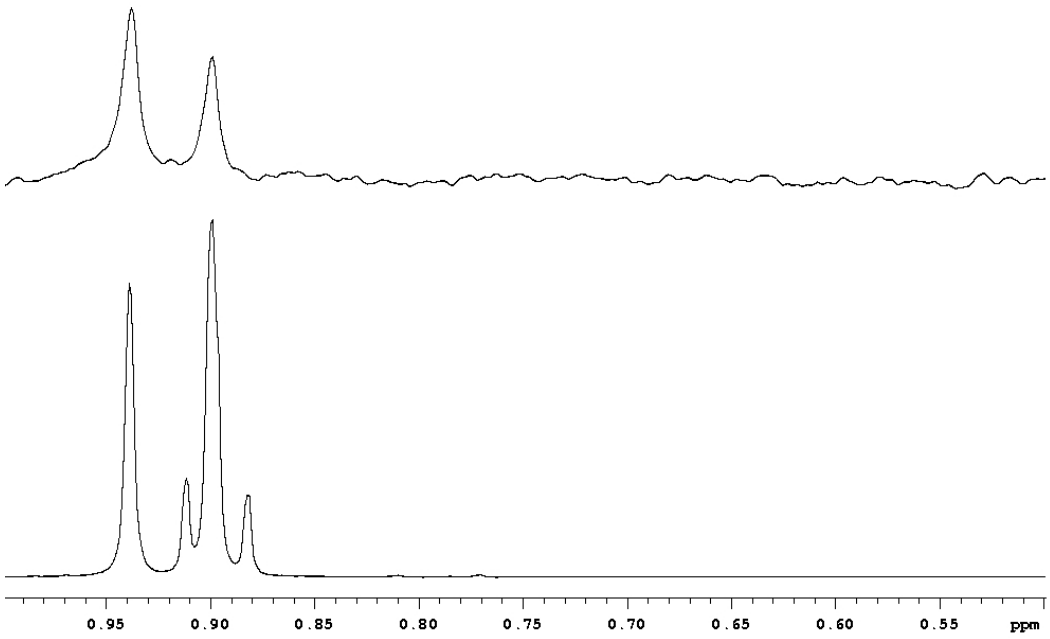

Figure 14: *Magnification of the above spectrum showing only geminal methyl peaks (C9, C10) (top). Reference ^{1}H spectrum shown (bottom)*

Results & Discussion

TLM is an attractive lead molecule for KAS directed anti-TB drug development. In order to direct the synthesis of TLM analogs with more potent binding to KasA we set out to explore unoccupied cavities near the TLM binding site. To this end, we synthesized and characterized a series of panthetheine analogs (pantoylamides). We hypothesized that TLM and a pantoylamide would simultaneously bind to adjacent sub-sites within the KasA active site. We used ILOE-NMR to probe two crucial questions related to this hypothesis. Firstly, do the ligands in fact bind simultaneously in the active site or is ligand binding mutually exclusive? Secondly what is the orientation of these ligands relative to one another?

In order to test these questions 2D NOESY spectra were collected for a mixture of pantoylamide and TLM in the presence of KasA. Initially no off diagonal peaks corresponding to interligand NOE (ILOE) were observed. Subsequent rounds of experiments eventually showed ILOE peaks and it became immediately obvious that signal strength was highly dependent on enzyme concentration. Additionally, the relative concentrations of the ligands in solution were also shown to effect NOE signal strength. Finally, the optimum protein concentration was set to 25 μM or greater, while with respect to ligand concentration, excess pantoylamide over TLM showed consistently better ILOE signal strength. We hypothesized that the greater binding affinity

of TLM over pantoylamide was the greatest contributing factor toward this result.

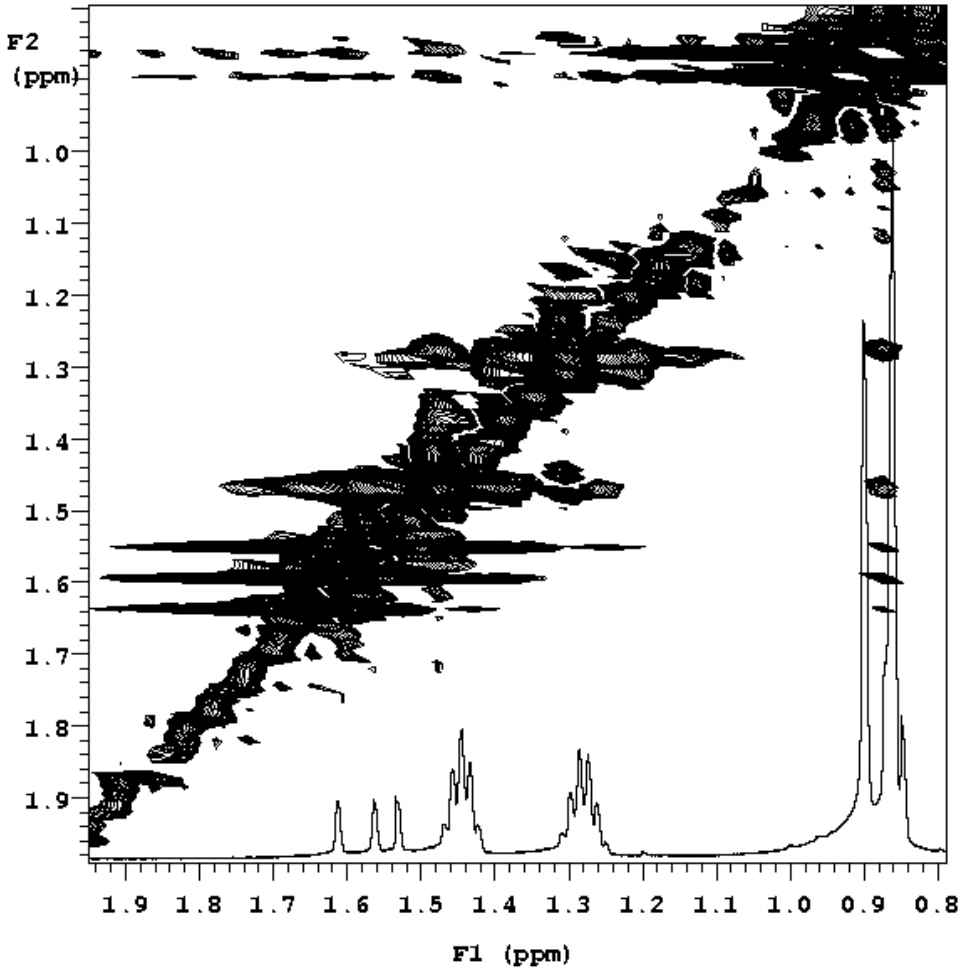

Figure 15: *NOESY spectrum in the presence of 25μM KasA showing ILOE between TLM methyls (1.57 -1.65ppm) and PK940 terminal methyl (.88ppm)*

The off diagonal peak corresponding to an ILOE signal in the presence of enzyme and subsequent control experiments indicated that the ligands were in fact bound to sub-sites within KasA (Figure 15). Upon close examination of the spectra we observe ILOE signals between the TLM methyl region (containing all three TLM methyl 1.57 -1.65 ppm) and the PK940 methyl region (0.92 - 0.88ppm)(Figure 15). The ^{1}H NMR combined with HMBC peak assignments for PK940 shows singlet proton peaks corresponding to the geminal methyl groups (C9, C10) with chemical shifts 0.91 and 0.88 ppm and a doublet of doublets corresponding to terminal methyl (C1) with a chemical shift of approximately 0.88ppm (Figures 10 and 15). The apparent stacking of the methyl peaks with chemical shifts differing by less than 0.005 presents a challenge in interpreting these data.

Nonetheless we assigned the ILOE between TLM and PK940 to the terminal methyl of PK940 based on the appearance of these peaks slightly downfield relative to the PK methyl cluster (Figure 15). Additionally, these peaks have chemical shifts equal to other NOE signals from each of the PK940 methylenes (C2 and C3, 1.49 and 1.31ppm respectively); expected to give an NOE to the terminal methyl (C1). Given the proximity of the geminal methyls to each other (C9 and C10, Figure 8) we would expect NOE signals including these groups to be mutually inclusive. That is, the presence of only one ILOE arguably eliminates the geminal methyls as the interaction partners with TLM (Figures 13 and 14). However, we sought to reconfirm this

assignment with further experimentation. Deconvolution of these enigmatic ILOE peaks would require both an increase in signal strength as well as a simplification of the spectra. To this end, we employed a method first described by Shaka *et al* (*41, 42*) affording both increased signal strength and spectral simplification. Significantly, to our knowledge this technique has never been employed in this manner.

The double pulsed field gradient spin echo (DPFGSE) technique was used to select the PK940 methyl region (including methyls C1, C9 and C10). This experiment again showed ILOE to all three methyl groups on TLM (negative peaks at 1.57-1.65ppm, Figure 16B) in presence of enzyme and no signal in the absence of enzyme (Figure 16C). Figure 16A shows the ^{1}H reference spectrum for the TLM/PK940 mixture.

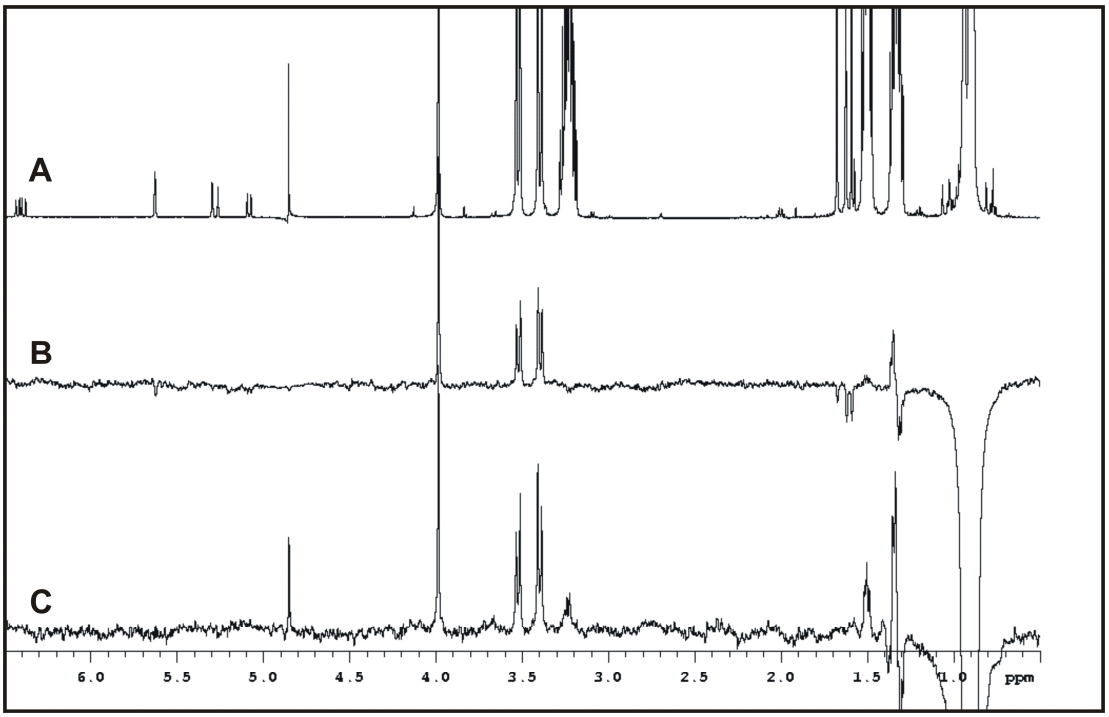

Figure 16: *DPFGSE experiments selecting PK940 Methyl groups in the presence and absence of enzyme*

We hypothesized, given these data, that the multiple signals (involving PK940 C1 (.88ppm) and all 3 TLM methyls (1.57-1.56ppm)) could be due to a loose fit of the ligands in the active site of WT-KasA. Recalling the results presented in Chapter 2, TLM binds to C171Q KasA with 10 fold greater binding affinity. These experiments were repeated with mutant protein with the hope that tighter binding would clarify our data set. The data however gave identical ILOE spectra. These data reaffirmed our hypothesis that the ligands bind to specific sub-sites within the active site. Recently, we have repeated these experiments with the *E. coli* homolog, FabF, with identical

results. These results are very encouraging not only as a positive control for our hypothesis but for the potential application of our designed analogs as broad spectrum anti-microbial agents.

The data presented in Figures 16 and 17 were consistent with the 2-D NOESY data. Figure 17A, shown here as an ^{1}H reference, shows a magnification of the upfield (0-1.65ppm) region containing PK940 methylenes (C2,C3), PK940 terminal methyl (C1) and all 3 TLM methyl groups. Figure 17B shows a control experiment where an *intra*-ligand NOE between the PK940 C2 and PK940 C1 doublet of doublets is observed. Figure 17C shows the through space interaction of TLM methyl protons (C7, 1.65ppm) exclusively with the PK940 C1 doublet of doublets. Further DPFGSE experiments were consistent with the hypothesis that the terminal methyl of PK940 (C1) was within 10 Å (NOE limit) of all three TLM methyl groups. Selective inversion of the individual methyls on TLM showed ILOE to the PK940 (C1) doublet of doublets, but not to the geminal methyl singlets, solidifying our interpretation of these data (Figure 17C).

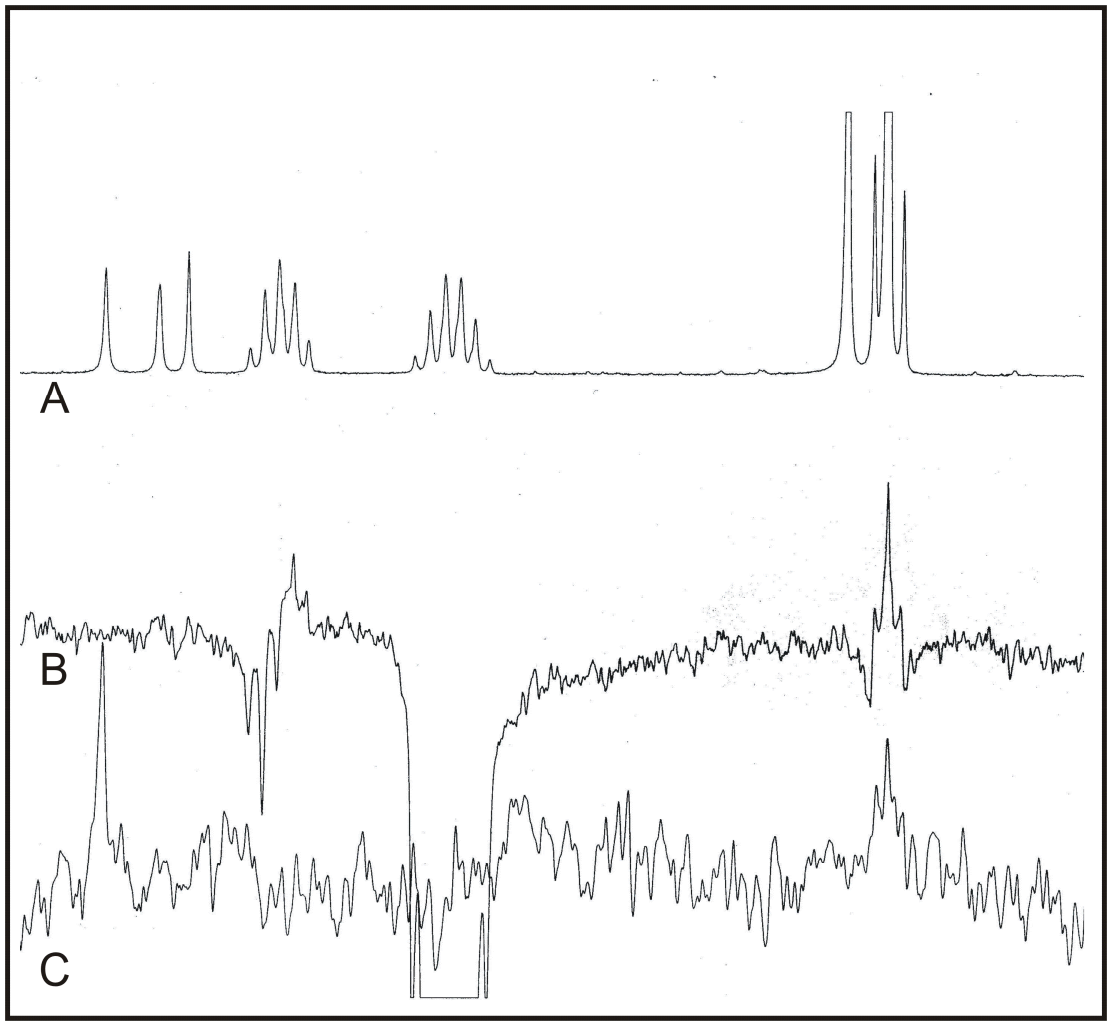

Figure 17: A. *focused upfield region of ^{1}H NMR* **B.** *Inversion of PK940 methylene (C2) and resultant terminal methyl (C1) NOE.* **C.** *TLM methyl inversion and resultant terminal methyl (C1) ILOE*

With our reaffirmation of the relative ligand binding modes we sought to estimate the distances between the terminal C1 methyl of PK940 and all three TLM methyls. Subsequent standard 2D NOESY experiments were used to estimate these distances. The intensity of the *intra*-ligand NOE between the

terminal TLM isoprene protons were used as a standard since the distance between these nuclei can be accurately determined to be 1.85 Å based on a H-C-H bond angle of 117° and a C-H bond length of 1.09 Å. The integrated volume of each NOE peak was used to rank the intensities relative to this standard (Table 5). Using this technique the distances to between C1 on PK940 and the 5 and 3 position methyls were estimated to be approximately equal at 3 Å.

Table 5: *Standard and ILOE Cross-peak Volumes and Estimated Distances*

ILOE	Relative Cross-peak Volume	Ratio ILOE/Standard	Estimated Distance
$H_{(TLM)}$-$H_{(TLM)}$	100.0	1	1.85 Å
$C6_{(TLM)}$-$C1_{(PK)}$ (1.57p)	56.3	.563	2.7 Å
$C7_{(TLM)}$-$C1_{(PK)}$ (1.65p)	48.0	.480	2.8 Å
$C12_{(TLM)}$-$C1_{(PK)}$ (1.61p)	75.0	.750	2.3 Å

Although we observe compelling data reporting on the relative orientation and distance of ligands bound to specific subsites within KasA we sought a visual explanation of these data. Structural models designed to corroborate our NMR data were constructed based on superimposed structures of homologous proteins. X-ray crystal structures for all three FAS *E. coli* KAS proteins are present in the Protein Data Bank (PDB) in complex with a variety

of ligands. The conenzyme A (CoA) dependent KASIII (FabH) X-ray crystal structure with CoA bound was solved and deposited in the PDB(*43*). The overall fold of this protein is similar to that of FabB, the Acp dependent *E. coli* KasII. The phosphopantetheine prothetic group of CoA and Acp are of course identical therefore both FabB and FabH both contain pantetheine binding channels with specific interactions that mediate substrate binding. The FabB-TLM and FabH-CoA crystal structures were overlaid in order to visualize the relative positions to TLM and CoA. The Pymol protein structure visualization program was used to superimpose these structures and a 12 atom pair fitting was used to overlay the conserved Cysteine and Histidine residues (Figures 18 and 19). The enzymes catalytic asparagine (FabH) and histidine (FabB) residues as well as the active site helices (Nα3) overlay well (Figures 18 and 19). Significantly, these structural models correlate with all of our NMR data acquired to date as well as our initial hypothesis that the orientation of specifically bound ligands could be probed using ILOE. Taken together these data provide compelling evidence that TLM-pantoylamide adducts would show enhanced KAS inhibition.

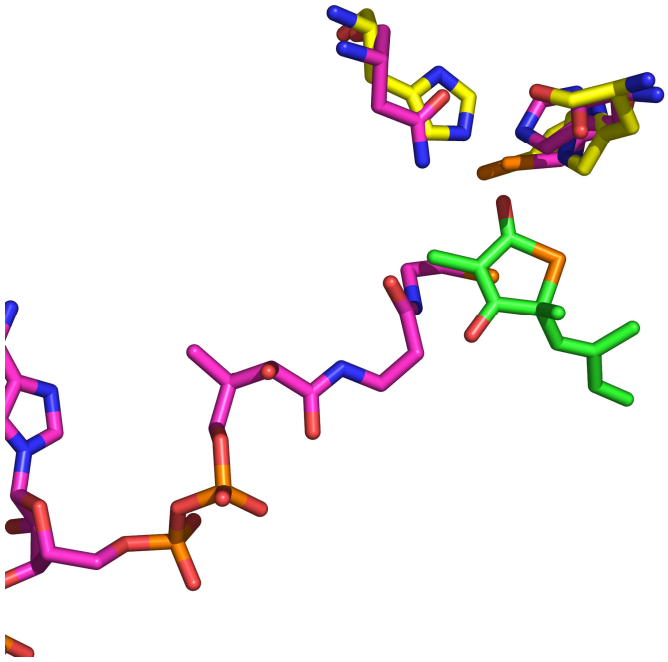

Figure 18: *FabB-TLM / FabH CoA overlay showing the relative orientation of TLM and Pantetheine binding site*

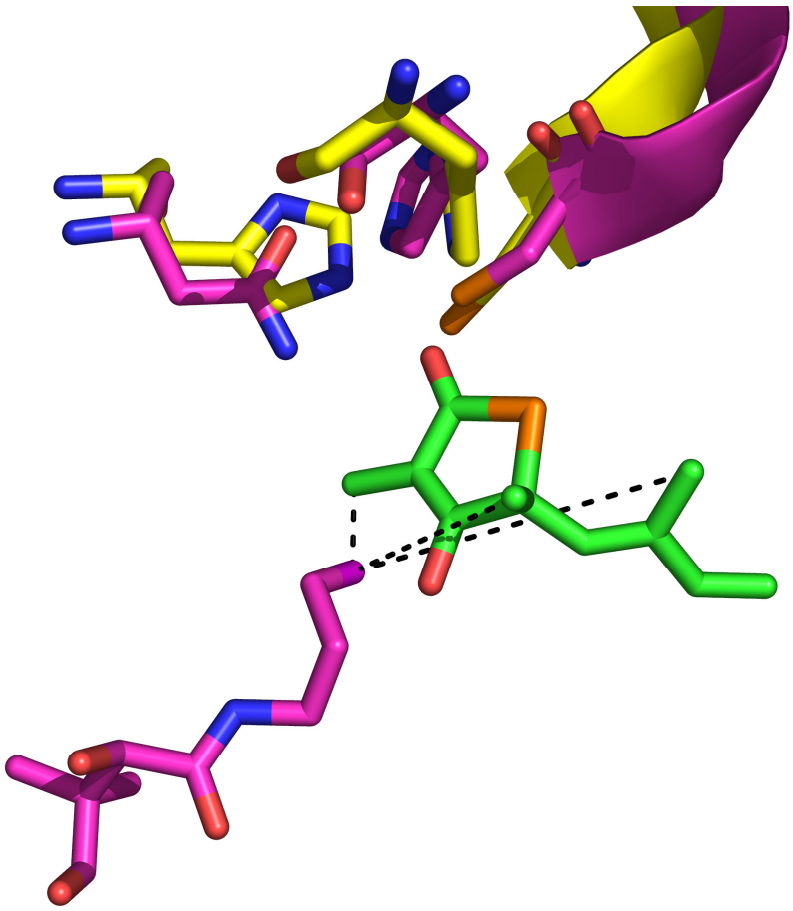

Figure 19: *PK940 (remaining CoA hidden) (magenta) and TLM (green) showing model of interaction consistent with observed ILOE data. Other overlaid structural components were removed for clarity.*

These models illustrate the utility of structural superposition in visualizing unoccupied sub-sites and encouraged us to extend these studies to models that include platencimycin and cerulenin. The relative orientation of TLM and Platensimycin (PMN) is shown in Figure 20 using an overlay of C164Q (FabF)-PMN and FabB-TLM. PMN occupies an additional subsite near but

not overlaid with the pantetheine binding site illustrating a number of additional interactions that could be potentially exploited by a more broad SAR study.

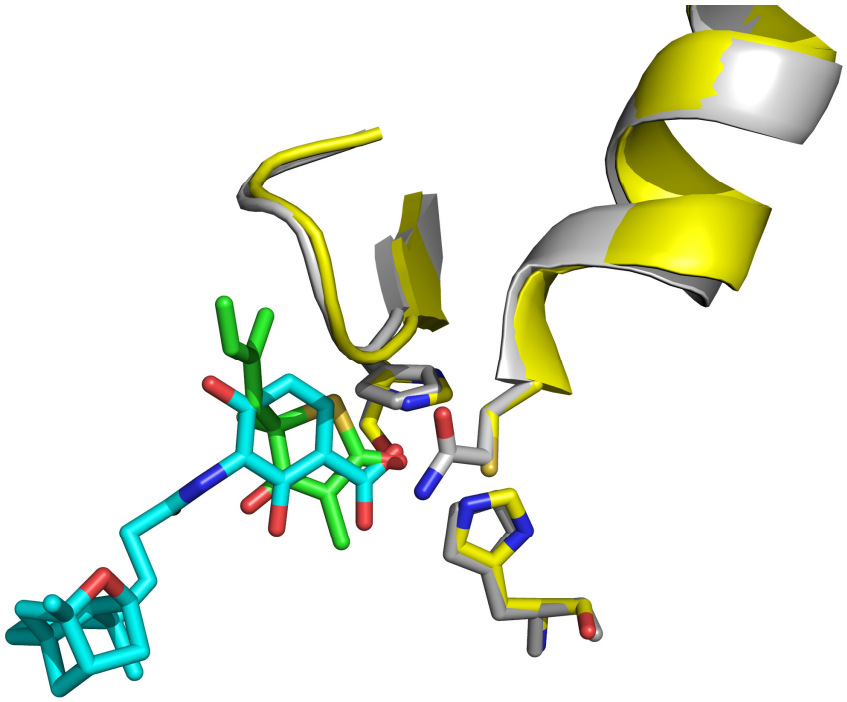

Figure 20: *FabF-Platensimycin / FabB TLM overlay*

Given the reported sensitivity of TLM binding to changes at the isoprene and the proximity of the 3 position methyl to the pantethenine binding channel, we've been encouraged, based on these data, to undertake an inhibitor synthesis program based on 3 position modifications to the TLM pharmacophore. These analogs include a 3 position TLM-pantoylamide adduct with varied linker lengths (Figure 21, compound 2a-c). Importantly,

these data have ignited the enthusiasm of a very talented and experienced post-doctoral synthetic organic chemist, Dr. B. Gopal Reddy, who has recently joined the Tonge group. Dr. Reddy has designed a synthesis for such TLM analogs (Figures 21 and 22) based on the reported synthesis of (5*R*) TLM from D-alanine (Figure 2) (*28*).

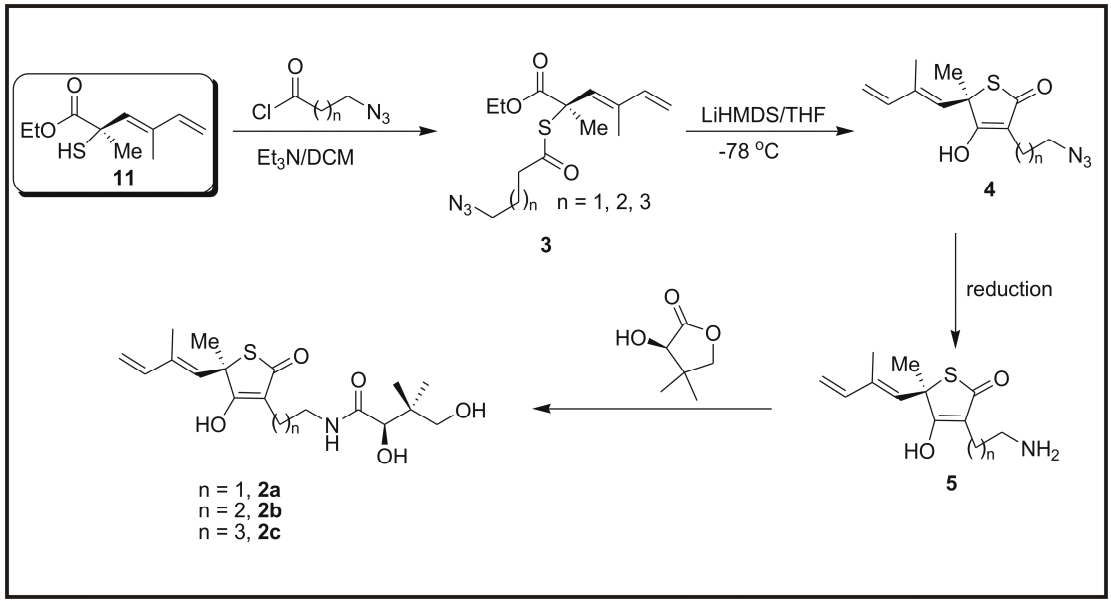

Figure 21: *Proposed TLM-Pantoylamide synthesis with varied linker length, based on an intermediate in a previously reported TLM synthesis(28)*

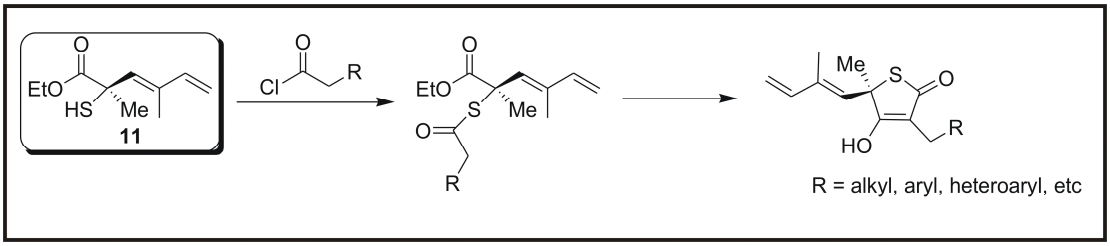

Figure 22: *Synthesis of additional TLM analogs*

Significantly, we have achieved our initial goal in reducing the number of compounds needed for SAR with KasA by probing specific interactions within two ligand binding sub-sites. We can now exploit these specific interactions in subsequent SAR studies by synthesizing a relatively small set of compounds. Undoubtedly, we will learn valuable lessons from the *in vitro* binding data of the TLM-pantoylamide adducts with varied linker lengths. Additionally, we would predict that these compounds retain favorable *in vivo* activity based on their physico-chemical properties. With clogP's between 1.1 and 1.6 and molecular weights of less than 400 the TLM adducts still retain their complete satisfaction of Lipinski's rule of 5.

References:

(1) Oishi, H., Noto, T., Sasaki, H., Suzuki, K., Hayashi, T., Okazaki, H., Ando, K., and Sawada, M. (1982) Thiolactomycin, a new antibiotic. I. Taxonomy of the producing organism, fermentation and biological properties. *J Antibiot (Tokyo) 35*, 391-5.

(2) Sasaki, H., Oishi, H., Hayashi, T., Matsuura, I., Ando, K., and Sawada, M. (1982) Thiolactomycin, a new antibiotic. II. Structure elucidation. *J Antibiot (Tokyo) 35*, 396-400.

(3) Brown, M. S., Akopiants, K., Resceck, D. M., McArthur, H. A., McCormick, E., and Reynolds, K. A. (2003) Biosynthetic origins of the natural product, thiolactomycin: a unique and selective inhibitor of type II dissociated fatty acid synthases. *J Am Chem Soc 125*, 10166-7.

(4) Noto, T., Miyakawa, S., Oishi, H., Endo, H., and Okazaki, H. (1982) Thiolactomycin, a new antibiotic. III. In vitro antibacterial activity. *J Antibiot (Tokyo) 35*, 401-10.

(5) Miyakawa, S., Suzuki, K., Noto, T., Harada, Y., and Okazaki, H. (1982) Thiolactomycin, a new antibiotic. IV. Biological properties and chemotherapeutic activity in mice. *J Antibiot (Tokyo) 35*, 411-9.

(6) Slayden, R. A., Lee, R. E., Armour, J. W., Cooper, A. M., Orme, I. M., Brennan, P. J., and Besra, G. S. (1996) Antimycobacterial action of thiolactomycin: an inhibitor of fatty acid and mycolic acid synthesis. *Antimicrob Agents Chemother 40*, 2813-9.

(7) Kim, P., Zhang, Y. M., Shenoy, G., Nguyen, Q. A., Boshoff, H. I., Manjunatha, U. H., Goodwin, M. B., Lonsdale, J., Price, A. C., Miller, D. J., Duncan, K., White, S. W., Rock, C. O., Barry, C. E., 3rd, and Dowd, C. S. (2006) Structure-activity relationships at the 5-position of thiolactomycin: an intact (5R)-isoprene unit is required for activity against the condensing enzymes from Mycobacterium tuberculosis and Escherichia coli. *J Med Chem 49*, 159-71.

(8) Ohata, K., and Terashima, S. (2007) Synthesis and biological activity of enantiomeric pairs of 5-vinylthiolactomycin congeners. *Bioorg Med Chem Lett 17*, 4070-4.

(9) Ondeyka, J. G., Zink, D. L., Young, K., Painter, R., Kodali, S., Galgoci, A., Collado, J., Tormo, J. R., Basilio, A., Vicente, F., Wang, J., and Singh, S. B. (2006) Discovery of bacterial fatty acid synthase inhibitors from a Phoma species as antimicrobial agents using a new antisense-based strategy. *J Nat Prod 69*, 377-80.

(10) Jones, S. M., Urch, J. E., Kaiser, M., Brun, R., Harwood, J. L., Berry, C., and Gilbert, I. H. (2005) Analogues of thiolactomycin as potential antimalarial agents. *J Med Chem 48*, 5932-41.

(11) Barco, P., Cardoso, R. F., Hirata, R. D., Leite, C. Q., Pandolfi, J. R., Sato, D. N., Shikama, M. L., de Melo, F. F., Mamizuka, E. M., Campanerut, P. A., and Hirata, M. H. (2006) pncA mutations in pyrazinamide-resistant Mycobacterium tuberculosis clinical isolates from the southeast region of Brazil. *J Antimicrob Chemother 58*, 930-5.

(12) Menner, N., Gunther, I., Orawa, H., Roth, A., Rambajan, I., Wagner, J., Hahn, H., Persaud, S., and Ignatius, R. (2005) High frequency of multidrug-resistant Mycobacterium tuberculosis isolates in Georgetown, Guyana. *Trop Med Int Health 10*, 1215-8.

(13) Lipinski, C. A., Lombardo, F., Dominy, B. W., and Feeney, P. J. (2001) Experimental and computational approaches to estimate solubility and permeability in drug discovery and development settings. *Adv Drug Deliv Rev 46*, 3-26.

(14) Price, A. C., Choi, K. H., Heath, R. J., Li, Z., White, S. W., and Rock, C. O. (2001) Inhibition of beta-ketoacyl-acyl carrier protein synthases by thiolactomycin and cerulenin. Structure and mechanism. *J Biol Chem 276*, 6551-9.

(15) Hayashi, T., Yamamoto, O., Sasaki, H., Kawaguchi, A., and Okazaki, H. (1983) Mechanism of action of the antibiotic thiolactomycin inhibition

of fatty acid synthesis of Escherichia coli. *Biochem Biophys Res Commun 115*, 1108-13.

(16) Jackowski, S., Zhang, Y. M., Price, A. C., White, S. W., and Rock, C. O. (2002) A missense mutation in the fabB (beta-ketoacyl-acyl carrier protein synthase I) gene confers tiolactomycin resistance to Escherichia coli. *Antimicrob Agents Chemother 46*, 1246-52.

(17) Tsay, J. T., Rock, C. O., and Jackowski, S. (1992) Overproduction of beta-ketoacyl-acyl carrier protein synthase I imparts thiolactomycin resistance to Escherichia coli K-12. *J Bacteriol 174*, 508-13.

(18) Slayden, R. A., Lee, R. E., and Barry, C. E., 3rd. (2000) Isoniazid affects multiple components of the type II fatty acid synthase system of Mycobacterium tuberculosis. *Mol Microbiol 38*, 514-25.

(19) Nishida, I., Kawaguchi, A., and Yamada, M. (1986) Effect of thiolactomycin on the individual enzymes of the fatty acid synthase system in Escherichia coli. *J Biochem (Tokyo) 99*, 1447-54.

(20) Copeland, R. A., Pompliano, D. L., and Meek, T. D. (2006) Drug-target residence time and its implications for lead optimization. *Nat Rev Drug Discov 5*, 730-9.

(21) Ehrlich, P. (1913) Address in pathology on chemotherapeutics : Scientific principles, methods, and results. *Lancet 2*, 445-451.

(22) Ojima, M., Inada, Y., Shibouta, Y., Wada, T., Sanada, T., Kubo, K., and Nishikawa, K. (1997) Candesartan (CV-11974) dissociates slowly from the angiotensin AT(1) receptor. *European Journal of Pharmacology 319*, 137-146.

(23) Lewandowicz, A., Tyler, P. C., Evans, G. B., Furneaux, R. H., and Schramm, V. L. (2003) Achieving the ultimate physiological goal in transition state analogue inhibitors for purine nucleoside phosphorylase. *J Biol Chem 278*, 31465-8.

(24) Kamal, A., Shaik, A. A., Azeeza, S., Malik, M. S., and Sandbhor, M. (2006) Chemoenzymatic synthesis of (5S)- and (5R)-hydroxymethyl-3,5-dimethyl-4-(methoxymethoxy)-5H-thiophen-2-one: a precursor of

thiolactomycin and determination of its absolute configuration. *Tetrahedron: Asymmetry 17*, 2890-2895.

(25) J. Wang, C.-L., and Salvino, J. M. (1984) Total ssynthesis of (±) thiolactomycin. *Tetrahedron Letters 25*, 5243-5246.

(26) Chambers, M., S.; Thomas,E., J. . (1997) Asymmetric synthesis of 5,5-disubstituted thiotetronic acids using an allyl xanthate to dithiocarbonate rearrangement: total synthesis of (5S)-thiolactomycin with revision of the absolute configuration of the natural *J. Chem. Soc., Perkin Trans. 1*, 417 - 432.

(27) Ohata, K., and Terashima, S. (2006) Efficient synthesis of enantiomeric pairs of thiolactomycin and its 3-demethyl derivative. *Tetrahedron Letters 47*, 2787-2791.

(28) McFadden, J. M., Frehywot, G. L., and Townsend, C. A. (2002) A flexible route to (5R)-thiolactomycin, a naturally occurring inhibitor of fatty acid synthesis. *Org Lett 4*, 3859-62.

(29) Sakya, S. M., Suarez-Contreras, M., Dirlam, J. P., O'Connell, T. N., Hayashi, S. F., Santoro, S. L., Kamicker, B. J., George, D. M., and Ziegler, C. B. (2001) Synthesis and structure-activity relationships of thiotetronic acid analogues of thiolactomycin. *Bioorg Med Chem Lett 11*, 2751-4.

(30) Jones, S. M., Urch, J. E., Brun, R., Harwood, J. L., Berry, C., and Gilbert, I. H. (2004) Analogues of thiolactomycin as potential anti-malarial and anti-trypanosomal agents. *Bioorg Med Chem 12*, 683-92.

(31) Jones, A. L., Herbert, D., Rutter, A. J., Dancer, J. E., and Harwood, J. L. (2000) Novel inhibitors of the condensing enzymes of the type II fatty acid synthase of pea (Pisum sativum). *Biochem J 347 Pt 1*, 205-9.

(32) Senior, S. J., Illarionov, P. A., Gurcha, S. S., Campbell, I. B., Schaeffer, M. L., Minnikin, D. E., and Besra, G. S. (2003) Biphenyl-based analogues of thiolactomycin, active against Mycobacterium tuberculosis mtFabH fatty acid condensing enzyme. *Bioorg Med Chem Lett 13*, 3685-8.

(33) Senior, S. J., Illarionov, P. A., Gurcha, S. S., Campbell, I. B., Schaeffer, M. L., Minnikin, D. E., and Besra, G. S. (2004) Acetylene-based analogues of thiolactomycin, active against Mycobacterium tuberculosis mtFabH fatty acid condensing enzyme. *Bioorg Med Chem Lett 14*, 373-6.

(34) Bhowruth, V., Brown, A. K., Senior, S. J., Snaith, J. S., and Besra, G. S. (2007) Synthesis and biological evaluation of a C5-biphenyl thiolactomycin library. *Bioorg Med Chem Lett 17*, 5643-6.

(35) Sassetti, C. M., Boyd, D. H., and Rubin, E. J. (2003) Genes required for mycobacterial growth defined by high density mutagenesis. *Mol Microbiol 48*, 77-84.

(36) McFadden, J. M., Medghalchi, S. M., Thupari, J. N., Pinn, M. L., Vadlamudi, A., Miller, K. I., Kuhajda, F. P., and Townsend, C. A. (2005) Application of a flexible synthesis of (5R)-thiolactomycin to develop new inhibitors of type I fatty acid synthase. *J Med Chem 48*, 946-61.

(37) Hajduk, P. J., Dinges, J., Miknis, G. F., Merlock, M., Middleton, T., Kempf, D. J., Egan, D. A., Walter, K. A., Robins, T. S., Shuker, S. B., Holzman, T. F., and Fesik, S. W. (1997) NMR-based discovery of lead inhibitors that block DNA binding of the human papillomavirus E2 protein. *J Med Chem 40*, 3144-50.

(38) Hajduk, P. J., Meadows, R. P., and Fesik, S. W. (1997) Discovering high-affinity ligands for proteins. *Science 278*, 497,499.

(39) Shuker, S. B., Hajduk, P. J., Meadows, R. P., and Fesik, S. W. (1996) Discovering high-affinity ligands for proteins: SAR by NMR. *Science 274*, 1531-4.

(40) Pellecchia, M., Sem, D. S., and Wuthrich, K. (2002) NMR in drug discovery. *Nat Rev Drug Discov 1*, 211-9.

(41) Van, Q. N., and Shaka, A. J. (1998) Improved cross peak detection in two-dimensional proton NMR spectra using excitation sculpting. *J Magn Reson 132*, 154-8.

(42) Van, Q. N., Smith, E. M., and Shaka, A. J. (1999) Observation of long-range small-molecule NOEs using a neoteric sensitivity enhancement scheme. *J Magn Reson 141*, 191-4.

(43) Davies, C., Heath, R. J., White, S. W., and Rock, C. O. (2000) The 1.8 A crystal structure and active-site architecture of beta-ketoacyl-acyl carrier protein synthase III (FabH) from escherichia coli. *Structure 8*, 185-95.

Bibliography:

Chapter 1:

1. Bloom, B. R., and Murray, C. J. (1992) Tuberculosis: commentary on a reemergent killer, *Science (New York, N.Y 257*, 1055-1064.
2. Kochi, A. (1991) The global tuberculosis situation and the new control strategy of the World Health Organization, *Tubercle 72*, 1-6.
3. Zink, A. R., Sola, C., Reischl, U., Grabner, W., Rastogi, N., Wolf, H., and Nerlich, A. G. (2003) Characterization of Mycobacterium tuberculosis complex DNAs from Egyptian mummies by spoligotyping, *Journal of clinical microbiology 41*, 359-367.
4. Donoghue, H. D., Spigelman, M., Greenblatt, C. L., Lev-Maor, G., Kahila Bar-Gal, G., Matheson, C., Vernon, K., G Nerlich, A., and R Zink, A. (2004) Tuberculosis: from prehistory to Robert Koch, as revealed by ancient DNA, *The Lancet Infectious Diseases 4*, 584-592.
5. Dye, C., Scheele, S., Dolin, P., Pathania, V., and Raviglione, M. C. (1999) Consensus statement. Global burden of tuberculosis: estimated incidence, prevalence, and mortality by country. WHO Global Surveillance and Monitoring Project, *Jama 282*, 677-686.
6. Chackerian, A. A., Alt, J. M., Perera, T. V., Dascher, C. C., and Behar, S. M. (2002) Dissemination of Mycobacterium tuberculosis is influenced by host factors and precedes the initiation of T-cell immunity, *Infection and immunity 70*, 4501-4509.
7. Dannenberg, A. M., Jr. (1982) Pathogenesis of pulmonary tuberculosis, *The American review of respiratory disease 125*, 25-29.
8. Szekely, R., Waczek, F., Szabadkai, I., Nemeth, G., Hegymegi-Barakonyi, B., Eros, D., Szokol, B., Pato, J., Hafenbradl, D., Satchell, J., Saint-Joanis, B., Cole, S. T., Orfi, L., Klebl, B. M., and Keri, G. (2008) A novel drug discovery concept for tuberculosis: Inhibition of bacterial and host cell signalling, *Immunology letters 116*, 225-231.
9. Walburger, A., Koul, A., Ferrari, G., Nguyen, L., Prescianotto-Baschong, C., Huygen, K., Klebl, B., Thompson, C., Bacher, G., and Pieters, J. (2004) Protein kinase G from pathogenic mycobacteria promotes survival within macrophages, *Science (New York, N.Y 304*, 1800-1804.
10. Kusner, D. J. (2005) Mechanisms of mycobacterial persistence in tuberculosis, *Clinical immunology (Orlando, Fla 114*, 239-247.
11. Malik, Z. A., Denning, G. M., and Kusner, D. J. (2000) Inhibition of Ca(2+) signaling by Mycobacterium tuberculosis is associated with reduced phagosome-lysosome fusion and increased survival within human macrophages, *The Journal of experimental medicine 191*, 287-302.
12. Malik, Z. A., Thompson, C. R., Hashimi, S., Porter, B., Iyer, S. S., and Kusner, D. J. (2003) Cutting edge: Mycobacterium tuberculosis blocks

Ca2+ signaling and phagosome maturation in human macrophages via specific inhibition of sphingosine kinase, *J Immunol 170*, 2811-2815.
13. Saunders, B. M., and Britton, W. J. (2007) Life and death in the granuloma: immunopathology of tuberculosis, *Immunology and cell biology 85*, 103-111.
14. Hiriyanna, K. T., and Ramakrishnan, T. (1986) Deoxyribonucleic acid replication time in Mycobacterium tuberculosis H37 Rv, *Archives of microbiology 144*, 105-109.
15. Sacchettini, J. C., Rubin, E. J., and Freundlich, J. S. (2008) Drugs versus bugs: in pursuit of the persistent predator Mycobacterium tuberculosis, *Nature reviews 6*, 41-52.
16. Middlebrook, G. (1952) Sterilization of tubercle bacilli by isonicotinic acid hydrazide and the incidence of variants resistant to the drug in vitro, *American review of tuberculosis 65*, 765-767.
17. Zimhony, O., Cox, J. S., Welch, J. T., Vilcheze, C., and Jacobs, W. R., Jr. (2000) Pyrazinamide inhibits the eukaryotic-like fatty acid synthetase I (FASI) of Mycobacterium tuberculosis, *Nature medicine 6*, 1043-1047.
18. Boshoff, H. I., Mizrahi, V., and Barry, C. E., 3rd. (2002) Effects of pyrazinamide on fatty acid synthesis by whole mycobacterial cells and purified fatty acid synthase I, *Journal of bacteriology 184*, 2167-2172.
19. Zhang, Y., Wade, M. M., Scorpio, A., Zhang, H., and Sun, Z. (2003) Mode of action of pyrazinamide: disruption of Mycobacterium tuberculosis membrane transport and energetics by pyrazinoic acid, *The Journal of antimicrobial chemotherapy 52*, 790-795.
20. Beggs, W. H., and Andrews, F. A. (1974) Chemical characterization of ethambutol binding to Mycobacterium smegmatis, *Antimicrobial agents and chemotherapy 5*, 234-239.
21. Takayama, K., and Kilburn, J. O. (1989) Inhibition of synthesis of arabinogalactan by ethambutol in Mycobacterium smegmatis, *Antimicrobial agents and chemotherapy 33*, 1493-1499.
22. Rawat, R., Whitty, A., and Tonge, P. J. (2003) The isoniazid-NAD adduct is a slow, tight-binding inhibitor of InhA, the Mycobacterium tuberculosis enoyl reductase: adduct affinity and drug resistance, *Proceedings of the National Academy of Sciences of the United States of America 100*, 13881-13886.
23. Gumbo, T., Louie, A., Liu, W., Brown, D., Ambrose, P. G., Bhavnani, S. M., and Drusano, G. L. (2007) Isoniazid bactericidal activity and resistance emergence: integrating pharmacodynamics and pharmacogenomics to predict efficacy in different ethnic populations, *Antimicrobial agents and chemotherapy 51*, 2329-2336.
24. Barco, P., Cardoso, R. F., Hirata, R. D., Leite, C. Q., Pandolfi, J. R., Sato, D. N., Shikama, M. L., de Melo, F. F., Mamizuka, E. M., Campanerut, P. A., and Hirata, M. H. (2006) pncA mutations in pyrazinamide-resistant Mycobacterium tuberculosis clinical isolates

from the southeast region of Brazil, *The Journal of antimicrobial chemotherapy 58*, 930-935.
25. Menner, N., Gunther, I., Orawa, H., Roth, A., Rambajan, I., Wagner, J., Hahn, H., Persaud, S., and Ignatius, R. (2005) High frequency of multidrug-resistant Mycobacterium tuberculosis isolates in Georgetown, Guyana, *Trop Med Int Health 10*, 1215-1218.
26. Frieden, T. R., Sterling, T., Pablos-Mendez, A., Kilburn, J. O., Cauthen, G. M., and Dooley, S. W. (1993) The emergence of drug-resistant tuberculosis in New York City, *The New England journal of medicine 328*, 521-526.
27. Hayward, A. C., and Coker, R. J. (2000) Could a tuberculosis epidemic occur in London as it did in New York?, *Emerging infectious diseases 6*, 12-16.
28. Banerjee, A., Dubnau, E., Quemard, A., Balasubramanian, V., Um, K. S., Wilson, T., Collins, D., de Lisle, G., and Jacobs, W. R., Jr. (1994) inhA, a gene encoding a target for isoniazid and ethionamide in Mycobacterium tuberculosis, *Science (New York, N.Y 263*, 227-230.
29. Cox, H. S., Morrow, M., and Deutschmann, P. W. (2008) Long term efficacy of DOTS regimens for tuberculosis: systematic review, *BMJ (Clinical research ed 336*, 484-487.
30. Heath, R. J., and Rock, C. O. (2004) Fatty acid biosynthesis as a target for novel antibacterials, *Curr Opin Investig Drugs 5*, 146-153.
31. Liu, J., Barry, C. E., 3rd, Besra, G. S., and Nikaido, H. (1996) Mycolic acid structure determines the fluidity of the mycobacterial cell wall, *The Journal of biological chemistry 271*, 29545-29551.
32. Barry, C. E., 3rd, Lee, R. E., Mdluli, K., Sampson, A. E., Schroeder, B. G., Slayden, R. A., and Yuan, Y. (1998) Mycolic acids: structure, biosynthesis and physiological functions, *Progress in lipid research 37*, 143-179.
33. Brindley, D. N., Matsumura, S., and Bloch, K. (1969) Mycobacterium phlei Fatty Acid Synthetase[mdash]A Bacterial Multienzyme Complex, *Nature 224*, 666-669.
34. Carlisle-Moore, L., Gordon, C. R., Machutta, C. A., Miller, W. T., and Tonge, P. J. (2005) Substrate recognition by the human fatty-acid synthase, *The Journal of biological chemistry 280*, 42612-42618.
35. Edwards, P., Nelsen, J. S., Metz, J. G., and Dehesh, K. (1997) Cloning of the fabF gene in an expression vector and in vitro characterization of recombinant fabF and fabB encoded enzymes from Escherichia coli, *FEBS Lett 402*, 62-66.
36. Schaeffer, M. L., Agnihotri, G., Volker, C., Kallender, H., Brennan, P. J., and Lonsdale, J. T. (2001) Purification and biochemical characterization of the Mycobacterium tuberculosis beta-ketoacyl-acyl carrier protein synthases KasA and KasB, *The Journal of biological chemistry 276*, 47029-47037.
37. Olsen, J. G., Kadziola, A., von Wettstein-Knowles, P., Siggaard-Andersen, M., and Larsen, S. (2001) Structures of beta-ketoacyl-acyl

carrier protein synthase I complexed with fatty acids elucidate its catalytic machinery, *Structure 9*, 233-243.
38. Bergler, H., Fuchsbichler, S., Hogenauer, G., and Turnowsky, F. (1996) The enoyl-[acyl-carrier-protein] reductase (FabI) of Escherichia coli, which catalyzes a key regulatory step in fatty acid biosynthesis, accepts NADH and NADPH as cofactors and is inhibited by palmitoyl-CoA, *European journal of biochemistry / FEBS 242*, 689-694.
39. Lai, C. Y., and Cronan, J. E. (2003) Beta-ketoacyl-acyl carrier protein synthase III (FabH) is essential for bacterial fatty acid synthesis, *The Journal of biological chemistry 278*, 51494-51503.
40. Sassetti, C. M., Boyd, D. H., and Rubin, E. J. (2003) Genes required for mycobacterial growth defined by high density mutagenesis, *Molecular microbiology 48*, 77-84.
41. Bhatt, A., Kremer, L., Dai, A. Z., Sacchettini, J. C., and Jacobs, W. R., Jr. (2005) Conditional depletion of KasA, a key enzyme of mycolic acid biosynthesis, leads to mycobacterial cell lysis, *Journal of bacteriology 187*, 7596-7606.
42. Parish, T., Roberts, G., Laval, F., Schaeffer, M., Daffe, M., and Duncan, K. (2007) Functional complementation of the essential gene fabG1 of Mycobacterium tuberculosis by Mycobacterium smegmatis fabG but not Escherichia coli fabG, *Journal of bacteriology 189*, 3721-3728.
43. Silva, R. G., Rosado, L. A., Santos, D. S., and Basso, L. A. (2008) Mycobacterium tuberculosis beta-ketoacyl-ACP reductase: alpha-secondary kinetic isotope effects and kinetic and equilibrium mechanisms of substrate binding, *Archives of biochemistry and biophysics 471*, 1-10.
44. Sullivan, T. J., Truglio, J. J., Boyne, M. E., Novichenok, P., Zhang, X., Stratton, C. F., Li, H. J., Kaur, T., Amin, A., Johnson, F., Slayden, R. A., Kisker, C., and Tonge, P. J. (2006) High affinity InhA inhibitors with activity against drug-resistant strains of Mycobacterium tuberculosis, *ACS chemical biology 1*, 43-53.
45. Xu, H., Sullivan, T. J., Sekiguchi, J. I., Kirikae, T., Ojima, I., Stratton, C. F., Mao, W., Rock, F. L., Alley, M. R., Johnson, F., Walker, S. G., and Tonge, P. J. (2008) Mechanism and Inhibition of saFabI, the Enoyl Reductase from Staphylococcus aureus, *Biochemistry*.
46. Silver, L. L. (2003) Novel inhibitors of bacterial cell wall synthesis, *Curr Opin Microbiol 6*, 431-438.
47. Chain, E., Florey, H. W., Gardner, A. D., Heatley, N. G., Jennings, M. A., Orr-Ewing, J., and Sanders, A. G. (1940) PENICILLIN AS A CHEMOTHERAPEUTIC AGENT, *The Lancet 236*, 226-228.
48. Newman, D. J., Cragg, G. M., and Snader, K. M. (2003) Natural products as sources of new drugs over the period 1981-2002, *Journal of natural products 66*, 1022-1037.

49. Pelaez, F. (2006) The historical delivery of antibiotics from microbial natural products--can history repeat?, *Biochem Pharmacol 71*, 981-990.

Chapter 2:

1. Heath, R. J., and Rock, C. O. (2002) The Claisen condensation in biology, *Nat Prod Rep 19*, 581-596.
2. Haapalainen, A. M., Merilainen, G., and Wierenga, R. K. (2006) The thiolase superfamily: condensing enzymes with diverse reaction specificities, *Trends in biochemical sciences 31*, 64-71.
3. Mathieu, M., Zeelen, J. P., Pauptit, R. A., Erdmann, R., Kunau, W. H., and Wierenga, R. K. (1994) The 2.8 A crystal structure of peroxisomal 3-ketoacyl-CoA thiolase of Saccharomyces cerevisiae: a five-layered alpha beta alpha beta alpha structure constructed from two core domains of identical topology, *Structure 2*, 797-808.
4. Mathieu, M., Modis, Y., Zeelen, J. P., Engel, C. K., Abagyan, R. A., Ahlberg, A., Rasmussen, B., Lamzin, V. S., Kunau, W. H., and Wierenga, R. K. (1997) The 1.8 A crystal structure of the dimeric peroxisomal 3-ketoacyl-CoA thiolase of Saccharomyces cerevisiae: implications for substrate binding and reaction mechanism, *Journal of molecular biology 273*, 714-728.
5. Modis, Y., and Wierenga, R. K. (1999) A biosynthetic thiolase in complex with a reaction intermediate: the crystal structure provides new insights into the catalytic mechanism, *Structure 7*, 1279-1290.
6. White, S. W., Zheng, J., Zhang, Y. M., and Rock. (2005) The structural biology of type II fatty acid biosynthesis, *Annu Rev Biochem 74*, 791-831.
7. Price, A. C., Choi, K. H., Heath, R. J., Li, Z., White, S. W., and Rock, C. O. (2001) Inhibition of beta-ketoacyl-acyl carrier protein synthases by thiolactomycin and cerulenin. Structure and mechanism, *The Journal of biological chemistry 276*, 6551-6559.
8. von Wettstein-Knowles, P., Olsen, J. G., McGuire, K. A., and Henriksen, A. (2006) Fatty acid synthesis. Role of active site histidines and lysine in Cys-His-His-type beta-ketoacyl-acyl carrier protein synthases, *The FEBS journal 273*, 695-710.
9. von Wettstein-Knowles, P., Olsen, J., Arnvig Mcguire, K., and Larsen, S. (2000) Molecular aspects of beta-ketoacyl synthase (KAS) catalysis, *Biochem Soc Trans 28*, 601-607.
10. Khandekar, S. S., Gentry, D. R., Van Aller, G. S., Warren, P., Xiang, H., Silverman, C., Doyle, M. L., Chambers, P. A., Konstantinidis, A. K., Brandt, M., Daines, R. A., and Lonsdale, J. T. (2001) Identification, substrate specificity, and inhibition of the Streptococcus pneumoniae beta-ketoacyl-acyl carrier protein synthase III (FabH), *The Journal of biological chemistry 276*, 30024-30030.

11. Wang, J., Soisson, S. M., Young, K., Shoop, W., Kodali, S., Galgoci, A., Painter, R., Parthasarathy, G., Tang, Y. S., Cummings, R., Ha, S., Dorso, K., Motyl, M., Jayasuriya, H., Ondeyka, J., Herath, K., Zhang, C., Hernandez, L., Allocco, J., Basilio, A., Tormo, J. R., Genilloud, O., Vicente, F., Pelaez, F., Colwell, L., Lee, S. H., Michael, B., Felcetto, T., Gill, C., Silver, L. L., Hermes, J. D., Bartizal, K., Barrett, J., Schmatz, D., Becker, J. W., Cully, D., and Singh, S. B. (2006) Platensimycin is a selective FabF inhibitor with potent antibiotic properties, *Nature 441*, 358-361.
12. Young, K., Jayasuriya, H., Ondeyka, J. G., Herath, K., Zhang, C., Kodali, S., Galgoci, A., Painter, R., Brown-Driver, V., Yamamoto, R., Silver, L. L., Zheng, Y., Ventura, J. I., Sigmund, J., Ha, S., Basilio, A., Vicente, F., Tormo, J. R., Pelaez, F., Youngman, P., Cully, D., Barrett, J. F., Schmatz, D., Singh, S. B., and Wang, J. (2006) Discovery of FabH/FabF inhibitors from natural products, *Antimicrobial agents and chemotherapy 50*, 519-526.
13. Surolia, A., Ramya, T. N., Ramya, V., and Surolia, N. (2004) 'FAS't inhibition of malaria, *The Biochemical journal 383*, 401-412.
14. Barry, C. E., 3rd, Slayden, R. A., and Mdluli, K. (1998) Mechanisms of isoniazid resistance in Mycobacterium tuberculosis, *Drug Resist Updat 1*, 128-134.
15. Mdluli, K., Slayden, R. A., Zhu, Y., Ramaswamy, S., Pan, X., Mead, D., Crane, D. D., Musser, J. M., and Barry, C. E., 3rd. (1998) Inhibition of a Mycobacterium tuberculosis beta-ketoacyl ACP synthase by isoniazid, *Science (New York, N.Y 280*, 1607-1610.
16. Bhatt, A., Kremer, L., Dai, A. Z., Sacchettini, J. C., and Jacobs, W. R., Jr. (2005) Conditional depletion of KasA, a key enzyme of mycolic acid biosynthesis, leads to mycobacterial cell lysis, *Journal of bacteriology 187*, 7596-7606.
17. Slayden, R. A., Lee, R. E., Armour, J. W., Cooper, A. M., Orme, I. M., Brennan, P. J., and Besra, G. S. (1996) Antimycobacterial action of thiolactomycin: an inhibitor of fatty acid and mycolic acid synthesis, *Antimicrobial agents and chemotherapy 40*, 2813-2819.
18. Rawat, R., Whitty, A., and Tonge, P. J. (2003) The isoniazid-NAD adduct is a slow, tight-binding inhibitor of InhA, the Mycobacterium tuberculosis enoyl reductase: adduct affinity and drug resistance, *Proceedings of the National Academy of Sciences of the United States of America 100*, 13881-13886.
19. Odriozola, J. M., and Bloch, K. (1977) Effects of phosphatidylcholine liposomes on the fatty acid synthetase complex from Mycobacterium smegmatis, *Biochimica et biophysica acta 488*, 198-206.
20. Veyron-Churlet, R., Guerrini, O., Mourey, L., Daffe, M., and Zerbib, D. (2004) Protein-protein interactions within the Fatty Acid Synthase-II system of Mycobacterium tuberculosis are essential for mycobacterial viability, *Molecular microbiology 54*, 1161-1172.

21. Oishi, H., Noto, T., Sasaki, H., Suzuki, K., Hayashi, T., Okazaki, H., Ando, K., and Sawada, M. (1982) Thiolactomycin, a new antibiotic. I. Taxonomy of the producing organism, fermentation and biological properties, *J Antibiot (Tokyo) 35*, 391-395.
22. Hamada, S., Fujiwara, T., Shimauchi, H., Ogawa, T., Nishihara, T., Koga, T., Nehashi, T., and Matsuno, T. (1990) Antimicrobial activities of thiolactomycin against gram-negative anaerobes associated with periodontal disease. f1, *Oral Microbiol Immunol 5*, 340-345.
23. Noto, T., Miyakawa, S., Oishi, H., Endo, H., and Okazaki, H. (1982) Thiolactomycin, a new antibiotic. III. In vitro antibacterial activity, *J Antibiot. (Tokyo) 35*, 401-410.
24. Kim, P., Zhang, Y. M., Shenoy, G., Nguyen, Q. A., Boshoff, H. I., Manjunatha, U. H., Goodwin, M. B., Lonsdale, J., Price, A. C., Miller, D. J., Duncan, K., White, S. W., Rock, C. O., Barry, C. E., 3rd, and Dowd, C. S. (2006) Structure-activity relationships at the 5-position of thiolactomycin: an intact (5R)-isoprene unit is required for activity against the condensing enzymes from Mycobacterium tuberculosis and Escherichia coli, *J Med Chem 49*, 159-171.
25. Hayashi, T., Yamamoto, O., Sasaki, H., Kawaguchi, A., and Okazaki, H. (1983) Mechanism of action of the antibiotic thiolactomycin inhibition of fatty acid synthesis of Escherichia coli, *Biochemical and biophysical research communications 115*, 1108-1113.
26. Miyakawa, S., Suzuki, K., Noto, T., Harada, Y., and Okazaki, H. (1982) Thiolactomycin, a new antibiotic. IV. Biological properties and chemotherapeutic activity in mice, *J Antibiot (Tokyo) 35*, 411-419.
27. Jackowski, S., Zhang, Y. M., Price, A. C., White, S. W., and Rock, C. O. (2002) A missense mutation in the fabB (beta-ketoacyl-acyl carrier protein synthase I) gene confers tiolactomycin resistance to Escherichia coli, *Antimicrobial agents and chemotherapy 46*, 1246-1252.
28. Tsay, J. T., Rock, C. O., and Jackowski, S. (1992) Overproduction of beta-ketoacyl-acyl carrier protein synthase I imparts thiolactomycin resistance to Escherichia coli K-12, *Journal of bacteriology 174*, 508-513.
29. Nishida, I., Kawaguchi, A., and Yamada, M. (1986) Effect of thiolactomycin on the individual enzymes of the fatty acid synthase system in Escherichia coli, *J Biochem (Tokyo) 99*, 1447-1454.
30. He, X., Mueller, J. P., and Reynolds, K. A. (2000) Development of a scintillation proximity assay for beta-ketoacyl-acyl carrier protein synthase III, *Anal Biochem 282*, 107-114.
31. Schaeffer, M. L., Carson, J. D., Kallender, H., and Lonsdale, J. T. (2004) Development of a scintillation proximity assay for the Mycobacterium tuberculosis KasA and KasB enzymes involved in mycolic acid biosynthesis, *Tuberculosis (Edinb) 84*, 353-360.
32. Jones, A. L., Gane, A. M., Herbert, D., Willey, D. L., Rutter, A. J., Kille, P., Dancer, J. E., and Harwood, J. L. (2003) Beta-ketoacyl-acyl carrier

protein synthase III from pea (Pisum sativum L.): properties, inhibition by a novel thiolactomycin analogue and isolation of a cDNA clone encoding the enzyme, *Planta 216*, 752-761.
33. Kim, P., Barry, C. E., and Dowd, C. S. (2006) Novel route to 5-position vinyl derivatives of thiolactomycin: Olefination vs. deformylation, *Tetrahedron Lett 47*, 3447-3451.
34. McFadden, J. M., Frehywot, G. L., and Townsend, C. A. (2002) A flexible route to (5R)-thiolactomycin, a naturally occurring inhibitor of fatty acid synthesis, *Org Lett 4*, 3859-3862.
35. McFadden, J. M., Medghalchi, S. M., Thupari, J. N., Pinn, M. L., Vadlamudi, A., Miller, K. I., Kuhajda, F. P., and Townsend, C. A. (2005) Application of a flexible synthesis of (5R)-thiolactomycin to develop new inhibitors of type I fatty acid synthase, *J Med Chem 48*, 946-961.
36. Witkowski, A., Joshi, A. K., Lindqvist, Y., and Smith, S. (1999) Conversion of a beta-ketoacyl synthase to a malonyl decarboxylase by replacement of the active-site cysteine with glutamine, *Biochemistry 38*, 11643-11650.
37. Nomura, S., Horiuchi, T., Omura, S., and Hata, T. (1972) The action mechanism of cerulenin. I. Effect of cerulenin on sterol and fatty acid biosynthesis in yeast, *J Biochem (Tokyo) 71*, 783-796.
38. Schaeffer, M. L., Agnihotri, G., Volker, C., Kallender, H., Brennan, P. J., and Lonsdale, J. T. (2001) Purification and biochemical characterization of the Mycobacterium tuberculosis beta-ketoacyl-acyl carrier protein synthases KasA and KasB, *The Journal of biological chemistry 276*, 47029-47037.
39. Changsen, C., Franzblau, S. G., and Palittapongarnpim, P. (2003) Improved green fluorescent protein reporter gene-based microplate screening for antituberculosis compounds by utilizing an acetamidase promoter, *Antimicrobial agents and chemotherapy 47*, 3682-3687.
40. Hackbarth, C. J., Unsal, I., and Chambers, H. F. (1997) Cloning and sequence analysis of a class A beta-lactamase from Mycobacterium tuberculosis H37Ra, *Antimicrobial agents and chemotherapy 41*, 1182-1185.
41. Newton, G. L., Unson, M. D., Anderberg, S. J., Aguilera, J. A., Oh, N. N., delCardayre, S. B., Av-Gay, Y., and Fahey, R. C. (1999) Characterization of Mycobacterium smegmatis mutants defective in 1-d-myo-inosityl-2-amino-2-deoxy-alpha-d-glucopyranoside and mycothiol biosynthesis, *Biochemical and biophysical research communications 255*, 239-244.
42. Lambalot, R. H., and Walsh, C. T. (1995) Cloning, overproduction, and characterization of the Escherichia coli holo-acyl carrier protein synthase, *The Journal of biological chemistry 270*, 24658-24661.
43. Thomas, J., and Cronan, J. E. (2005) The enigmatic acyl carrier protein phosphodiesterase of Escherichia coli: genetic and enzymological characterization, *The Journal of biological chemistry 280*, 34675-34683.

44. Thomas, J., Rigden, D. J., and Cronan, J. E. (2007) Acyl carrier protein phosphodiesterase (AcpH) of Escherichia coli is a non-canonical member of the HD phosphatase/phosphodiesterase family, *Biochemistry 46*, 129-136.
45. Tsai, Y. C., and Johnson, K. A. (2006) A new paradigm for DNA polymerase specificity, *Biochemistry 45*, 9675-9687.
46. Copeland, R. A., Williams, J. M., Giannaras, J., Nurnberg, S., Covington, M., Pinto, D., Pick, S., and Trzaskos, J. M. (1994) Mechanism of selective inhibition of the inducible isoform of prostaglandin G/H synthase, *Proceedings of the National Academy of Sciences of the United States of America 91*, 11202-11206.
47. Houtzager, V., Ouellet, M., Falgueyret, J. P., Passmore, L. A., Bayly, C., and Percival, M. D. (1996) Inhibitor-induced changes in the intrinsic fluorescence of human cyclooxygenase-2, *Biochemistry 35*, 10974-10984.
48. Gey Van Pittius, N. C., Gamieldien, J., Hide, W., Brown, G. D., Siezen, R. J., and Beyers, A. D. (2001) The ESAT-6 gene cluster of Mycobacterium tuberculosis and other high G+C Gram-positive bacteria, *Genome biology 2*, RESEARCH0044.
49. Sridharan, S., Wang, L., Brown, A. K., Dover, L. G., Kremer, L., Besra, G. S., and Sacchettini, J. C. (2007) X-ray crystal structure of Mycobacterium tuberculosis beta-ketoacyl acyl carrier protein synthase II (mtKasB), *Journal of molecular biology 366*, 469-480.
50. Copeland, R. A., Pompliano, D. L., and Meek, T. D. (2006) Drug-target residence time and its implications for lead optimization, *Nat Rev Drug Discov 5*, 730-739.

Chapter 3:

(1) Price, A. C., Choi, K. H., Heath, R. J., Li, Z., White, S. W., and Rock, C. O. (2001) Inhibition of beta-ketoacyl-acyl carrier protein synthases by thiolactomycin and cerulenin. Structure and mechanism. *J Biol Chem 276*, 6551-9.
(2) Jones, A. L., Gane, A. M., Herbert, D., Willey, D. L., Rutter, A. J., Kille, P., Dancer, J. E., and Harwood, J. L. (2003) Beta-ketoacyl-acyl carrier protein synthase III from pea (Pisum sativum L.): properties, inhibition by a novel thiolactomycin analogue and isolation of a cDNA clone encoding the enzyme. *Planta 216*, 752-61.
(3) Wang, J., Soisson, S. M., Young, K., Shoop, W., Kodali, S., Galgoci, A., Painter, R., Parthasarathy, G., Tang, Y. S., Cummings, R., Ha, S., Dorso, K., Motyl, M., Jayasuriya, H., Ondeyka, J., Herath, K., Zhang, C., Hernandez, L., Allocco, J., Basilio, A., Tormo, J. R., Genilloud, O., Vicente, F., Pelaez, F., Colwell, L., Lee, S. H., Michael, B., Felcetto, T., Gill, C., Silver, L. L., Hermes, J. D., Bartizal, K., Barrett, J., Schmatz, D., Becker, J. W., Cully, D., and Singh, S. B. (2006) Platensimycin is a

selective FabF inhibitor with potent antibiotic properties. *Nature 441*, 358-61.

(4) White, S. W., Zheng, J., Zhang, Y. M., and Rock. (2005) The structural biology of type II fatty acid biosynthesis. *Annu Rev Biochem 74*, 791-831.

(5) Young, K., Jayasuriya, H., Ondeyka, J. G., Herath, K., Zhang, C., Kodali, S., Galgoci, A., Painter, R., Brown-Driver, V., Yamamoto, R., Silver, L. L., Zheng, Y., Ventura, J. I., Sigmund, J., Ha, S., Basilio, A., Vicente, F., Tormo, J. R., Pelaez, F., Youngman, P., Cully, D., Barrett, J. F., Schmatz, D., Singh, S. B., and Wang, J. (2006) Discovery of FabH/FabF inhibitors from natural products. *Antimicrob Agents Chemother 50*, 519-26.

(6) Wang, J., Kodali, S., Lee, S. H., Galgoci, A., Painter, R., Dorso, K., Racine, F., Motyl, M., Hernandez, L., Tinney, E., Colletti, S. L., Herath, K., Cummings, R., Salazar, O., Gonzalez, I., Basilio, A., Vicente, F., Genilloud, O., Pelaez, F., Jayasuriya, H., Young, K., Cully, D. F., and Singh, S. B. (2007) Discovery of platencin, a dual FabF and FabH inhibitor with in vivo antibiotic properties. *Proc Natl Acad Sci U S A 104*, 7612-6.

(7) Sridharan, S., Wang, L., Brown, A. K., Dover, L. G., Kremer, L., Besra, G. S., and Sacchettini, J. C. (2007) X-ray crystal structure of Mycobacterium tuberculosis beta-ketoacyl acyl carrier protein synthase II (mtKasB). *J Mol Biol 366*, 469-80.

(8) Kortemme, T., and Creighton, T. E. (1995) Ionisation of cysteine residues at the termini of model alpha-helical peptides. Relevance to unusual thiol pKa values in proteins of the thioredoxin family. *J Mol Biol 253*, 799-812.

(9) Schaeffer, M. L., Carson, J. D., Kallender, H., and Lonsdale, J. T. (2004) Development of a scintillation proximity assay for the Mycobacterium tuberculosis KasA and KasB enzymes involved in mycolic acid biosynthesis. *Tuberculosis (Edinb) 84*, 353-60.

(10) Frydrych, I., and Mlejnek, P. (2007) Serine protease inhibitors N-alpha-Tosyl-L-Lysinyl-Chloromethylketone (TLCK) and N-Tosyl-L-Phenylalaninyl-Chloromethylketone (TPCK) are potent inhibitors of activated caspase proteases. *J Cell Biochem*.

(11) Schaeffer, M. L., Agnihotri, G., Volker, C., Kallender, H., Brennan, P. J., and Lonsdale, J. T. (2001) Purification and biochemical characterization of the Mycobacterium tuberculosis beta-ketoacyl-acyl carrier protein synthases KasA and KasB. *J Biol Chem 276*, 47029-37.

(12) Plietker, B. (2003) RuO4-catalyzed ketohydroxylation of olefins. *J Org Chem 68*, 7123-5.

(13) Karim, M. R., and Sampson, P. (1990) pp 598-605.

(14) Ogawa, K., Terada, T., Muranaka, Y., Hamakawa, T., Hashimoto, S., and Fujii, S. (1986) Studies of hypolipidemic agents. I. Syntheses and hypolipidemic activities of 1-substituted 2-alkanone derivatives. *Chem Pharm Bull (Tokyo) 34*, 1118-27.

(15) Heath, R. J., and Rock, C. O. (2002) The Claisen condensation in biology. *Nat Prod Rep 19*, 581-96.
(16) Haapalainen, A. M., Merilainen, G., and Wierenga, R. K. (2006) The thiolase superfamily: condensing enzymes with diverse reaction specificities. *Trends Biochem Sci 31*, 64-71.

Chapter 4:

(1) Oishi, H., Noto, T., Sasaki, H., Suzuki, K., Hayashi, T., Okazaki, H., Ando, K., and Sawada, M. (1982) Thiolactomycin, a new antibiotic. I. Taxonomy of the producing organism, fermentation and biological properties. *J Antibiot (Tokyo) 35*, 391-5.
(2) Sasaki, H., Oishi, H., Hayashi, T., Matsuura, I., Ando, K., and Sawada, M. (1982) Thiolactomycin, a new antibiotic. II. Structure elucidation. *J Antibiot (Tokyo) 35*, 396-400.
(3) Brown, M. S., Akopiants, K., Resceck, D. M., McArthur, H. A., McCormick, E., and Reynolds, K. A. (2003) Biosynthetic origins of the natural product, thiolactomycin: a unique and selective inhibitor of type II dissociated fatty acid synthases. *J Am Chem Soc 125*, 10166-7.
(4) Noto, T., Miyakawa, S., Oishi, H., Endo, H., and Okazaki, H. (1982) Thiolactomycin, a new antibiotic. III. In vitro antibacterial activity. *J Antibiot (Tokyo) 35*, 401-10.
(5) Miyakawa, S., Suzuki, K., Noto, T., Harada, Y., and Okazaki, H. (1982) Thiolactomycin, a new antibiotic. IV. Biological properties and chemotherapeutic activity in mice. *J Antibiot (Tokyo) 35*, 411-9.
(6) Slayden, R. A., Lee, R. E., Armour, J. W., Cooper, A. M., Orme, I. M., Brennan, P. J., and Besra, G. S. (1996) Antimycobacterial action of thiolactomycin: an inhibitor of fatty acid and mycolic acid synthesis. *Antimicrob Agents Chemother 40*, 2813-9.
(7) Kim, P., Zhang, Y. M., Shenoy, G., Nguyen, Q. A., Boshoff, H. I., Manjunatha, U. H., Goodwin, M. B., Lonsdale, J., Price, A. C., Miller, D. J., Duncan, K., White, S. W., Rock, C. O., Barry, C. E., 3rd, and Dowd, C. S. (2006) Structure-activity relationships at the 5-position of thiolactomycin: an intact (5R)-isoprene unit is required for activity against the condensing enzymes from Mycobacterium tuberculosis and Escherichia coli. *J Med Chem 49*, 159-71.
(8) Ohata, K., and Terashima, S. (2007) Synthesis and biological activity of enantiomeric pairs of 5-vinylthiolactomycin congeners. *Bioorg Med Chem Lett 17*, 4070-4.
(9) Ondeyka, J. G., Zink, D. L., Young, K., Painter, R., Kodali, S., Galgoci, A., Collado, J., Tormo, J. R., Basilio, A., Vicente, F., Wang, J., and Singh, S. B. (2006) Discovery of bacterial fatty acid synthase inhibitors from a Phoma species as antimicrobial agents using a new antisense-based strategy. *J Nat Prod 69*, 377-80.

(10) Jones, S. M., Urch, J. E., Kaiser, M., Brun, R., Harwood, J. L., Berry, C., and Gilbert, I. H. (2005) Analogues of thiolactomycin as potential antimalarial agents. *J Med Chem 48*, 5932-41.
(11) Barco, P., Cardoso, R. F., Hirata, R. D., Leite, C. Q., Pandolfi, J. R., Sato, D. N., Shikama, M. L., de Melo, F. F., Mamizuka, E. M., Campanerut, P. A., and Hirata, M. H. (2006) pncA mutations in pyrazinamide-resistant Mycobacterium tuberculosis clinical isolates from the southeast region of Brazil. *J Antimicrob Chemother 58*, 930-5.
(12) Menner, N., Gunther, I., Orawa, H., Roth, A., Rambajan, I., Wagner, J., Hahn, H., Persaud, S., and Ignatius, R. (2005) High frequency of multidrug-resistant Mycobacterium tuberculosis isolates in Georgetown, Guyana. *Trop Med Int Health 10*, 1215-8.
(13) Lipinski, C. A., Lombardo, F., Dominy, B. W., and Feeney, P. J. (2001) Experimental and computational approaches to estimate solubility and permeability in drug discovery and development settings. *Adv Drug Deliv Rev 46*, 3-26.
(14) Price, A. C., Choi, K. H., Heath, R. J., Li, Z., White, S. W., and Rock, C. O. (2001) Inhibition of beta-ketoacyl-acyl carrier protein synthases by thiolactomycin and cerulenin. Structure and mechanism. *J Biol Chem 276*, 6551-9.
(15) Hayashi, T., Yamamoto, O., Sasaki, H., Kawaguchi, A., and Okazaki, H. (1983) Mechanism of action of the antibiotic thiolactomycin inhibition of fatty acid synthesis of Escherichia coli. *Biochem Biophys Res Commun 115*, 1108-13.
(16) Jackowski, S., Zhang, Y. M., Price, A. C., White, S. W., and Rock, C. O. (2002) A missense mutation in the fabB (beta-ketoacyl-acyl carrier protein synthase I) gene confers tiolactomycin resistance to Escherichia coli. *Antimicrob Agents Chemother 46*, 1246-52.
(17) Tsay, J. T., Rock, C. O., and Jackowski, S. (1992) Overproduction of beta-ketoacyl-acyl carrier protein synthase I imparts thiolactomycin resistance to Escherichia coli K-12. *J Bacteriol 174*, 508-13.
(18) Slayden, R. A., Lee, R. E., and Barry, C. E., 3rd. (2000) Isoniazid affects multiple components of the type II fatty acid synthase system of Mycobacterium tuberculosis. *Mol Microbiol 38*, 514-25.
(19) Nishida, I., Kawaguchi, A., and Yamada, M. (1986) Effect of thiolactomycin on the individual enzymes of the fatty acid synthase system in Escherichia coli. *J Biochem (Tokyo) 99*, 1447-54.
(20) Copeland, R. A., Pompliano, D. L., and Meek, T. D. (2006) Drug-target residence time and its implications for lead optimization. *Nat Rev Drug Discov 5*, 730-9.
(21) Ehrlich, P. (1913) Address in pathology on chemotherapeutics : Scientific principles, methods, and results. *Lancet 2*, 445-451.
(22) Ojima, M., Inada, Y., Shibouta, Y., Wada, T., Sanada, T., Kubo, K., and Nishikawa, K. (1997) Candesartan (CV-11974) dissociates slowly from the angiotensin AT(1) receptor. *European Journal of Pharmacology 319*, 137-146.

(23) Lewandowicz, A., Tyler, P. C., Evans, G. B., Furneaux, R. H., and Schramm, V. L. (2003) Achieving the ultimate physiological goal in transition state analogue inhibitors for purine nucleoside phosphorylase. *J Biol Chem 278*, 31465-8.
(24) Kamal, A., Shaik, A. A., Azeeza, S., Malik, M. S., and Sandbhor, M. (2006) Chemoenzymatic synthesis of (5S)- and (5R)-hydroxymethyl-3,5-dimethyl-4-(methoxymethoxy)-5H-thiophen-2-one: a precursor of thiolactomycin and determination of its absolute configuration. *Tetrahedron: Asymmetry 17*, 2890-2895.
(25) J. Wang, C.-L., and Salvino, J. M. (1984) Total ssynthesis of (±) thiolactomycin. *Tetrahedron Letters 25*, 5243-5246.
(26) Chambers, M., S.; Thomas,E., J. . (1997) Asymmetric synthesis of 5,5-disubstituted thiotetronic acids using an allyl xanthate to dithiocarbonate rearrangement: total synthesis of (5S)-thiolactomycin with revision of the absolute configuration of the natural *J. Chem. Soc., Perkin Trans. 1*, 417 - 432.
(27) Ohata, K., and Terashima, S. (2006) Efficient synthesis of enantiomeric pairs of thiolactomycin and its 3-demethyl derivative. *Tetrahedron Letters 47*, 2787-2791.
(28) McFadden, J. M., Frehywot, G. L., and Townsend, C. A. (2002) A flexible route to (5R)-thiolactomycin, a naturally occurring inhibitor of fatty acid synthesis. *Org Lett 4*, 3859-62.
(29) Sakya, S. M., Suarez-Contreras, M., Dirlam, J. P., O'Connell, T. N., Hayashi, S. F., Santoro, S. L., Kamicker, B. J., George, D. M., and Ziegler, C. B. (2001) Synthesis and structure-activity relationships of thiotetronic acid analogues of thiolactomycin. *Bioorg Med Chem Lett 11*, 2751-4.
(30) Jones, S. M., Urch, J. E., Brun, R., Harwood, J. L., Berry, C., and Gilbert, I. H. (2004) Analogues of thiolactomycin as potential anti-malarial and anti-trypanosomal agents. *Bioorg Med Chem 12*, 683-92.
(31) Jones, A. L., Herbert, D., Rutter, A. J., Dancer, J. E., and Harwood, J. L. (2000) Novel inhibitors of the condensing enzymes of the type II fatty acid synthase of pea (Pisum sativum). *Biochem J 347 Pt 1*, 205-9.
(32) Senior, S. J., Illarionov, P. A., Gurcha, S. S., Campbell, I. B., Schaeffer, M. L., Minnikin, D. E., and Besra, G. S. (2003) Biphenyl-based analogues of thiolactomycin, active against Mycobacterium tuberculosis mtFabH fatty acid condensing enzyme. *Bioorg Med Chem Lett 13*, 3685-8.
(33) Senior, S. J., Illarionov, P. A., Gurcha, S. S., Campbell, I. B., Schaeffer, M. L., Minnikin, D. E., and Besra, G. S. (2004) Acetylene-based analogues of thiolactomycin, active against Mycobacterium tuberculosis mtFabH fatty acid condensing enzyme. *Bioorg Med Chem Lett 14*, 373-6.
(34) Bhowruth, V., Brown, A. K., Senior, S. J., Snaith, J. S., and Besra, G. S. (2007) Synthesis and biological evaluation of a C5-biphenyl thiolactomycin library. *Bioorg Med Chem Lett 17*, 5643-6.

(35) Sassetti, C. M., Boyd, D. H., and Rubin, E. J. (2003) Genes required for mycobacterial growth defined by high density mutagenesis. *Mol Microbiol 48*, 77-84.
(36) McFadden, J. M., Medghalchi, S. M., Thupari, J. N., Pinn, M. L., Vadlamudi, A., Miller, K. I., Kuhajda, F. P., and Townsend, C. A. (2005) Application of a flexible synthesis of (5R)-thiolactomycin to develop new inhibitors of type I fatty acid synthase. *J Med Chem 48*, 946-61.
(37) Hajduk, P. J., Dinges, J., Miknis, G. F., Merlock, M., Middleton, T., Kempf, D. J., Egan, D. A., Walter, K. A., Robins, T. S., Shuker, S. B., Holzman, T. F., and Fesik, S. W. (1997) NMR-based discovery of lead inhibitors that block DNA binding of the human papillomavirus E2 protein. *J Med Chem 40*, 3144-50.
(38) Hajduk, P. J., Meadows, R. P., and Fesik, S. W. (1997) Discovering high-affinity ligands for proteins. *Science 278*, 497,499.
(39) Shuker, S. B., Hajduk, P. J., Meadows, R. P., and Fesik, S. W. (1996) Discovering high-affinity ligands for proteins: SAR by NMR. *Science 274*, 1531-4.
(40) Pellecchia, M., Sem, D. S., and Wuthrich, K. (2002) NMR in drug discovery. *Nat Rev Drug Discov 1*, 211-9.
(41) Van, Q. N., and Shaka, A. J. (1998) Improved cross peak detection in two-dimensional proton NMR spectra using excitation sculpting. *J Magn Reson 132*, 154-8.
(42) Van, Q. N., Smith, E. M., and Shaka, A. J. (1999) Observation of long-range small-molecule NOEs using a neoteric sensitivity enhancement scheme. *J Magn Reson 141*, 191-4.
(43) Davies, C., Heath, R. J., White, S. W., and Rock, C. O. (2000) The 1.8 A crystal structure and active-site architecture of beta-ketoacyl-acyl carrier protein synthase III (FabH) from escherichia coli. *Structure 8*, 185-95.